INDEX

LIST OF ABBREVIATIONS

br	broad signal (NMR)
d	doublet
DFT	Density functional theory
DSC	Differential scanning calorimetry
ε-CL	ε-Caprolactone
ESI-MS	Electrospray ionization mass spectrometry
Et	Ethyl
GPC	Gel permeation chromatography
I	Initiator
iPr	iso-Propyl
J	Coupling constant (NMR)
LA	Lactide
m	multiplet (NMR)
M	Monomer
MALDI-TOF-MS	Matrix assisted laser desorption ionization time-of-flight mass spectrometry
Me	Methyl
Mn_{exp}	Experimental number-average molar mass

Mn_{th}	Theoretic number-average molar mass
Mw	Weight-average molar mass
NMR	Nuclear magnetic resonance
OR	Alkoxide group
PCL	Poly(ε-Caprolactone)
PDI	Polydispersity index
Ph	Phenyl
PHB	Poly(3-hydroxybutyrate)
PLA	Poly(lactide)
PPP-H	Phosphinophenyl-phosphine ligand
Pr	Probability of heterotactic enchainment
R	Alkyl moiety
ROP	Ring Opening Polymerization
t	Triplet (NMR)
THF	Tetrahydrofurane
TOF	Turnover frequency
β BL	β-butyrolactone
δ	chemical shift (NMR)
δ-VL	δ-Valerolactone

ABSTRACT

This thesis is concerned with the synthesis and characterization of new metal systems as efficient initiators for Ring Opening Polymerization (ROP) of cyclic esters.

The compounds synthesized contain a metal center featuring a tridentade monoanionic phosphido pincer ligand as ancillary ligand and alkyl or amido groups as nucleofilic groups.

Phosphido-diphosphine pincer ligands represent an original coordination environment to support reactive metal centers traditionally employed in this kind of catalysis such as Group 3 metals, zinc and aluminum.

The chapters of the present work are based on each other, but they can be read independently.

The first chapter is an introduction showing the background of this thesis. The growing interest in biodegradable polyesters, a short description of their properties and their main applications in a variety of fields are described. Moreover an overview of the different methods to synthesize these polymers and of the countless metal systems as active initiators for this polymerization is showed.

The key objectives of this work are discussed in the Chapters 2 to 4. Each chapter regards the synthesis and characterization of new metal complexes and their ability as efficient catalysts in the ROP of lactides and lactones, for each class of metals investigated. A brief description of the most representative examples of catalysts for ROP of cyclic esters in literature

introduces the work reported in a specific chapter and a summary of all results obtained completes the discussion.

The second chapter report the investigation of the catalytic activity of bis(alkyl) Group 3 metal systems bearing phosphido-diphosphine pincer ligands. The experimental studies on the catalytic behavior of yttrium and scandium systems are performed in order to show how the catalytic activity is dependent on the nature of the metal center, the structure of the ancillary ligand and the polymerization conditions.

The third chapter regards the description of two new alkyl and amido zinc complexes bearing a tridentate monoanionic phosphorous-based pincer ligand. Variable temperature ^{1}H and ^{31}P NMR studies highlight a marked flexibility of the phosphido pincer ligand in the coordination at the metal center.

The fourth chapter reports the study of new alkyl aluminum complexes supported by phosphide diphosphine pincer ligands This class of aluminum complexes represent the first example of aluminum systems bearing purely phosphorous containing ligands explored in the ROP of cyclic esters.

Brief concluding remarks and an experimental part conclude all this thesis work.

1 INTRODUCTION

1.1 BIOPLASTICS

In the last 60 years, synthetic polymeric materials field has grown progressively up to forming one of the most attractive domains in materials science.

These materials can be easily produced, processed and handled and therefore provide a wide variety of applications. Conventional plastics like polyethylene (PE), polypropylene (PP), polyvinylchloride (PVC), polystyrene (PS), and poly(ethylene terephthalate) (PET) possess excellent properties such as lightness, durability, non-degradability and non-corrosivity to acids and alkalis. However, the high durability of these synthetic polymers has caused a crisis in solid waste management. This, together with the dwindling fossil resources, the increasing oil prices and the growing environmental awareness lead to modern approaches towards green and sustainable chemistry which focus on the substitution of petrochemical-based plastics with bioplastics.[1, 2, 3, 4, 5]

The term bioplastics (also called organic plastics, biobased plastic materials or artificial biopolymers [3]) has up to now no consistent definition. In general it includes polymers which are derived from renewable biomass sources, (biorenewable materials), and/or are biodegradable plastic materials.[1, 6]

The class of bioplastics includes primarily four polymer types: polysaccharides, polyesters, polyurethanes and polyamides (for an overview see Table 1.1).[5]

Table 1.1 Overview of currently most important groups and types of bioplastics

Type of polymer	Bioplastics (group)
Polysaccharides	Starch and cellulose polymers
Polyesters	Poly(lactic acid) (PLA), Polyglycolide (PGA), Poly-ε-caprolactone (PCL), Polytrimethyleneterephthalate (PTT), Polybutyleneterephthalate (PBT), Polybutylene succinate (PBS), Polyhydroxyalkanoates (PHAs)
Polyurethanes	Polyurethanes (PURs)
Polyamides	Nylon

Beside their advantageous properties which are characteristic for plastics, bioplastics derived from annually renewable biomass sources provide a new source of income for the agricultural sector and offer a higher independence of fossil resources like crude oil or gas. They fulfill the principles of sustainable chemistry.

Their use in packaging and for single-use disposal products [1] helps to solve the problems of solid waste management and allows for contributions to environmental protection.

According to a definition by IUPAC, biodegradation means the breakdown of a substance to its constituents, catalyzed by enzymes or whole microorganisms. [7] This process is highly influenced not only by the primary chemical structure of these materials but also by their solid-state morphology and ordering phenomena such as crystallinity and orientation.[1]

As a definition of the term biodegradability, a German standard test method exists since 1998, which is entitled “test of the compostability of plastics” (Figure 1.1). In addition to an analysis of the chemical composition (e.g. of any heavy metals present) this standard test includes probing the complete degradability in laboratory experiments, probing the degradability under real-life conditions and the quality of the resulting compost. To be classified as biodegradable, in laboratory experiments more than 60% of the organic carbon must be converted within a maximum of six months; moreover under real-life conditions of composting more than 90% of the plastic is required to be degraded to fragments not more than 2 mm in size.[8]

Fig. 1.1: Symbol for the certification of biodegradability of plastics according to the German standard test method DIN V54900. [9]

1.2 POLYESTERS

As to synthetic biodegradable polymers, aliphatic polyesters are representatives. Nowadays, aliphatic polyesters, such as poly(lactide) and poly(ε-caprolactone), polyglycolide, polybutyrolactone, are commercially produced and their output continue to increase.

1.2.1 Polylactide

Polylactide (PLA) or poly(lactic acid) is an aliphatic polyester which can be produced by polymerization of either l4actic acid or lactide (3,6-dimethyl-1,4-dioxane-2,5-dione), the cyclic diester of lactic acid.

The monomer, i.e. lactic acid, can be synthesized by biological and chemical methods. However, biological method is generally preferred [9] (Scheme 1.1). It is based on the fermentation of starch and other polysaccharides, which are easily available from corn, sugar beet, sugar cane, potatoes, and other biomasses. The majority of the world's commercially produced lactic acid is by bacterial fermentation, allowing the production of 99.5% of the L-isomer and 0.5% of the D-isomer of lactic acid.

Whereas chemically synthesized lactic acid gives the racemic mixture (50% D and 50% L). During the fermentation process, the conditions like pH, temperature and in some cases the agitation are monitored closely to get the maximum yield with the purity of material.

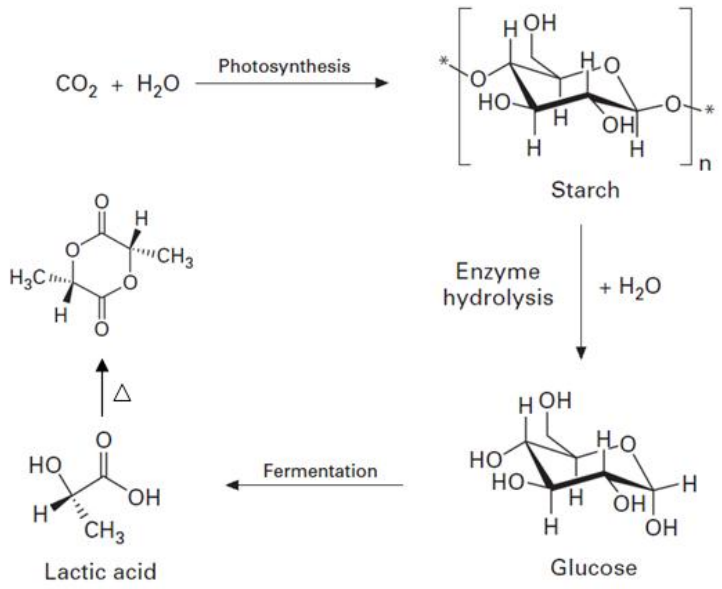

Scheme 1.1: Production of lactic acid and lactide from renewable resources

Based on the 12 principles of green chemistry introduced by P. T. Anastas and J. C. Warner,[10] PLA can be described as sustainable polymer in context of green chemistry. It can be made from inexpensive annually renewable resources and after its lifetime it can be recycled or it degrades through hydrolysis of the ester linkages by microorganisms and enzymes or simple acidic or alkaline catalysis into non-toxic, harmless natural products.

Thus PLA is a low-impact greenhouse gas polymer because the CO_2 generated during the biodegradation is balanced by an equal amount taken from the atmosphere during the growth of plant feedstock (Scheme. 1.2). [11]

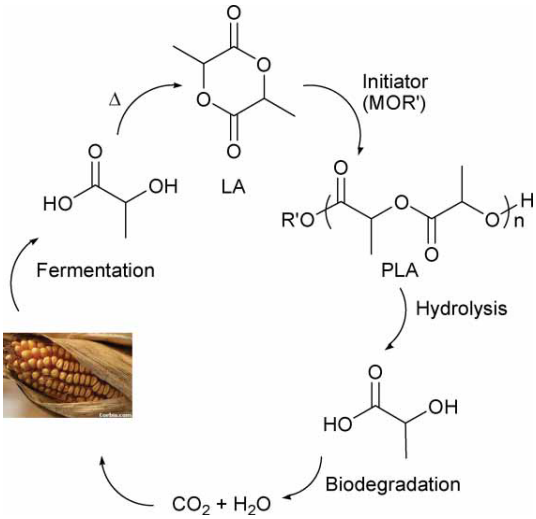

Scheme 1.2: The life cycle of PLA

Moreover, this polymer is bioassimilable since its hydrolysis in physiological media gives lactic acid, non-toxic component that can be eliminated via Krebs cycle as water and carbon dioxide.

Polylactide provides many advantageous properties such as bioresorbability, biocompatibility, biodegradability, both in vivo and in the environment, bacteriostatic and antifungal characteristics, high transparency, grease and oil resistance, high odour and flavour barrier, weather stability, elastic recovery and good resilience and thermal bonding capabilities.

Isotactic PLA benefits from its excellent mechanical properties like its thermoplastic processability which allows for the easily conversion into films, • fibers, spun-bond and melt-blown products on existing processing equipment. Due to these favourable intrinsic properties PLA provides a versatile range of possible applications reaching from specialized biomedical and pharmaceutical products [12] (drug delivery systems, sutures, surgical implants, devices for bone surgery like bone plates, screws, pins,

etc.) to widespread use as coatings, fibers, films and packages including agricultural and civil engineering materials (mulch films, plant pots, root covers, shing lines, string), geotextiles (sand bags, erosion protection, drainage), clothing and furnishings (casual wear, towels, mats), nonwovens as personal hygiene products (wipes, diapers, pad liners), packaging materials (wrapping, containers, coated paper, bags) and industrial uses (filters, drainage bags, tapes, ropes, carpets).[13]

By the mid-1990s, market pressures for sustainable plastics and improvements to monomer production enabled cost reductions and facilitated its use in consumer articles, fiber technology, and packaging. PLA is now being manufactured on a 140,000 ton scale annually in the USA by Natureworks LLC, (e.g. Natureworks™, Ingeo™) and on a smaller scale by several enterprises in the EU and Japan. [14]

The physical properties, hydrolysis and biodegradation behavior of PLA can be controlled not only by altering the averaged molecular weight and its distribution; in order to meet also the requirements of specific applications it is even possible to modify the properties of PLA by tailoring the macromolecular architecture and microstructure. Thus, the stereocontrol is an important parameter because the polymer's tacticity influences its properties, e. g. isotactic PLA is crystalline whereas atactic PLA is amorphous. The PLA tacticity depends on the type of lactide selected.

Lactide exists in different enantiomeric forms: the pure entantiomers, (*S,S*)-Lactide, (L-Lactide) and (*R,R*)-Lactide, (D-Lactide), the racemic mixture, *rac*-Lactide, (D-Lactide and L-Lactide 50:50 mixture) and *meso*-Lactide, D,L-Lactide (Fig 1.2).

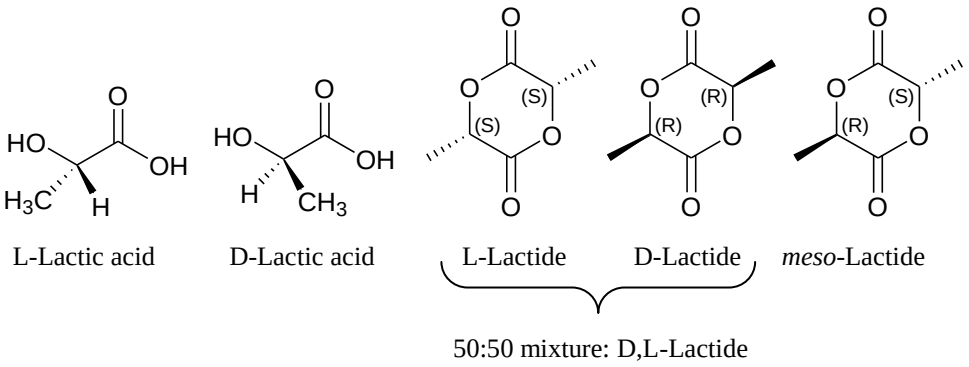

Fig 1.2: Stereoisomers of lactic acid and lactide

When pure D- or L-lactide is polymerized, optically pure poly(D-lactide) ({RRRR}n) and poly(L-lactide) ({SSSS}n) are obtained as isotactic polymers, respectively.

With D,L-Lactide it is possible to have three different stereoregular microstructures: heterotactic PLA, ({SSRR}n), isotactic stereoblock PLA, ([{SSSS}n{RRRR}n]m) and stereocomplex of isotactic PLA, ({SSSS}n + ({RRRR}n).

The polymerization of *meso*-lactide leads to the formation of syndiotactic PLA, ({RSRS}n), and of heterotactic PLA, (Fig 1.3).

Optically pure isotactic PLA is a semi-cystalline, hard and rather brittle material and has an equilibrium melting point of 207°C, but due to impurities, slight racemization and crystal defects the typical melting point ranges from 170 to 180°C.

Whereas the stereocomplex PLA exhibited a high melting temperature of 230°C.

On the contrary, syndiotactic, heterotactic and atactic PLA are amorphous, transparent polymers with a softening point observed around 60°C. The amorphous polymer is soluble in most common organic solvents such as

ketones, tetrahydofurane, benzene, acetonitrile, dioxane and chlorinated solvents whereas the crystalline material is only soluble in chlorinated solvents or benzene at elevated temperatures.[15]

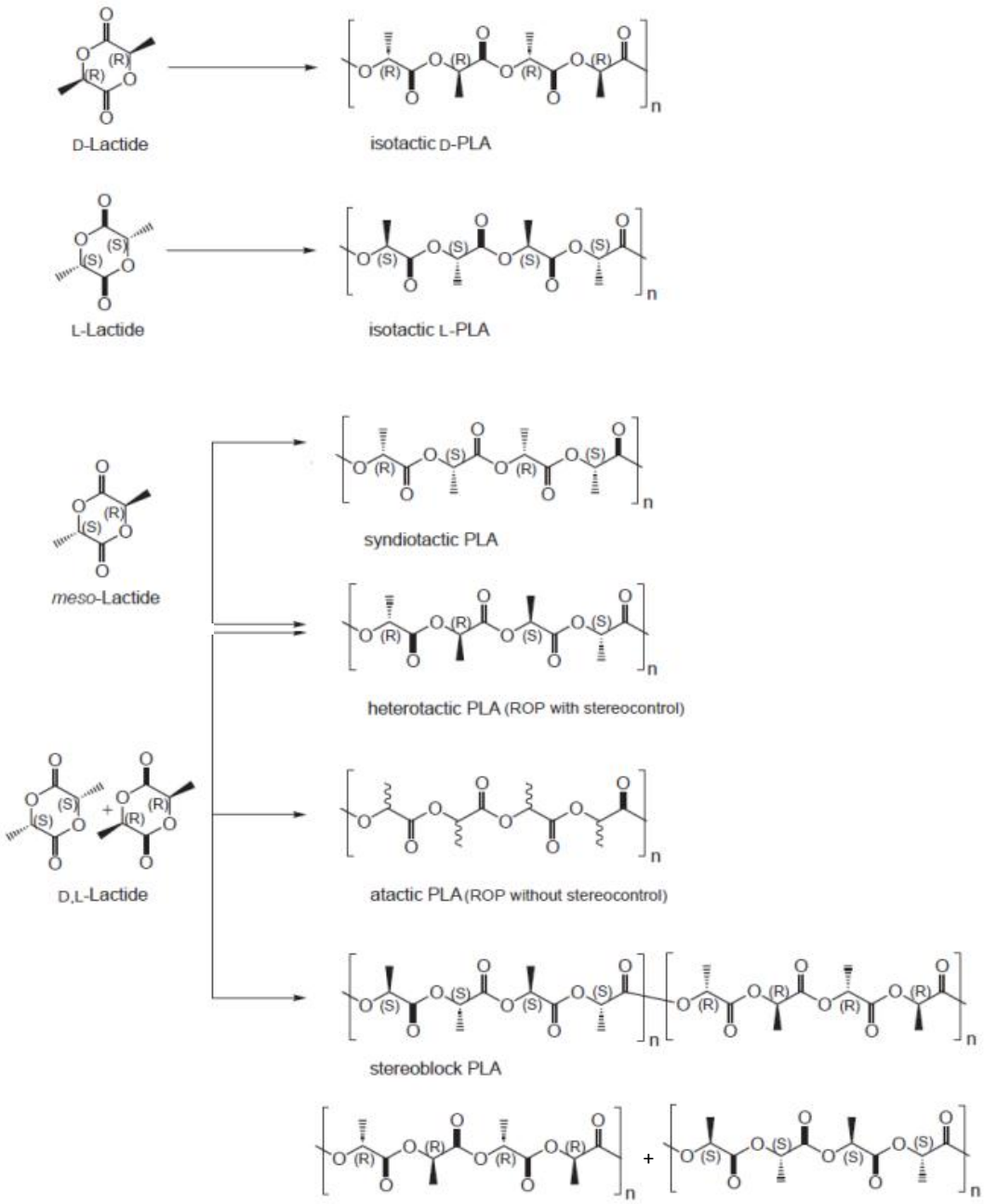

Fig 1.3: Microstructures of polylactide

1.2.2 Polycaprolactone

Poly(caprolactone) (PCL) is an aliphatic polyester composed of hexanoate repeat units. It is a semicrystalline polymer with a degree of crystallinity which can reach 69%.[16]

ε-Caprolactone (ε-CL), a cyclic ester, is the monomer used to obtain the polymer. It is still mainly produced through the Bayer Williger oxidation of cyclohexanone with peracids or hydrogen peroxide (Scheme 1.3 a) [17] by companies such as Perstorp (through a subsidiary previously owned by Solvay), BASF and Daicel. However, reports in the patent literature make mention of the possible availability of ε-caprolactone from starch, [18] (Scheme 1.3 b) making poly(ε-caprolactone) a polymer with high industrial potential.

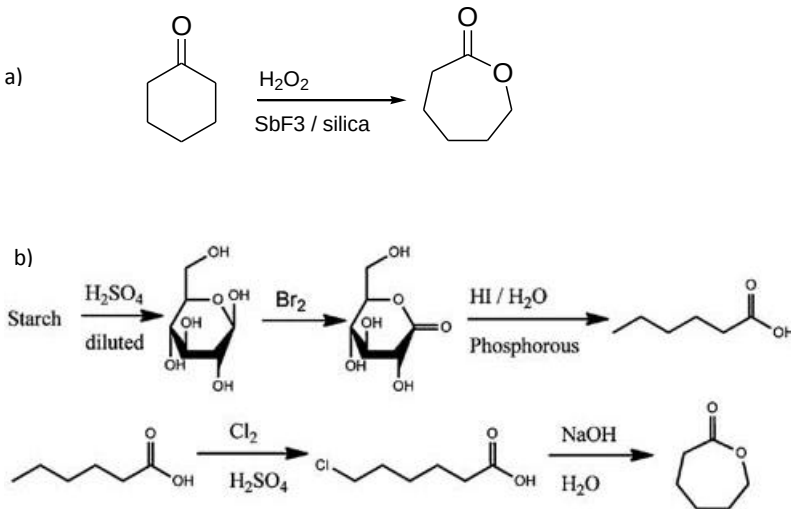

Scheme 1.3: Synthesis of ε-caprolactone monomer a) via the Bayer Williger oxidation process and b) from renewable resources

At room temperature, PCL is highly soluble in chloroform, dichloromethane, carbon tetrachloride, benzene, toluene, cyclohexanone and 2-nitropropane; slightly soluble in acetone, 2-butanone, ethyl acetate, dimethylformamide and acetonitrile; and insoluble in alcohols, petroleum ether, diethyl ether and water.[19]

PCL displays the rare property of being miscible with many other polymers (such as poly(vinyl chloride), poly(styrene–acrylonitrile), poly(acrylonitrile butadiene styrene), poly(bisphenol-A) and other polycarbonates, nitrocellulose and cellulose butyrate), and is also mechanically compatible with others (polyethylene, polypropylene, natural rubber, poly- (vinyl acetate), and poly(ethylene–propylene) rubber).

Like polylactide, PCL is a biocompatible, biodegradable polymer and can be obtained from renewable resources.[20]

It biodegrades within several months to several years depending on the molecular weight, the degree of crystallinity of the polymer, and the conditions of degradation.

Many microbes in nature are able to completely biodegrade PCL. The polymer degrades by end chain scission at higher temperatures while it degrades by random chain scission at lower temperatures.[21] PCL degradation is autocatalyzed by the carboxylic acids liberated during hydrolysis but it can also be catalyzed by enzymes, resulting in faster decomposition.[21]

PCL has uses in different fields such as scaffolds in tissue engineering,[22] , in long-term drug delivery systems [23] (in particular contraceptives delivery), in microelectronics, as adhesives and in packaging. [24]

Poly(caprolactone) is now produced industrially by companies such as Solvay Interox (CAPA®), which was recently acquired by the Perstorp

group of Sweden, Dow Union Carbide (Tone®) and Daicel (Placcel®), and the demand for this polymer is ever increasing.[25]

1.2.3 Copolymers of Lactide and ε-Caprolactone

In recent years, (Lactide)/(ε-caprolactone) copolymers are among the most widely used polymeric materials in medical and pharmaceutical applications due to their physical properties and nontoxicity to humans. Biodegradable sutures, artificial skin, resorbable prostheses, and controlled drug release,[1, 26] are examples of the applications of these polymeric materials, since these copolymers can be metabolized and remove from the body via normal metabolic pathways.[26c]

Copolymerization or blending of PLA with PCL could allow the fabrication of a variety of biodegradable and biocompatible polymers with improved properties in comparison to those of the parent homopolyesters.

For example, PLA presents good mechanical properties but poor elasticity; PCL exhibits remarkable drug permeability, elasticity, and thermal properties but poor mechanical strength. Because the glass transition temperature of PLAs is above body temperature, these materials are stiff with poor elasticity in the human body. On the contrary, PCL is in the rubbery state at room temperature, exhibiting a glass transition temperature of -60 °C.

So, it is possible to obtained copolymers with properties from rigid thermoplastics to elastomeric rubbers,[27] with tensile strengths ranging from 0.6 to 48 MPa and also elongation [28].

Moreover, PCL degrades much slower than PLA. Therefore, copolymers of poly(lactide) and poly(ε-caprolactone) could be suitable for applications where elasticity and degradability are required in the same product. [29] Moreover, the PCL drug permeability and the rapid degradation rate of PLA

may be combined in their copolymers, making drug delivery systems with adjustable properties depending on the composition. [30]

By varying the copolymer composition, monomer sequencing, and molecular weight, the copolymer properties can be tailored to meet the requirements of various applications. Therefore, the synthesis of ε-CL/LA copolymers has been widely studied focusing on either block [31], or random [32] copolymers.

1.2.4 Synthesis of polyesters

Generally, polymers are available via two polymerization routes: (1) by direct polycondensation of corresponding hydroxyacid or (2) by ring-opening polymerization of lactide and lactone (Scheme 1.4)

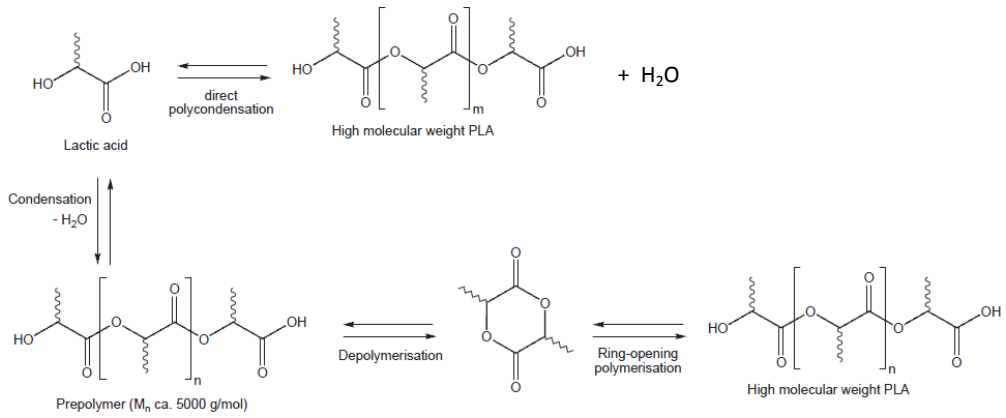

Scheme 1.4: Schematic polymerization routes to PLA

Direct polycondensation

The direct polycondensation of lactic acid is the oldest technique to obtain PLA and was introduced by Carruthers and coworkers already in 1932. [33] The polymerization proceeds by the successive reaction of polymer end-groups which results in the gradual growth of polymer chains.

Braud et al. synthesized PCL oligomers by polycondensation of 6-hydroxyhexanoic acid under vacuum. The reaction was performed without the addition of catalyst and was complete in 6 h at a temperature that was gradually increased from 80 to 150 °C. [34]

The polymers obtained by polycondesation have low molecular weights, because it is hard to remove derived water completely from the highly viscous reaction mixture and this is the main disadvantage of direct polycondensation polymerization, so it restricts its use. Moreover, the streoregularity, e. g. for polylactide, cannot be controlled during the course of polymerization. The polymer thus possesses inferior mechanical properties.

Polymers with high molecular weights can be obtained by different techniques. For example, high molecular weight PLA can also be synthesized azeotropically, a high-boiling solvent (e.g. diphenyl ether, bp 259°C) is used to drive the removal of water in the direct esterification process to obtain high-molecular weight PLA. [35]

Also use of enzyme is noteworthy, polymerization of 6-hydroxycaproic acid using lipase from *Candida antarctica* under vacuum gave rise to PCLs with an high average molecular weight and a polydispersity under 1.5 in 2 days. [36]

Ring-Opening Polymerization (ROP)

High-molecular weight polymers can be directly synthesized by ring-opening polymerization of cyclic esters, a process which can be initiated by a large variety of species, ranging from metal complexes to nucleophilic organocatalysts, to enzymes. [37] [38]

The ring-opening polymerization is thermodynamically favorable, due to the relief of the lactone ring strain. [39] Only low concentration of initiator and relatively low reaction temperatures (< 130°C, in solution) are needed to obtain full conversion of the monomer. By altering the monomer to initiator ratio, the molecular weight of the polymers can be adjusted. In addition, the setting of reaction conditions (e.g. the choice of initiator) allows for a good control of polymerization and therefore provides tailoring of the properties related to the microstructure and the molecular architecture of the polymer. This makes the ROP a precise tool for the production of well-defined polyesters.[1]

Depending of the nature of initiator three prevalent types of mechanisms are discussed for the ring-opening polymerization: 1) the cationic polymerization mechanism, 2) the anionic polymerization mechanism, 3) the coordination insertion mechanism.

Cationic polymerization mechanism

The cationic ROP of lactones occurs in the presence of alkylating agents, acylating agents, Lewis acids and protic acids, such as carbenium ion donors, triethyloxonium tetrafluoroborate, borontrifluoride, and trifluoroacetic acid. [40]

The initiation step of cationic polymerization occurs when the exocyclic oxygen of the monomeric carbonyl is either alkylated or protonated by the initiator, causing the resulting O–CH bond to become positively charged. Nucleophilic attack by a second monomer breaks this bond to create another electrophilic carbenium ion. The propagation step of this polymerization

repeats as nucleophilic attack by additional monomers continues until the polymerization is terminated by a monofunctional nucleophile like water. In cationic polymerization high temperature causes racemization, since the second monomer attack at chiral center propagating chain. However, the racemization can be minimized at temperature >50°C but at this temperature the rate of reaction is very slow and does not yield high molecular weight polymer (Scheme 1.5).

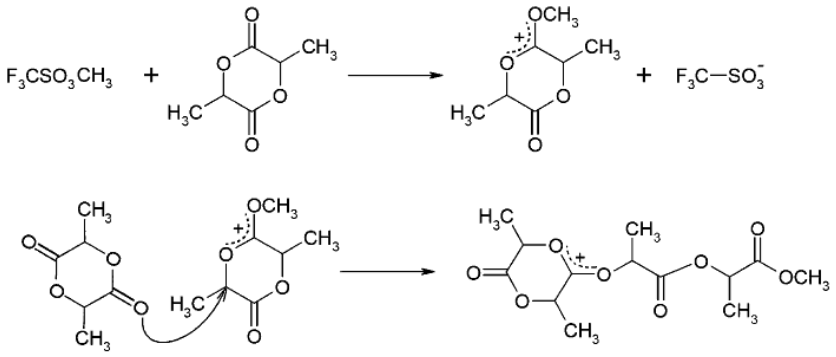

Scheme 1.5: Cationic ring opening polymerization of PLA[39]

Anionic polymerization mechanism

The anionic ROP involves a nucleophilic anion of the initiator which attacks the carbonyl-C atom of the monomer, resulting in the cleavage of the C-O single bond. The resulting alkoxide species continues to propagate as new anion.

Although, this polymerization reaction possesses higher conversion rates in comparison to the cationic ROP, there is still the risk of partial racemization

if the monomer is deprotonated by the initiator or the active chain end. [41] (Scheme 1.6)

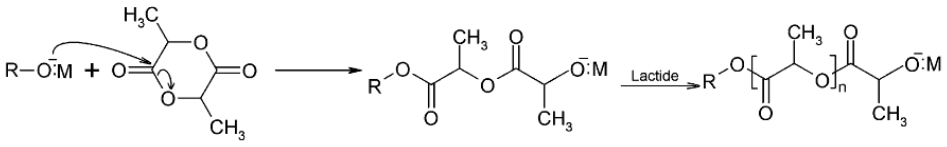

Scheme 1.6: Anionic ring opening polymerization of PLA[32]

Coordination–insertion mechanisms

It is the most widely studied method for the synthesis of high molecular weight aliphatic polyesters. In this method, metal initiators having a nucleophilic co-ligand (e.g., an amido, alkyl or alkoxide group), are used. According to such a mechanism, the Lewis acidic metal center coordinates and activates a cyclic ester, enabling it to be attacked by the metal-bound initiating group. The putative tetrahedral intermediate undergoes ring-opening to generate a ring-opened cycle with a specific chain end and a new metal alkoxide bond. The metal alkoxide subsequently goes on to bind, activate, and attack another monomer; this reaction repeats itself until the equilibrium conversion is reached and polymer is formed. Varying the polymerization conditions it can govern the polymerization rate, control, and any stereoselectivity; therefore it profoundly influences the physical and chemical properties of the polymeric material. [42, 43](Scheme 1.7)

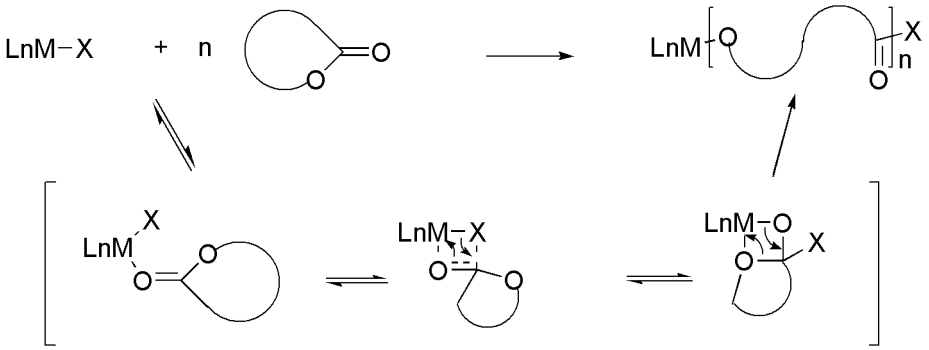

Scheme 1.7: Schematic coordination-insertion mechanism

Side reactions

Controlled polymerization reactions like the living ROP provide the possibility to predict and to regulate the physical properties of the obtained polymers. However, the living character of ROP can be observed only in the rarest cases due to side reactions like hydrolysis and chain transfer by transesterification (also designated as back-biting reactions). Intermolecular transesterification causes broadening of the molecular weight distribution, whereas intramolecular transesterification generates cyclic oligomers leading to the decrease of averaged molecular weights (Scheme 1.8).[42]

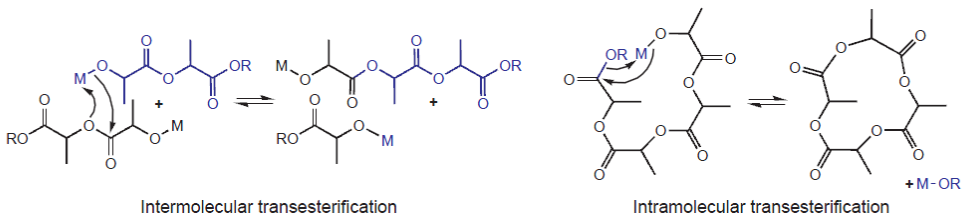

Scheme 1.8: Transesterification reactions

1.2.5 Initiator systems for the ROP of cyclic esters

During the past decades, various initiator systems have been investigated for the ROP of lactides and lactones. The initiator not only dictates the mechanism and therefore significantly influences the molecular weight and the molecular weight distribution but also affects the conversion rate and in some cases controls the stereochemistry of the obtained polymers. General requirements for initiators are well-behaved reaction control, high activity, fast initiation relative to propagation, minimal side reactions (transesterification), high tolerance towards impurities in the monomer, easy handling, colourlessness and odourlessness as well as low costs and toxicity. [44, 45]

For industrial production of PLA the most widely used initiator is still tin(II) ethylhexanoate ($SnOct_2$).[46] It is commercially available, easy to handle, and soluble in common organic solvents and in melt monomers. It is highly active (typical reaction times in bulk at 140-180 °C range from minutes to a few hours) and allows for the preparation of high-molecular-weight polymers (up to 10^5 Da in the presence of an alcohol).

Although $SnOct_2$ has been accepted as food additive by the FDA (Food and Drug Administration), the toxicity associated with most tin compounds is a considerable drawback in the case of biomedical applications.

Aluminum alkoxides have also proved to be efficient catalysts for the ROP of cyclic esters. The archetypal example, namely, $Al(Oi\text{-}Pr)_3$, has been largely used for mechanistic studies. However, it has been revealed to be significantly less active than $Sn(Oct)_2$ Moreover, an induction period of a

few minutes is systematically observed with $Al(Oi\text{-}Pr)_3$. This feature has been attributed to aggregation phenomenon.[47]

For all these reasons, $Al(Oi\text{-}Pr)_3$ is much less used for the preparation of biodegradable polyesters, and especially since aluminum ions do not belong to the human metabolism and are suspected of supporting Alzheimer's disease.

Much interest has thus been devoted to zinc and yttrium derivatives as potential nontoxic catalysts. Zinc powder itself is a relatively good polymerization catalyst that is used industrially. [48] Numerous zinc salts have also been investigated, so far, the best results regarding lactide conversion and degree of polymerization were observed with zinc(II) lactate, $Zn(Lact)_2$, which is commercially available and can be readily obtained from ZnO and ethyl lactate or lactide. Notably, $Zn(Lact)_2$ allows for a better control of the molecular weight of the resulting polymers compared with zinc powder.

McLain et al. [49]. were the first to report homoleptic yttrium alkoxides, $Y(OCH_2CH_2NMe_2)_3$, prepared by reaction of alcohol with the yttrium isopropoxide cluster compound. Their yttrium alkoxide is still one of the most active initiators, with a zero order dependence on lactide concentration.

Homoleptic metal amide/alkoxide complexes are effective initiators, but they are frequently rather difficult to characterize, poorly soluble, in some cases show complex kinetics, and lack any stereocontrol. Moreover, control of the polymerization is often complicated by the complex aggregated or even cluster structures of these derivatives and by the presence of several alkoxide ligands resulting in more than one growing-chain per metallic center. [50]

To overcome these limitations, researchers have investigated heteroleptic single-site complexes of general form [LnMX], where M is central metal atom surrounded by an ancillary ligand Ln. The steric and electronic properties of the ligand adjust the bonding of the metal center to the ligand, and therefore, influence the activity and stereoselectivity of the catalyst. X is the initiating group, a nucleophilic group, which also affects the polymerization activity of the complexes. It is possible, by employing appropriate combinations of Ln with M and X, to generate efficient catalysts which can precisely control the polymerization rate, molecular weight, molecular weight distribution, comonomer incorporation, and even polymer stereochemistry in lactide polymerization. [44 51]

Some of the ligand classes for single-site homogeneous catalysts are able to coordinate various metals and thus provide a wide range of applications.

The most commonly used anionic ligand classes include bisphenolates, aminidate β-diiminates, Schiff-bases, salen and salan ligands. All these ligands present oxygen and/or nitrogen as hard donor elements.[4, 42, 43]

As single-site homogeneous catalysts several metal complexes with metals from first to fourth group, some lanthanids, as well as iron, zinc, aluminium and tin, have been investigated and a wide array of ligand frameworks has been employed, generating a library of catalysts. [42, 43]

Growing attention has been attracted by organocatalysts, such as amines, phosphines and carbenes.[38]

Beside the organic or inorganic initiator systems, it is also possible to obtain polyesters by enzymatic ring-opening polymerization. Lipase from *Pseudomonas cepacia* (lipase PC) as well as protease (proteinase K) were able to yield PLA. Due to the relatively low catalytic activity and the fact that the reaction took place only at higher temperatures, which are unusual

for enzymatic reactions, the latter described system has up to now no industrial relevance.[1]

1.3 AIM OF THIS WORK

The Ring-Opening Polymerization of cyclic esters by metal complexes *via* coordination-insertion mechanism represents the most effective and versatile method for preparing aliphatic polyesters with a good control in terms of molecular weight, composition, microstructure and stereoselectivity.

Among the large variety of species investigated, the heteroleptic metal complexes of type [LMX], in which L is an ancillary ligand and X a nucleophilic group, have been shown to be especially interesting for their high catalytic efficiency and good control.

In the development of new and efficient catalytic systems a careful ligand design and an opportune choice of the metal are crucial features.

Ideally, the presence of sterically demanding ancillary ligands could tune the electronic and steric properties of the metal center, modulate its Lewis acidity, minimize the aggregation processes and limit deleterious transesterification reactions to enhance the catalytic activity and the degree of control on polymerization process**.**

Chelation, that is, the binding of a ligand to a metal through two or more bonds, is an efficient approach to realize this.

As previously discussed, several classes of chelating ligands have been explored as ancillary ligands for stabilizing reactive metal centers of the catalytic active species.

In this context the pincer-type ligands represent an valid alternative because of their unusual abilities in the stabilization of the metal center in coordination complexes.

Typically, the so-called pincer ligands of general formula ECE comprise an o-phenylene-derived backbone and a potentially E, C, E terdentate coordinating, monoanionic array, where E is a neutral two-electron donor such as NR_2, PR_2, OR_2, while C represents the anionic donor such as a arylic carbon or amido group.

Metal complexation with pincer ligands usually occurs with formation of two five-membered metallacycles to afford complexes with a rigid and robust structure.

In the last two decades pincer ligands have been synthesized with a wide range of donor atoms and the related pincer-metal complexes have been used in a variety of applications, in particular in catalytic chemistry.

On the contrary the examples of pincer based-metal complexes as initiators in the ring-opening polymerization of cyclic esters are completely unexplored.

In this work of thesis I describe the use of new phosphido pincer-type ligands, recently reported in literature, as ancillary ligands for the synthesis of new metal complexes as catalysts for the ring opening polymerization of the cyclic esters.

This type of ligands represents an original coordination environment in which an unusual phosphido anionic donor is flanked by phosphine neutral donors. A considerable coordinative flexibility is predictable for them because the phosphido moiety is an electronically flexible donor, as it can serve as an efficient σ and possibly π donor.

Moreover, the electronic and steric characteristic of the ligands can be finely modulated by introducing different substituent groups on the neutral phosphorous atoms .

In this work, two different diarylphosphido- disubstituted-phosphine ligands have been examinated:

[Ph-PPP-H] bis(2-diphenylphosphinophenyl)phosphine ligand and

[iPr-PPP-H], bis(2-di-isopropylphosphinophenyl)phosphine ligand

(see figure below).

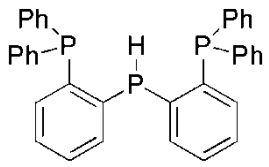

[Ph-PPP-H]

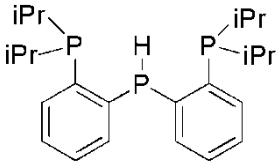

[iPr-PPP-H]

The role of the this innovative coordination environment on stability of the reactivity of different metal catalysts for the ring opening polymerization of several cyclic esters has been explored.

In general, the key parameters for the choice of metal are the polymerization control, rate and stereocontrol; further desirable features are low cost, tolerance abundance and low toxicity.

Among all metals exploited, rare-earth metal-based compounds are the most significant examples as they are very efficient catalysts for ROP of lactones due to their moderate acidity. Moreover, these compounds do not have any known toxicity.

Traditionally, zinc-based and aluminum-based complexes are also attractive initiators because they combine a very good ability in control of the polymerization reactions with relatively absence or low toxicity.

In literature examples of these metal complexes with ligands based on the hard donor elements, such as oxygen or/and nitrogen, have been largely investigated.

Differently, the use of soft donors-based ligands is rather uncommon.

In this work of thesis the synthesis of new yttrium, scandium, zinc and aluminum complexes with pincer ligands has been reported and their ability as initiators in the ring-opening polymerization of cyclic esters has been studied.

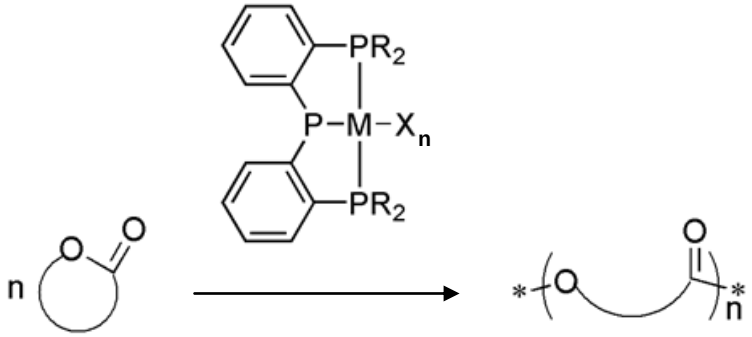

M = Y, Sc, Zn, Al

R = Ph, iPr

X = alkyl, amido, $-CH_2SiMe_3$

2 GROUP 3 METAL COMPLEXES

2.1 INTRODUCTION

In the last few years, rare-earth metal complexes emerged as very promising initiators, in view of their low toxicity, low cost, and high reactivity.[52, 53, 54]
A variety of lanthanide and group 3 metals alkoxides have been used as catalysts for ROP of cyclic ester. The first example of very efficient initiator was reported by McLain and Drysdale in 1991, [49, 55] with a complex formulated as $Y(OCH_2CH_2NMe_2)_3$. Then several rare-earth homoleptic alkoxide, $Ln(OR)_3$, have been found to be active in the polymerization of lactones and lactides.[56] Even if these homoleptic systems have shown an unprecedented high efficiency for the polymerization of cyclic esters, several drawbacks such as complicated equilibria phenomena (aggregations, ligand exchange) and multiple nuclearities have limited the control of the polymerization Efforts to obviate these problems focused on the use of supporting ligands designed to control the structure of the complexes and their polymerization reactivity. Based on the evolution of the group 3 and lanthanide organometallic chemistry, two types of complexes were independently studied: on one hand, organolanthanide metallocenes, which were earlier studied, [57] (Fig.2.1) and on the other hand, lanthanide complexes supported by non-cyclopentadienyl ligands, which appeared later on.[52, 53, 54] However, except Okuda's bimetallic complexes,[57a] no Cp-based

group 3 complexes have been reported to be active for the ROP of LA and those remain limited to the synthesis of polycaprolactone.[57b]

Fig.2.1: Representative examples of organolanthanide metallocenes.[6]

In an attempt to enhance and control this reactivity, recent research efforts have been directed toward substitution of the cyclopentadienyl framework by other anionic ligand systems.

Because of the hard Lewis acidic nature of the Group 3 metal ions, ligands based on the hard donor elements oxygen and nitrogen have been the most explored. Recently, a number of groups have reported single-site yttrium and scandium amide or alkoxide initiators bearing dianionic phenoxy based ligands, some of which showed high activity and good stereocontrol.[58, 59]

On the contrary, the examples of Group 3 metal complexes bearing ancillary ligands which include soft donors are quite rare (Fig.2.2).

Ma and Okuda described Group 3 metal complexes supported by ω-dithiaalkanediyl bridged bis(phenol)s, which showed high activity and heteroselectivity in the polymerization of D,L-lactide.[60] Remarkable

activities in the ROP of lactide were recently reported for novel bis(oxo/thiophosphinic)diamido yttrium complexes.[61]

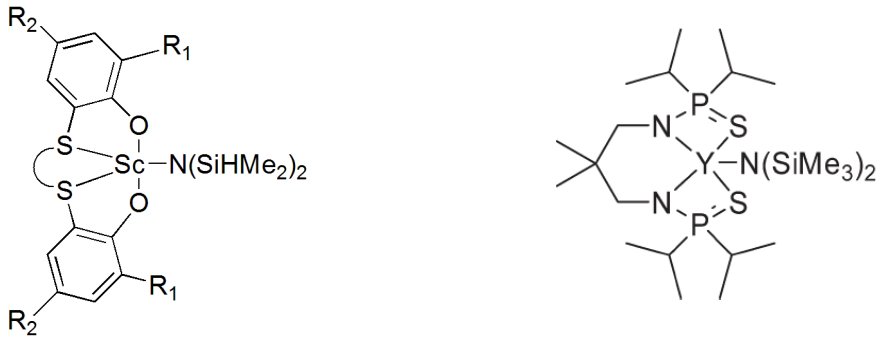

Fig.2.2: On the left ω- dithiaalkanediyl bridged bis(phenol) scandium complex; on the right bis(oxo/thiophosphinic)diamido yttrium complex

With this in mind, in this work of thesis the use of phosphorous- based ligands (*PPP*) as soft donors for supporting Group 3 metals complexes has been explored. These studies are interesting since softer donors, such as phosphorous and sulfur, could mediate the Lewis acidity of the metal center with remarkable consequences on the catalytic performances.

Here it is reported the synthesis of new yttrium and scandium alkyl complexes supported by tridentate phosphido-diphosphine ligands [62] and the study of their catalytic activity as initiators of ROP of polar monomer. .

2.2 RESULTS AND DISCUSSION

2.2.1 Synthesis and Characterization of Complexes

The phosphido-diphosphine ligands [(*o*-$C_6H_4PR_2)_2$P-H; R = Ph (**L1-H**); R = iPr (**L2-H**), Scheme 2.1] were synthesized according to previously published procedures.[62]

The reactions of **L1-H** or **L2-H** with 1 equivalent of the yttrium tris(alkyl) complex $Y(CH_2SiMe_3)_3(THF)_2$ took place at room temperature in THF. The reaction mixtures were kept stirring for 1 h to afford the yttrium bis(alkyl) complexes **1** and **3**. [(*o*-$C_6H_4PR_2)_2PM(CH_2SiMe_3)_2(THF)_n$] [M = Y, R = Ph (**1**), R = iPr (**3**)] as the only products in quantitative yields. (95– 97%; Scheme .2.1). Removal of the volatiles under reduced pressure yielded orange solids that were washed with a minimum amount of cold hexane to obtain the analytically pure complexes **1** and **3** which were characterized by NMR spectroscopy and elemental analysis.

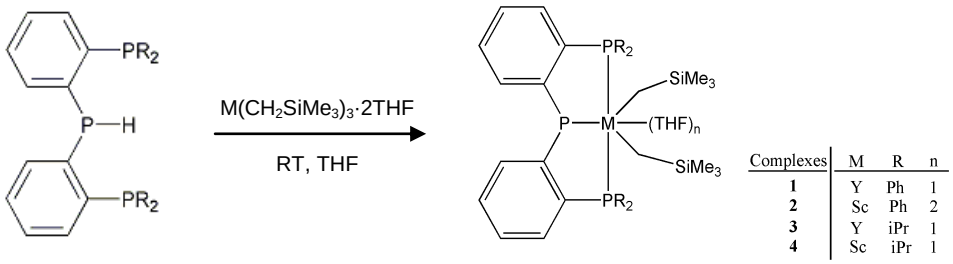

Complexes	M	R	n
1	Y	Ph	1
2	Sc	Ph	2
3	Y	iPr	1
4	Sc	iPr	1

Scheme 2.1: Synthetic route to complexes **1-4**

Solution ^{1}H and ^{31}P NMR studies of the reactions performed in C_6D_6 indicated that the neutral ligands **L1-H** and **L2-H** were deprotonated by one metal alkyl of $Y(CH_2SiMe_3)_3(THF)_2$ with the release of 1 equivalent of tetramethylsilane. NMR and elemental analysis were consistent with structures of one *PPP* pincer ligand, two CH_2SiMe_3 groups, and one coordinated THF molecule at the metal center.

The ^{1}H NMR spectrum of complex **1** showed sharp resonances for all protons. The methylene protons of $Y(CH_2SiMe_3)_2$ appeared as a doublet at δ = 0.11 ppm (J_{Y-H} = 3 Hz), different from the singlet resonance at δ = -0.71 ppm in the yttrium tris(alkyl) precursor. In the $^{31}P\{^{1}H\}$NMR spectrum the resonances, corresponding to the neutral and anionic phosphorous donors, are shifted downfield from the corresponding ligand precursor. A single resonance was observed for the two equivalent neutral phosphine donors, the chemical shift (-1.04 ppm) and $^{1}J_{Y-P}$ values (29 Hz) being consistent with a *mer* arrangement of the ligand around the metal center.(Fig.2.3)

NMR analysis showed that complex **3** exhibits a structure similar to that of complex **1**.

The homologous scandium complexes have been synthesized following a synthetic procedure similar to that described above. The reactions between $Sc(CH_2SiMe_3)_3$.$(THF)_2$ and 1 equivalent of the proligands **L1-H** or **L2-H** proceeded smoothly at room temperature via metal alkyl abstraction and generated complexes **2** and **4** [$(o\text{-}C_6H_4PR_2)_2PM(CH_2SiMe_3)_2(THF)_n$] [M = Sc, R = Ph (**2**), R = iPr (**4**)], respectively, in high yield (>97%; Scheme 2.1).

The ^{1}H NMR spectra showed that the resonances of the methylene protons of $Sc(CH_2SiMe_3)_2$ shifted downfield to δ = 0.72 ppm for **2** and to 0.16 ppm for **4** compared with the scandium trisalkyl complex (δ = -0.20 ppm).

As already discussed for complexes **1** and **3**, the scandium complexes **2** and **4** showed highly symmetric structures in solution. The ^{1}H NMR spectrum for the isopropyl substituted complex **4** showed a single resonance for the protons of the isopropyl groups and two doublet of doublets for the diasterotopic methyls' protons of the isopropyl groups. In the ^{31}P{^{1}H}NMR spectra of **2** and **4**, the two equivalent neutral phosphorous donors (at -0.75 and 14.67 ppm, respectively), which are diagnostic of a *mer* arrangement of the phosphido ligands appeared as doublets ($J_{P\,P}$ = 44–50 Hz

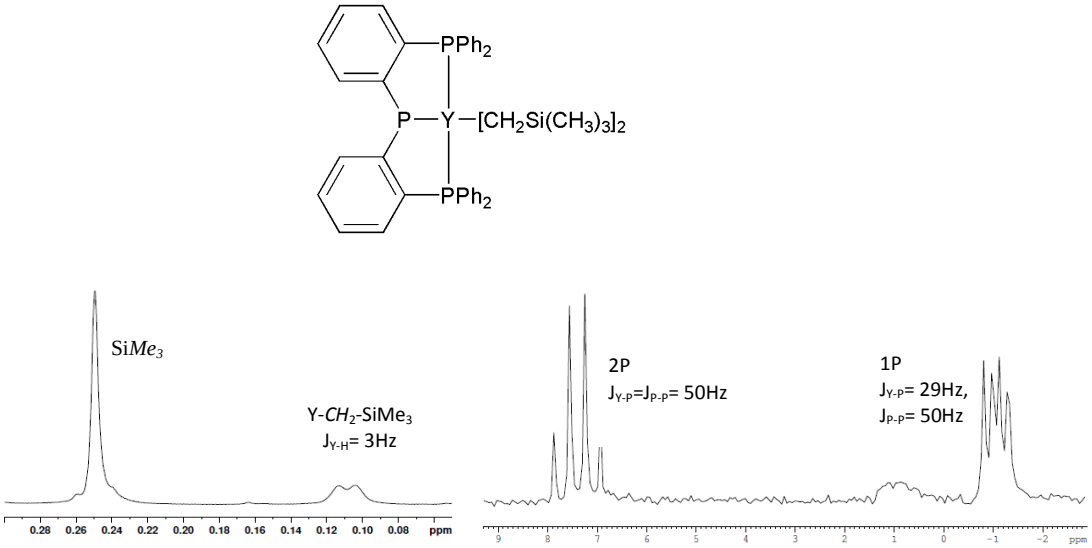

Figure 2.1: Aliphatic region of ^{1}H spectrum (on the left) and ^{31}P spectrum (on the right) of complex **1**

2.2.2 Ring-Opening Polymerization of ε-Caprolactone (ε-CL)

The phosphido pincer complexes **1–4** were tested as initiators for the ROP of ε-CL (Scheme 2.2); the results are summarized in Table 1

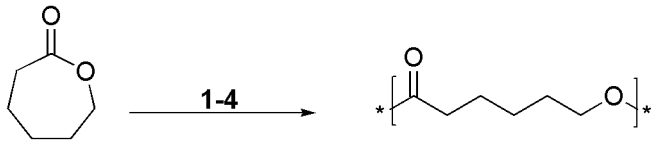

SCHEME 2.2: Ring-opening polymerization of ε-caprolactone initiated by complexes **1-4**

The polymers obtained were characterized by ^{1}H NMR and GPC analyses.
All complexes **1–4** resulted efficient initiators for the ROP of ε-CL. They showed exceptional ability to promote quantitative conversion of high amount of monomer under mild polymerization conditions (low concentration of catalyst at room temperature) with very high TOF (0.8– 4.4 x 10^4 mol_{CL}/mol_I h, runs 1–4, Table 2.1), among the highest reported in the literature.[52d]

Table 2.1 . Ring-opening Polymerization of ε-CL initiated by complexes **1-4.**

[a]Run	Cat	$[CL]_0/[I]_0$	Time (min)	[b] Conv (%)	[c]$M_{n\ GPC}$ (kDa)	[d]$M_{n\ calc}$ (kDa)	PDI
1	**1**	1000	1	73	86.4	83.2	1.40
2	**2**	1000	5	80	69.5	91.2	1.34
3	**3**	1000	5	91	61.4	134.7	1.46
4	**4**	1000	5	67	63.7	76.4	1.45
5[e]	**4**	1000	30	75	92.7	85.5	1.61
6	**1**	1000	30	100	132.8	114.1	1.71
7	**1**	1000	60	100	98.0	114.1	1.82
8[f]	**1**	3000	20	98	125.0	335.6	1.90
9[f]	**4**	2500	30	100	103.0	285.0	1.60

[a]All reactions were performed using 1 μmol of catalyst in 2 mL of toluene at room temperature. [b]Conversion of ε-CL as determined by ^{1}H NMR spectral data. [c] Experimental Mn and Mw/Mn values determined by GPC in THF against polystyrene standards and corrected using the Mark-Houwink factor [d] Mn_{calc} =114,14 x ($[\varepsilon\text{-CL}]_0/[I]_0$) x conversion ε-CL. [e] Solvent =2 mL of THF. [f]5mL of toluene

The catalytic activity depends on both the nature of the metal center and the structure of the ancillary ligand. Yttrium initiators **1** and **3** showed higher activities than the analogues scandium complexes **2** and **4**, according with literature data reporting that the complexes of smaller rare earth metals normally show lower activities. As a matter of fact, the decrease in ionic radii from Y → Sc and the consequent longer steric crowding created by the ancillary ligand around the active metal centre should disadvantage the coordination of the incoming ε-CL monomer, which is a necessary step required before ring-opening. The higher activity observed for the phenyl substituted complexes (run 1 vs. 3 and run 2 vs. run 4, Table 2.1) can be ascribed to the lower electron donating character of the phenyl groups and to the consequent increase of the Lewis acidity of the metal centre.

The polymerization medium played an important role in influencing the catalytic activity. A lower activity was observed when polymerization

experiments were performed in THF as a consequence of the presence of a competing coordinating solvent (run 4 vs. run 5, Table 2.1). Similar effects of the solvent in the polymerization rates promoted by Group 3 metal precursors have been often observed. [63]

These catalysts were able to afford high molecular weight polycaprolactones. The molecular weights obtained in entry 6, Table 2.1, by using 1 μmol of the yttrium initiator and 1000 equiv of the monomer are among the highest molecular weights observed for rare-earth metal initiated ε-CL polymerization. [64] Moreover, the M_{nGPC} values were in good agreement with the theoretical ones ($M_{n\ calc}$) assuming the growth of one polymer chain per metal center, (Table 2.1) implying that **1–4** behave as single site catalysts. A good molecular weight control was demonstrated by a linear increase in Mn with time and conversion (Table 2.2, Fig. 2.4).

Table 2.2. Ring Opening Polymerization of ε-CL promoted by **4** Relationship between time and Mn

Run	$[CL]_0/[I]_0$	Time (min)	Conv.[a] %	$M_{n\ GPC}$[b] (kDa)	$M_{n\ calc}$[c] (kDa)	PDI[b]
10	1000	10	36	36.7	41.0	1.48
11	1000	15	63	57.9	67.3	1.51
12	1000	20	67	65.6	73.4	1.53
13	1000	25	73	76.0	83.2	1.47
14	1000	30	87	99.4	96.9	1.48

All reactions were performed with **[**CL]= 0.5 M in 4 mL of toluene, [CL]/**4**=1000 , at 20°C. [a]Conversion of ε-CL as determined by ^{1}H NMR spectral data. [b] Experimental Mn and Mw/Mn values determined by GPC in THF against polystyrene standards and corrected using the Mark-Houwink factor of 0,58.
[c] Mn,calc =114,14 x ([ε-CL]/[I]) x conversion ε-CL .

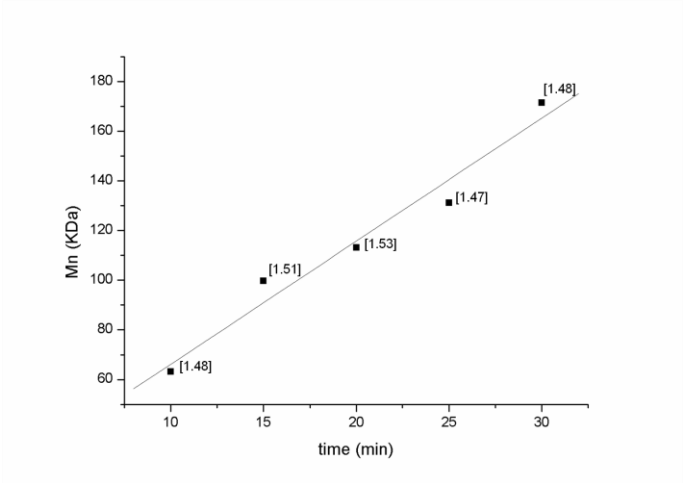

Figure 2.4: Plot of number-averaged molecular weights, Mn (kDa), and PDI values versus time (minutes) for PCLs produced by catalyst **4**.

The PDI values (1.34–1.90) are typical for rare-earth initiated ring-opening polymerization of ε-CL and, as reported in the literature, become broader when the Mn value decreases for longer reaction time, as a consequence of frequent transesterification reactions occurring after the monomer is totally consumed (cf. runs 1, 6, and 7, Table 2.1).

The same consequences are observed when the polymerization reaction is performed with a high monomer/initiator ratio (up to $[CL]_0/[I]_0 = 2000$, runs 8 and 9, Table 2.1). This may be due to bulk-transfer properties, resulting in an increase in chain-termination mechanisms as the concentration of monomer is increased. [65]

To determine the nature of the active species and of the initiating groups, a low molecular weight polymer sample was prepared and analyzed by ^{1}H NMR spectroscopy.

In the ^{1}H NMR spectrum of this sample, a triplet at 3.67 ppm, corresponding to the methylene protons adjacent to the terminal hydroxyl function of the polymer chain, was observed. An additional resonance, diagnostic for the presence of -CH_2SiMe_3 end group, was observed at 0.07 ppm. These observations supported the hypothesis that the reaction proceeds with initiation by the alkyl groups of the initiator and the oxygen-acyl bond cleavage of the cyclic ester.

To investigate the mechanism of insertion/coordination occurring during the polymerization of ε-CL I selected the more active yttrium complex **1** for more in-depth kinetic investigations, via ^{1}H NMR spectroscopic analysis.

The reaction kinetic features a pseudofirstorder dependence in ε-CL concentration, as reported in Figure 2.5: the semilogarithmic plot of ln($[\varepsilon\text{-CL}]_0/[\varepsilon\text{-CL}]_t$) versus time was linear with a slope of $(3.0 \pm 0.1) \times 10^{-2}$ s^{-1}.

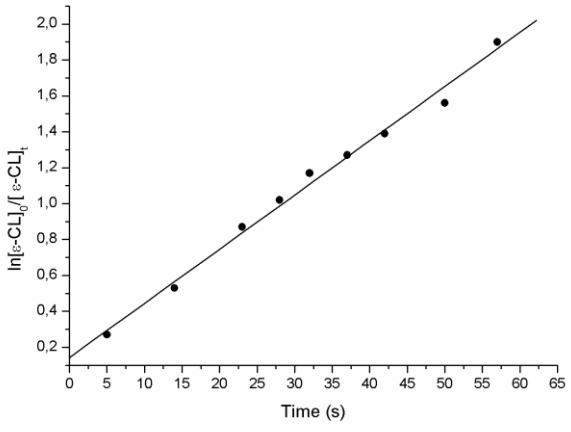

Figure 2.5. Pseudofirst-order kinetic plot for ROP of ε-CL promoted by **1**.
Pseudofirst-order rate is $(3.0 \pm 0.1) \times 10^{-2}$ s^{-1} ($[\varepsilon\text{-CL}]_0 = 0.5$M; $[\varepsilon\text{-CL}]_0/[I]_0 = 1000$; toluene as solvent;
T = 25°C).

2.2.3 Ring-Opening Polymerization (ROP) of *L*- and *D,L*-Lactide

The yttrium and scandium complexes **1–4** were assessed in the polymerization of *L*-LA and *rac*-LA.

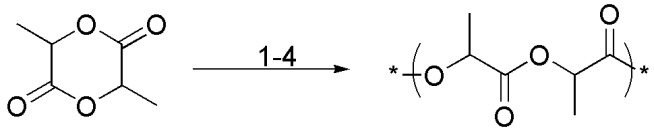

Scheme 2.3: Ring-opening polymerization of lactide initiated by complexes **1-4**

All explored complexes resulted active; representative results are reported in Table 2.3. The observed activities for yttrium initiators are high and comparable with other highly active bis(alkyl)-yttrium initiators bearing N,O multidentate ligands. [66] Both yttrium complexes **1** and **3** allowed almost quantitative monomer conversions in about 15 min (runs 1-4, Table 2.3).
The scandium complexes **2** and **4** showed lower catalytic activities than those obtained with the analogous yttrium complexes (runs 5–7, Table 2.3). This is coherent with the data reported in paragraph 2.2.2 about the ROP of ε-CL.

Table 2.3. Ring Opening Polymerization of *L*-Lactide initiated by complexes **1-4**

Run[a]	Cat	Time (min)	Solvent	Conv (%)	$M_{n(expt)}$[b] (kDa)	$M_{n(calc)}$[c] (kDa)	PDI
1	**1**	15	THF	79	21.5	23.1	1.25
2	**3**	15	THF	65	15.9	18.7	1.25
3	**1**	15	toluene	93	27.9	26.8	1.50
4	**3**	15	toluene	82	20.4	23.6	1.47
5	**2**	1200	toluene	23	6.4	6.6	1.50
6	**4**	1200	THF	38	8.1	10.9	1.20
7	**4**	1200	toluene	27	8.3	7.8	1.22
8[d]	**1**	180	THF	100	39.4	144.1	1.66
9[e]	**1**	15	-	69	10.6	19.9	1.44
10[e]	**3**	15	-	50	7.2	14.4	1.25
11[e]	**2**	60	-	44	3.5	12.6	1.31
12[e]	**4**	60	-	49	3.1	14.4	1.20

[a]All reactions were carried out at room temperature with $[L\text{-}LA]_0$ = 1 M and $[L\text{-}LA]_0/[I]_0$=200. [b]Experimental M_n and M_w/M_n values determined by GPC in THF using polystyrene standards and corrected using the Mark–Houwink factor. [c]Calculated M_n values considering one polymer chain per metal center. [d] Reaction carried out at RT with $[L\text{-}LA]_0$= 1M and $[L\text{-}LA]_0/[I]_0$=1000. [e]130 °C, solvent free, L-LA=0.288g, $[L\text{-}LA]_0/[I]_0$=200.

To obtain more insight about the nature of the real initiators of ROP of the lactide, a study of the structure of the chain end groups was performed. For this scope a polymerization experiment at low LA to initiator molar ratio ($[L\text{-}LA]_0/[I]_0$ = 100 : I = 2) was carried out. The polymerization reaction was performed in deuterated benzene and followed by NMR spectroscopy. The ^{1}H NMR analysis of the reaction mixture at about 70% of the monomer conversion showed two resonances of the same intensity, at 0.23 and 0.06 ppm, attributable to the CH_2SiMe_3 groups bounded to the metal center and to the growing chain, respectively.(Figure 2.6) [67]

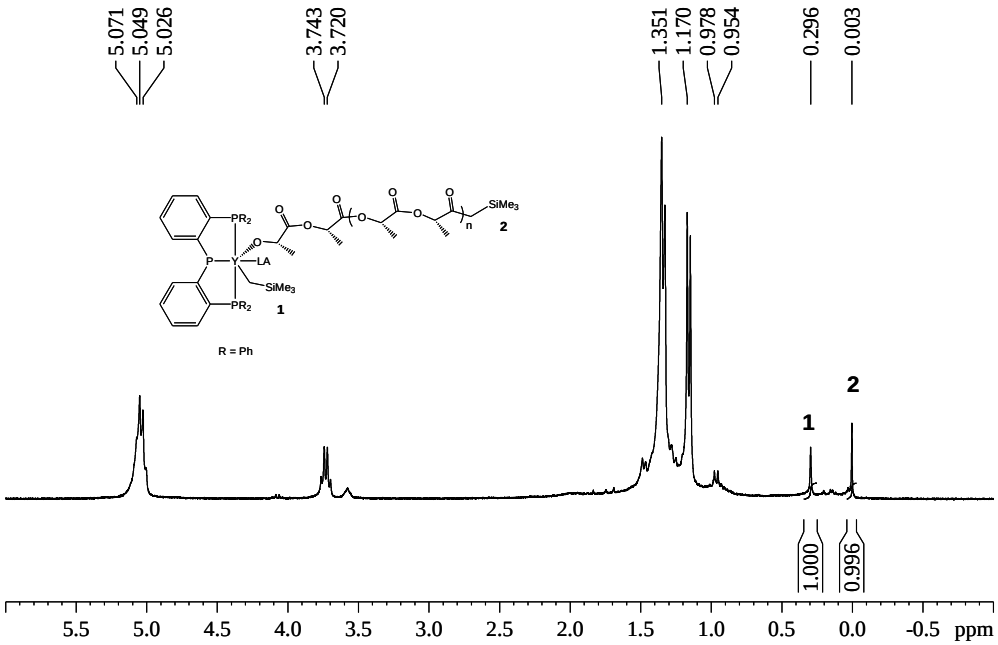

Figure 2.6. ^{1}H NMR spectrum of polymerization reaction of L-LA promoted by **1**. ($[L\text{-}LA]_0$ = 0.5 M, $[L\text{-}LA]_0/[I]_0$ = 100, rt, C_6D_6, polymerization time 2 mins, conversion 74%)

This observation is a clear evidence that the polymerization reaction proceeds via a coordination/insertion mechanism. The acyl oxygen atom of the monomer first coordinates to the metal center and this is followed by nucleophilic attack of the alkyl group on the carbonyl carbon atom with subsequent cleavage of the acyl-oxygen bond (Scheme 2.4).

It is also demonstrated that only one of the initiating groups at the metal center is involved in the polymerization reactions.

The nature of the initiating group was also confirmed by MALDI-TOF-MS analysis of oligomers formed by **1** at $[L\text{-}LA]_0/[I]_0$ = 20. The distribution of molecular weights showed that the most intense peaks are consistent with

linear both even-membered and odd-membered oligomers of the type H-$[OCH(CH_3)C(=O)]_{2n}$-CH_2SiMe_3.(Fig 2.7)

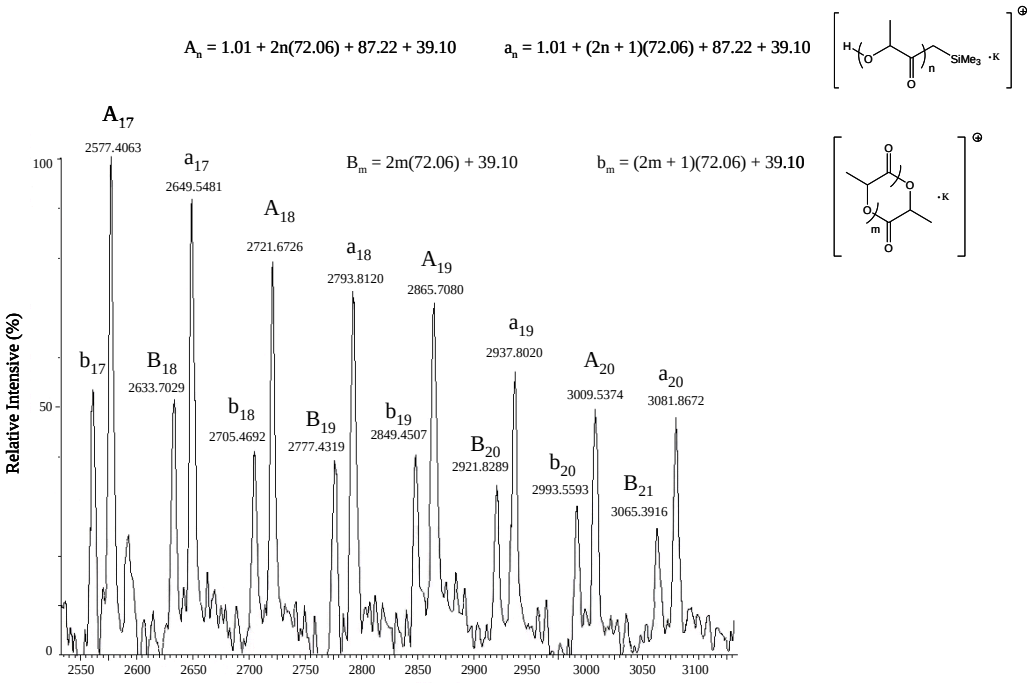

Figure 2.7. MALDI-TOF mass spectrum of the oligomer of L-lactide using **1** as initiator (doped with K+). Conditions: $[L\text{-}LA]_0$ = 0.1 mM, $[L\text{-}LA]_0/[I]_0$ = 20, RT, THF, 15 mins.

The MALDI-TOF-MS analysis also revealed the presence of cyclic oligomers arising from intramolecular transesterification processes (Scheme 2.4).

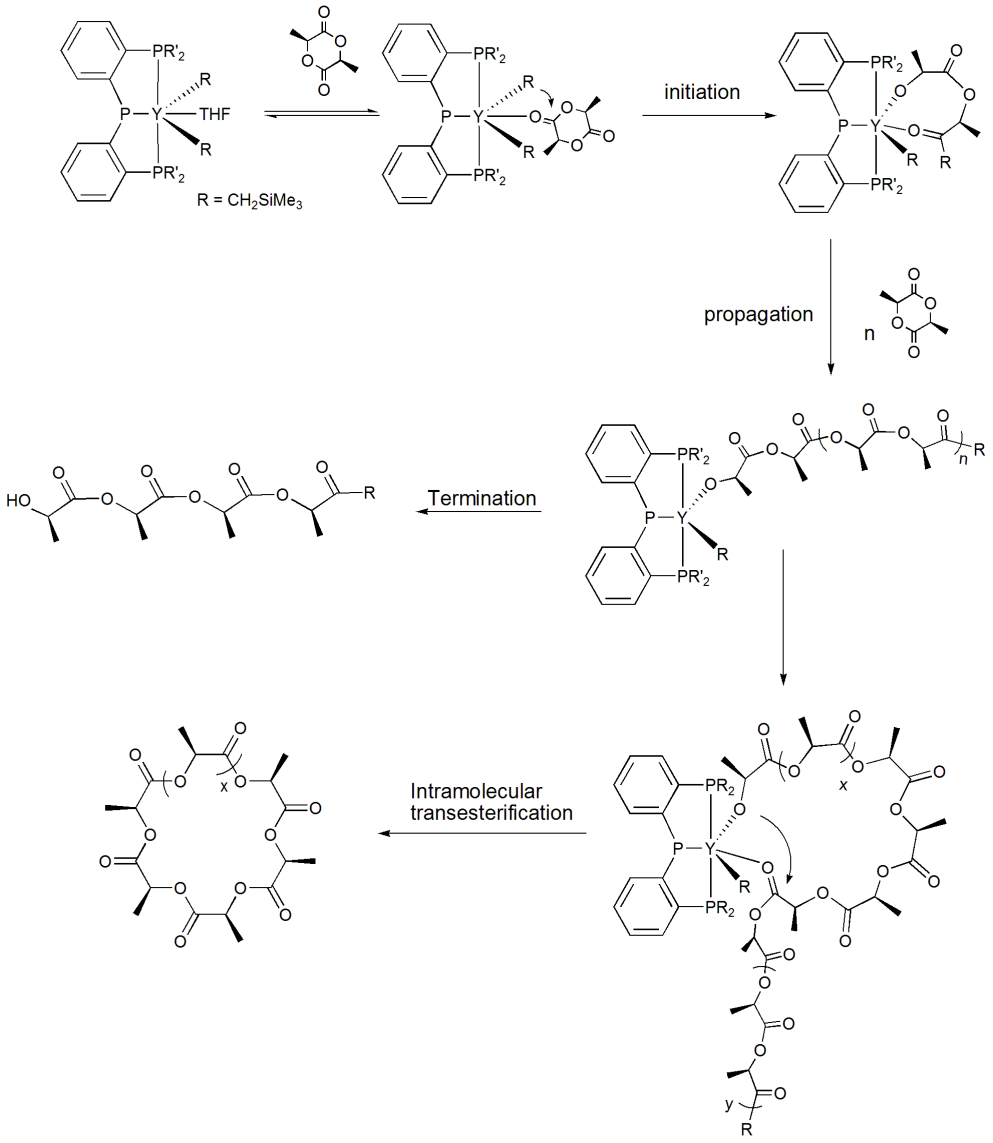

Scheme 2.4: Polymerization mechanism of L-LA

To investigate the possibility to obtain high molecular weight polymers a polymerization run with **1** and 1000 equiv of monomer was performed (run 8, Table 2.3). Remarkably high conversion up to 99% of monomer to PLA was achieved within 3 h using relatively low concentration of the initiator demonstrating that high conversion of the monomer can be obtained. The Mn experimental value is lower than the theoretical one and the molecular weight distribution is quite large. These observations suggest that, under these polymerization conditions, collateral transesterification reactions could be more frequent.

The more active yttrium complexes were selected for more in-depth kinetic investigations , *via* ^{1}H NMR spectroscopic analysis.

For both catalysts the reaction kinetics feature a pseudofirst-order dependence in LA concentration, as reported in Figure 2.8: the semilogarithmic plots of $\ln([\text{L-LA}]_0/[\text{L-LA}]_t)$ versus time were linear with a slope of (1.1 ± 0.1) x 10^{-3} and (3.0 ± 0.3) x 10^{-4} s^{-1} for **1** and **3**, respectively.[68]

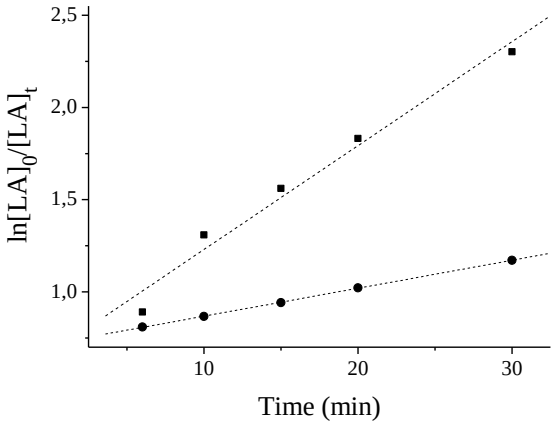

Fig. 2.8: Pseudofirst-order kinetic plots for ROP of L-LA promoted by 1 (■) and 3 (●). Pseudofirst-order rate constants are(1.1 ± 0.1) x 10^{-3} and (3.0 ± 0.3) x 10^{-4} $s^{-}1$ for 1 and for 3, respectively. ($[\text{L-LA}]_0$= 1M; $[\text{L-LA}]_0/[\text{I}]_0$= 200; THF as solvent; T= 25 °C)

The number-average molecular weight ($M_{n(expt)}$) of the resultant PLAs by **1** was found to increase linearly with monomer conversion (runs 13-18, Table 2.4, Fig. 2.9). Moreover, the $M_{n(expt)}$ values were in good agreement with the theoretical ones (Mn(calc)) assuming growth of one polymer chain per Y-initiator (Table 2.4).

Table 2.4. ROP of *L*-Lactide initiated by complexes **1**
Effect of the time/conversion

Run[a]	Time (min)	Conv (%)	$M_{n(expt)}$[b] (kDa)	$M_{n(calc)}$[c] (kDa)	M_w/M_n
13	1	19	8.7	5.8	1.27
14	3	40	14.0	11.5	1.22
15	6	60	17.0	17.3	1.28
16	10	73	19.8	21.3	1.25
17[d]	15	79	21.5	23.1	1.25
18	70	92	25.7	26.5	1.20

[a]All reactions were carried out at room temperature with $[L\text{-}LA]_0$ = 1 M and $[L\text{-}LA]_0/[\mathbf{1}]_0$=200, in THF. [b]Experimental M_n and M_w/M_n values determined by GPC in THF using polystyrene standards and corrected using the Mark–Houwink factor. [c]Calculated M_n values considering one polymer chain per metal center. [d]Run 1 in Tab.3.

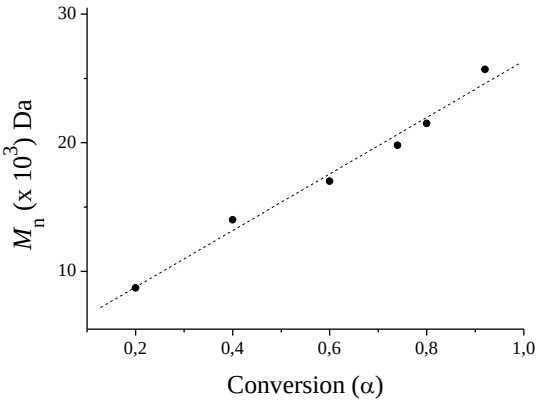

Figure 2.9: Plot of Mn versus monomer conversion (determinated by ^{1}H NMR) using **1** for L-LA polymerization

The small deviation observed in the early stages of the polymerization suggests that the initiation step is slow with respect to propagation, and this can be correlated to the low initiation efficiency of the alkyl group. In fact, it is commonly observed that alkyl and amido initiators such as -CH_2SiMe_3, -$N(SiMe_3)_2$, and -$N(SiHMe_2)_2$ are less efficient initiating groups for the ROP of lactide than isopropoxo initiating groups, which produce PLAs of predictable molecular weight and with narrower molecular weight distributions. [69]

The efficient control on the molecular weights of the produced PLAs was also expressed by the linear dependence of Mn versus the monomer-to-initiator ratio $[L\text{-}LA]_0/[I]_0$ in the feed, see Table 2.5, as illustrated in Figure 2.10

Table 2.5. Ring Opening Polymerization of L-Lactide initiated by complex **1**. Effect of the monomer-–to-initiator ratio

Run[a]	**Time min**	**$[L\text{-}LA]_0/[I]_0$**	**Conv %**	**$M_{n(expt)}$**[b] **(kDa)**	**$M_{n(calc)}$**[c] **(kDa)**	**M_w/M_n**
19	15	100	84	14.9	12.1	1.27
20	15	200	85	25.8	24.5	1.23
21	30	300	80	36.7	34.6	1.25
22	60	400	82	42.9	47.3	1.27
23	60	500	78	46.9	56.2	1.26

[a]All reactions were carried out at room temperature with $[I]_0$ = 5 mM in THF (2 mL). [b]Experimental M_n and M_w/M_n values determined by GPC in THF using polystyrene standards and a correction corrected using the Mark–Houwink factor of 0.58. [c]Calculated M_n values considering one polymer chain per metal center.

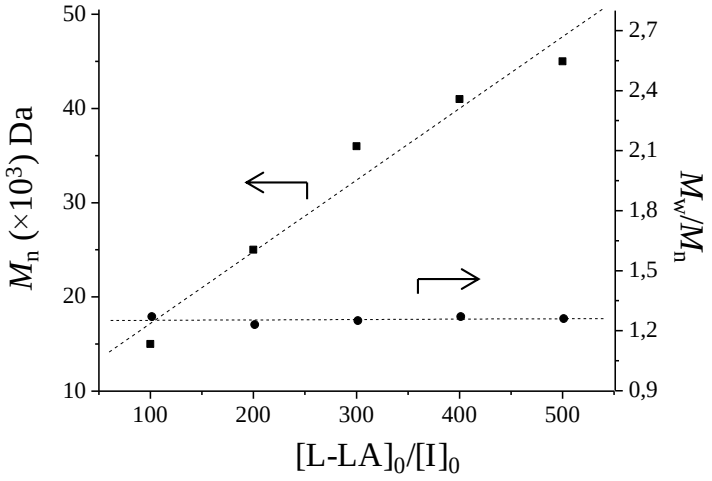

Fig. 2.10: Plot of number-averaged molecular weights Mn (■) and polidispersity indexes Mw/Mn (●) versus monomer-to-initiator ratio $[L\text{-}LA]_0/[I]_0$ for catalyst 1. ([1] = 5 mM, $[L\text{-}LA]_0/[I]_0$ = 100, 200, 300, 400, 500; THF as solvent; T = 20 °C).

All the PLAs obtained by **1** and **3** showed monomodal molecular weight distributions with narrow Mw/Mn ratio ranging from 1.25 to 1.27, indicative of a single-site character. Although these values are somewhat higher than those expected for a purely living polymerization (Mw/Mn < 1.1), the overall results are consistent with a ‘‘controlled-living’’ polymerization model. The deviation observed is due to the intermolecular and intramolecular transesterification processes as observed by the MALDI-TOF-MS analysis. These phenomena are frequently observed during ROP of LA promoted by Group 3 metal-based complexes.[58,68,69]

The homonuclear decoupled ^{1}H NMR spectra of the PLAs obtained by **1–4** showed that isotactic PLAs were produced from *L*-LA, suggesting that no epimerization side reactions occurred, (Fig. 2.11)

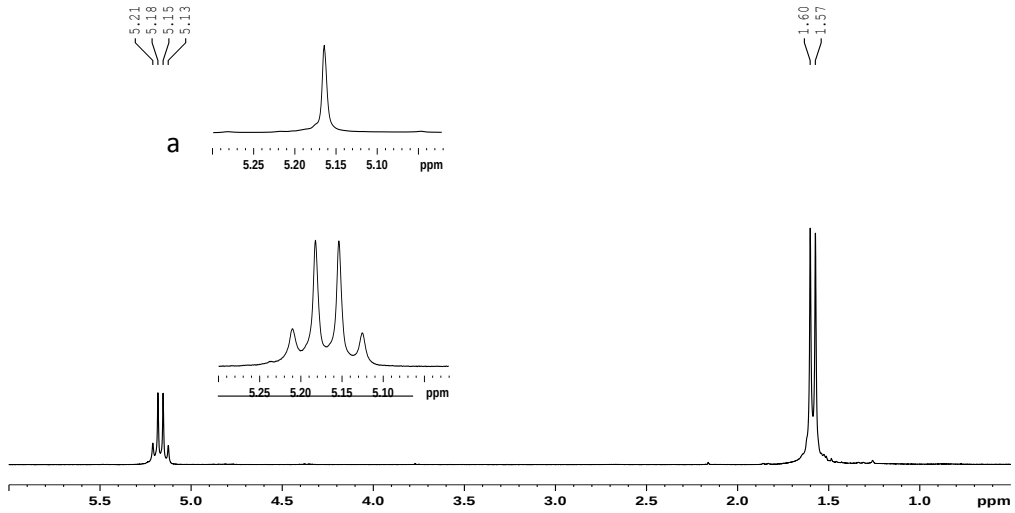

Fig 2.11. ^{1}H NMR spectrum of polylactyde (CDCl3, RT, 400MHz). The inserted figure (a) shows the methine resonance in the homonuclear decoupled 1H NMR of the same sample.

Polymerization of *rac*-LA was explored to evaluate the stereospecificity of the polymerization. Initiators **1** and **3** showed conversions of *rac*-LA in THF solution at room temperature similar to those obtained for polymerizations of *L*-LA. NMR analysis of the produced poly-*rac*-LAs revealed that the microstructure is slightly heterotactic (Pr = 0.63 and 0.64 for **1** and **3**, respectively).[58,70]

The same was observed in the polymerizations of *rac*-LA promoted by the scandium complexes **2** and **4**, the activity was analogous to that reported for the enantiopure monomers and the homonuclear decoupled ^{1}H NMR of the methine region of the PLA samples revealed a slightly heterotactic microstructure (Pr = 0.60 and 0.62 for **2** and **4**, respectively).

As previously observed for ε-CL polymerization promoted by rare earth catalyst systems, the solvent was found to have a strong influence on the catalyst performance.[9a,14] In toluene, higher catalytic activities (runs 1

versus 3 and 2 versus 4, Table 2.3) were observed and the PLAs produced showed monomodal and slightly broader molecular weight distributions.

A challenging target in the field of ring opening polymerization is the development of thermally robust initiators for *solvent-free* LA polymerization.

As the pincer ligands should impart a fair stability to metal complexes, I was interested in the investigation of the catalytic behavior of **1–4** under solvent-free polymerization conditions at higher temperature (T = 130 °C). For both yttrium complexes **1** and **3**, satisfactory monomer conversions were reached in short polymerization time (runs 9 and 10, Table 2). The analysis of molecular weights and molecular weight distributions indicated that complexes **1–3** are able to promote ROP of LA in such drastic conditions with a controlled manner. It is worth noting that the $M_{n(expt)}$ values were half of the theoretical ones ($M_{n(calc)}$) assuming growth of one polymer chain per Y-initiator. Thus, in absence of solvent and at high temperature, both alkyl groups on the yttrium center are able to initiate the polymerization.

The ^{1}H NMR analysis of the PLAs obtained showed, as expected, resonances diagnostic for the presence of $-CH_2SiMe_3$ end groups and resonances at 4.37 and 2.68 ppm that account for the presence of $HOCH(CH_3)C(=O)-$ end groups formed by the hydrolysis of the metal-chain bonds. The presence of these end groups indicates that a classical coordination/insertion mechanism is also operative for the solvent free polymerizations. These observations suggest that phosphido pincer ligands appear to be efficient ligands in stabilizing the oxophilic yttrium and scandium centers preventing, in addition, the decomposition of the complexes in drastic reaction conditions.

2.2.4 "Living-Immortal" Ring Opening Polymerization

The formation of macromolecules with controlled molecular weight is of primary interest and importance with specific physical and mechanical properties.

ROP reactions promoted by organometallic complexes often proceed in a "living controlled" fashion.[71] As depicted in Scheme 2.5, in such "classical living" ROP, there are (ideally) as many growing macromolecules as the total amount of active sites available from the catalyst molecule (therefore named "initiator"). This approach has inherent limitations and pitfalls: low catalytic productivity and potentially large contamination of the polymer with catalyst residues.

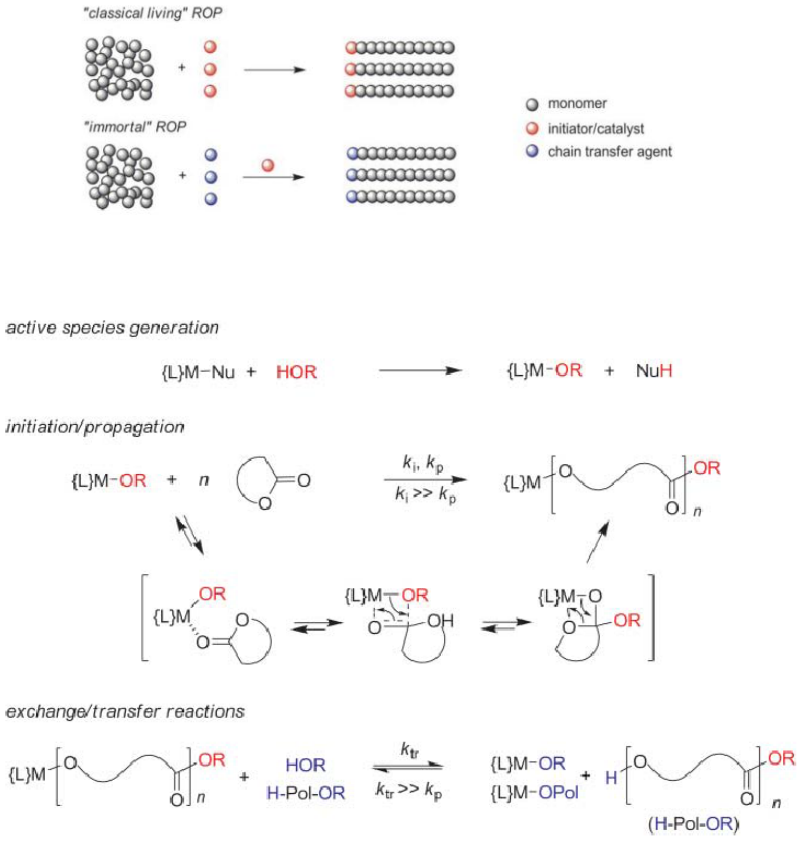

Scheme 2.5: Illustration of the distinction between "classical living" and "immortal" ROP process (on the left) and representation of coordination/insertion mechanism operative in the "immortal" ROP of cyclic esters (on the right). Scheme by: J-F. Carpentier et al.,*Dalton Trans.* **2010**, 39, 8363-8376.

The so-called "immortal" ROP (hereafter referred to as "iROP"), initially named as such by Inoue,[72] provides an efficient alternative to "classical living" ROP. This process involves a bicomponent system made of (*i*) a catalyst and (*ii*) an external nucleophile that acts simultaneously as the initiator and chain transfer agent (CTA). As shown in Scheme 2.5, the

number of growing polymer chains in an iROP exceeds the number of catalyst molecules (*e.g.*, a metallic species) used and is equal to the initial amount of CTA introduced. Hence, the process becomes "truly catalytic" with respect to both the monomer (as in a "classical living" ROP) *and* the polymer chains. In a general context of green and sustainable chemistry, the "catalytic" iROP strategy thus appears highly attractive, especially if performed in solvent-free conditions (bulk process).

With the aim to achieve a "living-immortal" polymerization and, at the same time, to optimize the degree of control on the ROP of cyclic esters, I tested the catalytic behavior of complexes **1**-**4** in presence of 2-propanol.

The polymerization data discussed in the previous paragraphs showed relatively high values of the PDI indexes (Tab. 2.1-2.5) in the polymerization of *L*-Lactide and *ε*-Caprolactone as a consequence of intramolecular transesterification processes occurring during the polymerization reactions, a phenomenon that is often observed in the ROP of cyclic esters promoted by Group 3 metal initiators. In fact, it is commonly observed that alkyl and amido initiators such as $-CH_2SiMe_3$ - $N(SiMe_3)_2$, and $-N(SiHMe_2)_2$ are less efficient initiating groups for the ROP of cyclic esters than isopropoxo initiating groups, which produce polymers of predictable molecular weight and with narrower molecular weight distributions.

To circumvent these limitations, suitable alkoxide initiators for polymerization can be generated *in situ* by alcoholisis of alkyl precursors with 2-propanol, to form initiating groups that efficiently mimic the propagating groups of the presumed active species. At the same time, the alcohol present in excess acts as a chain transfer agent allowing to achieve

"living-immortal" polymerizations which produce several polymer chains per metal center with a more efficient control on the molecular weights.

To this purpose, ε-CL was polymerized by complexes **1–4** in combination with different amounts of 2-propanol (Table 2.6 and Fig. 2.12). From the results listed in Table 2.5 (runs 1-6) emerged that the ratio of 2-propanol to the metal complex **1** had a crucial influence on the molecular weight of the obtained

polymers and their polydispersity index, whereas the polymerization rate was not significantly affected (run 6, Table 2.6).

Table 6. Ring-opening Polymerization of ε-CL initiated by complexes **1-4.**Effect of 2-propanol

[a]Run	Cat	$[iPrOH]_0/[I]_0$	[b] Conv. (%)	[c]$M_{n\ GPC}$ (kDa)	[d]$M_{n\ calc}$ (kDa)	PDI
1	**1**	2	100	30.0	43.9	1.29
2	**1**	4	100	21.1	23.3	1.13
3	**1**	8	100	13.7	13.4	1.16
4	**1**	15	100	6.4	7.1	1.19
5	**1**	40	85	2.6	2.9	1.13
6	**2**	4	70	14.1	15.9	1.12
7	**3**	4	100	18.3	22.8	1.15
8	**4**	4	92	31.7	21.0	1.16

[a]All reactions were performed using 1 μmol of catalyst, 1000 equivalent of ε-CL in 2 mL, in toluene at room temperature for 30 min. [b] Conversion of ε-CL as determined by ^{1}H NMR spectral data. [c]Experimental Mn and Mw/Mn values determined by GPC in THF against polystyrene standards and corrected using the Mark-Houwink factor of 0,58. [d] Mn_{calc} =114,14 x ($[\varepsilon\text{-CL}]_0/[I + iPrOH]_0$) x conversion ε-CL.

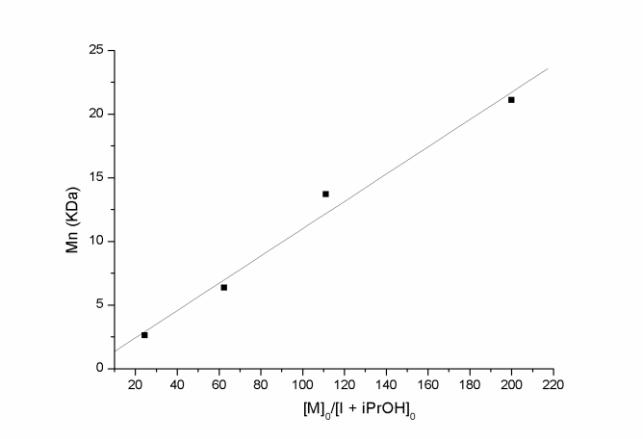

Figure 2.12: Plot of number-averaged molecular weights, Mn versus monomer-to-initiator ratio($[M]_0/[$**1**$+iPrOH]_0$

However, the excess of alcohol acts as an efficient chain-transfer agent, eventually yielding polymer chains with reduced molecular weights and narrower polydispersities.[73] The strict agreement between the experimental and the theoretical values of the Mn values highlighted that **1**, in the presence of an excess of 2-propanol, shows an ‘‘immortal character" leading to polymers with narrow molecular weight distributions, and with a Mn proportional to the equivalents of added 2-propanol. Thus, by choosing the opportune iPrOH/initiator ratio, it is possible to obtain polymer chains with the predicted molecular weights (see Fig. 2.8). The ^{1}H NMR spectrum of the low molecular weight polymer obtained in run 5 in Table 2.6, Figure 2.13, showed a doublet at 1.22 ppm and a septet at 5.01, diagnostic of the isopropyl chain-end groups.

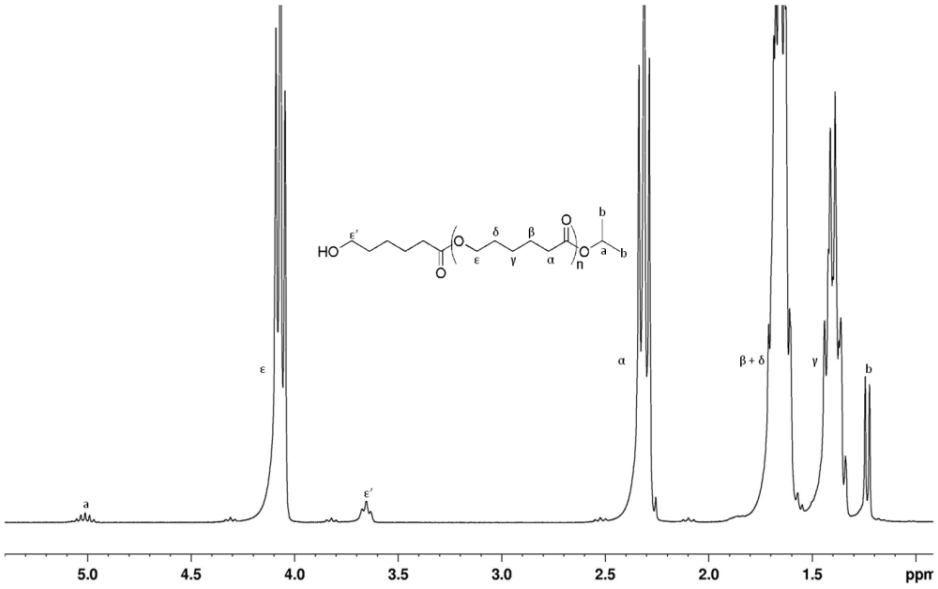

Fig 2.13. ^{1}H NMR spectrum (400 MHz, $CDCl_3$) A) the PCL obtained using **1**/ iPrOH=1/40 as initiator after quenching with wet *n*-hexane Conditions: $[\varepsilon\text{-CL}]_0/[Y]_0$ =1000) in toluene at room temperature (see run 5 , Table 6).

In the polymerization of *L*-Lactide, the catalytic system **1**/2-propanol in 1:2 ratio, showed approximately the same activity of the corresponding alkyl precursor (runs 9 and 10, Table 2.7).

The obtained PLA showed monomodal and narrow distribution of molecular weights with an excellent agreement between the experimental and calculated M_n values (run 10, Table 2.7). Increasing the alcohol/initiator ratio (5:1), polymer chains with reduced molecular weights and narrower polydispersities (PDI = 1.07) were achieved (run 11, Table 2.7). This confirms that the excess of alcohol acts as an efficient chain-transfer agent and that the growing chain/2-propanol exchange is very fast with respect to the chain propagation, indicating the living nature of the polymerization.

Table 2.7. Ring-opening Polymerization of L-LA. Effect of 2-Propanol

[a]Run	Cat	[L-LA]$_0$/[I]$_0$	[iPrOH]$_0$/[I]$_0$	[b]Time (h)	Conv. (%)	[c]M_n GPC (kDa)	[d]M_n calc (kDa)	[c]PDI
9	**1**	500	-	1	78	47.0	56.0	1.26
10	**1**	500	2	1	85	23.7	20.4	1.13
11	**1**	500	5	1	85	10.1	10.2	1.07
12[e]	**1**	2000	5	1	70	26.0	33.6	1.09
13	**3**	500	5	1	100	12.8	12.0	1.05
14	**2**	500	5	20	44	4.0	5.3	1.06

[a]All reactions were carried out at room temperature with [I]$_0$ = 5 mM in THF (2 mL). [b]Reaction times were not optimized. [e]Experimental M_n and M_w/M_n values (corrected using the Mark–Houwink factor of 0.58) were determined by GPC analysis in THF using polystyrene standards. [d]Calculated Mn of PLA =144,14 x ([L-LA]/[I$_0$ + iPrOH]) x conversion L-LA. [e] [I]$_0$ = 1.7mM in THF (6 mL).

To establish the termination and initiation steps of the polymerization reaction, end-group analysis of low molecular weight PLAs was performed by NMR spectroscopy. The ^{1}H NMR spectrum of the samples clearly showed the existence of HOCH(CH_3)CO- and -O CH(CH_3)$_2$ as exclusive chain end groups[59b,70](Figure 2.14).

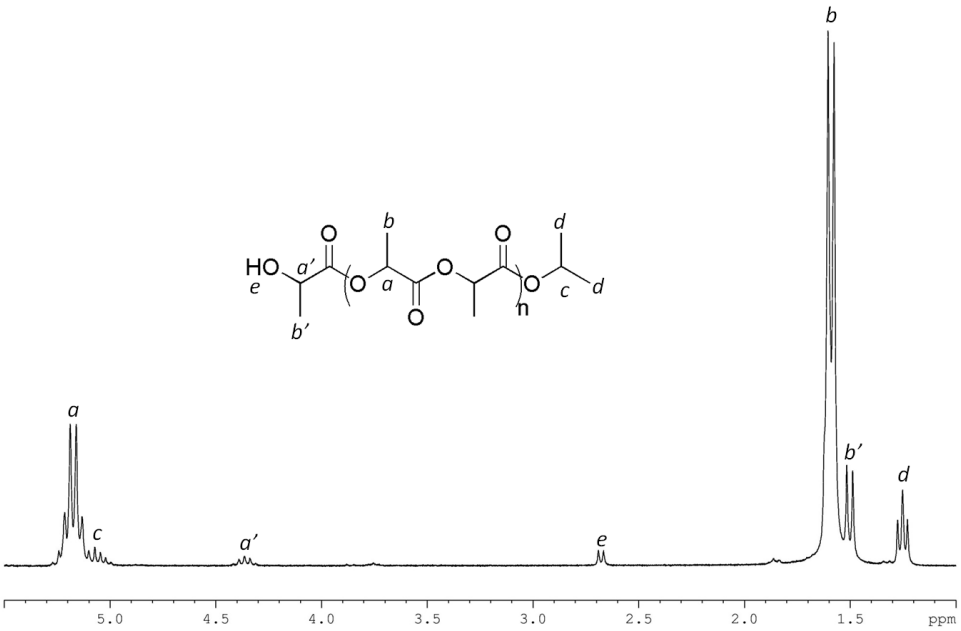

Figure 2.14. ^{1}H NMR spectrum (400 MHz, $CDCl_3$) of oligomers of L-LA obtained using **1**/iPrOH=1/5 as initiator after quenching with wet *n*-hexane Conditions: $[L\text{-}LA]_0/[Y]_0$ =20 in THF (2ml),at room temperature

The ESI-MS analysis further confirmed that only linear oligomers of the type H-$[OCH(CH_3)C(=O)]_{2n}$-$OCH(CH_3)_2$ were formed.(Fig.2.15) Less intense peaks consistent with linear oligomer chains with carboxylic acid end group, presumably arising from the hydrolysis of H-$[OCH(CH_3)C(=O)]_{2n}$-$OCH(CH_3)_2$ were also observed. No cyclic oligomers were detectable, differently from previously reported results for the ROP of lactide performed in the absence of alcohol. More significantly, elevated conversions and high molecular weight polymers were achieved by increasing the monomer to initiator ratio to 2000, still using 5 equiv of 2-propanol as chain-transfer agent (run 12, Table 2.7). In terms of productivity

and chain-transfer efficiency, these results are among the best reported for the ROP of lactide with metal-based initiators.[58c,58e,70]

At the same time, these experiments confirmed that the phosphido pincer ligands create a coordination environment efficient for stabilizing the oxophilic metal center, preventing irreversible decomposition of the initiator in the presence of alcohol. Analogously, a more efficient control over the polymerization reactions with substantially no variations of the catalytic activity were achieved when complexes **2** and **3** were used in combination with several equivalents of alcohol (runs 13 and 14 Table 2.7). In all cases, an excellent agreement between the theoretical and experimental values of the Mn and very narrow polydispersity of the obtained polymers were observed.

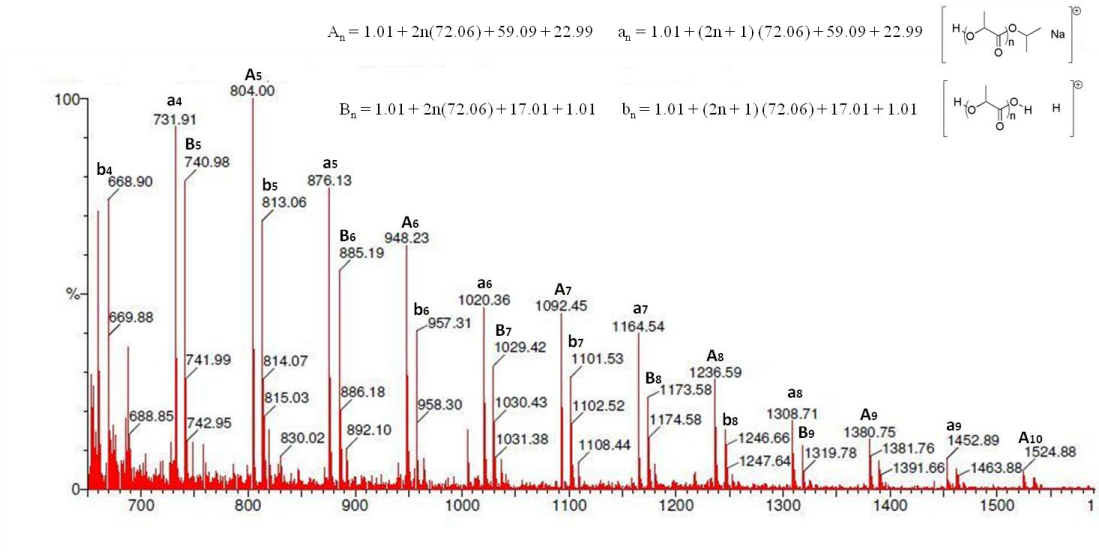

Figure 2.15. ESI-MS spectrum of oligomer of L-lactide using **1** as initiator

2.2.5 Synthesis of Diblock PCL–PLA Copolymers

The living behavior observed in the ROP of cyclic esters is an useful feature for the preparation of block copolymers. To this purpose, the initiator **1** was tested in copolymerization reactions of ε-CL and *L*-lactide. PCL–PLA block copolymers were obtained by sequential addition of the two monomers. ε-CL was first polymerized in toluene at room temperature for 5 min, and after formation of the first block, *L*-lactide was added and the solution was stirred at room temperature for additional 15 min.

The ^{1}H and ^{13}C NMR spectra of the polymer clearly showed the presence of the two blocks, (fig. 2.16). In the ^{13}C NMR spectrum, signals due to the random sequences of CL with *L*-LA, which typically appear between 173.4 and 169.7 ppm, were not observed. GPC analysis revealed a molecular weight higher than that for a pure PCL block on its own (maximum estimated Mn = 11,400 g mol^{-1}) and a monomodal distribution of the molecular weights (Mn = 18,500 g mol^{-1}; PDI = 1.72), in accordance with the formation of a PCL/PLA diblock copolymer.

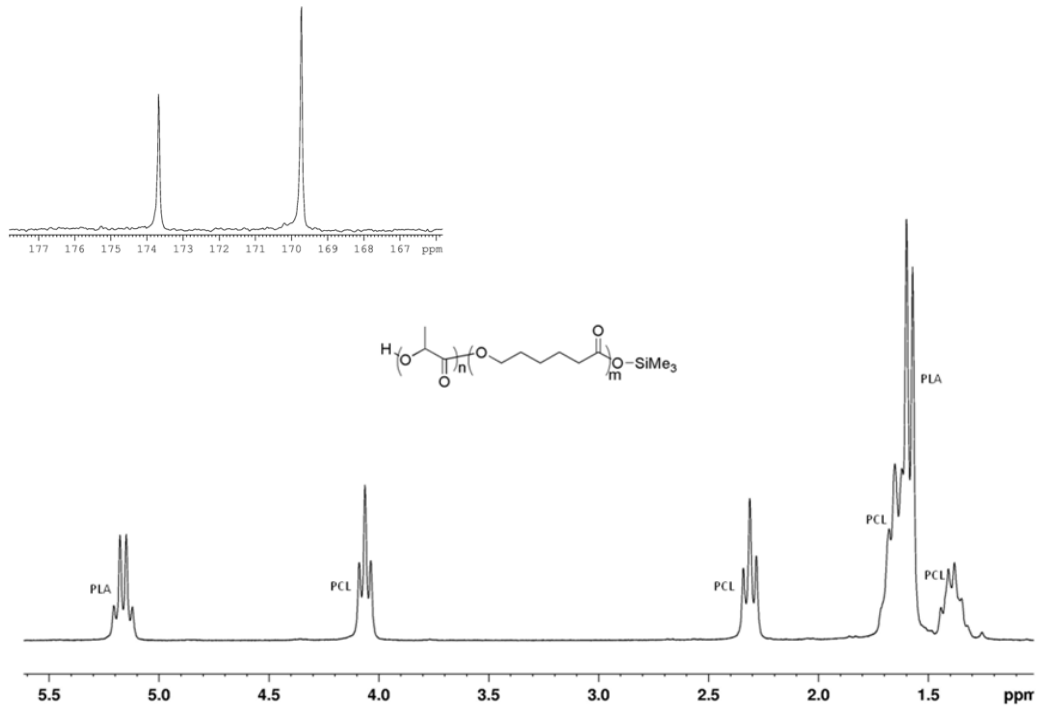

Figura 2.16: ^{1}H spectrum (400 MHz, $CDCl_3$) of copolymer ε-CL-block-*L*-LA and the carbonyl region of ^{13}C {^{1}H}(in high on the left).

In the production of PCL/PLA diblock copolymers, the importance of order in which the CL and LA monomers were added has been underlined in the literature. Several examples reported that when the CL monomer was polymerized first, the living PCL-macromolecules could initiate the PLA chain growth, to produce the desired PCL-*b*-PLA copolymers.[74] On the contrary, the addition of the monomers in the reverse order generally produced random copolymers, probably as a consequence of a faster transesterification rate of the growing PCL chain on the PLA chains, with respect to the CL homo-propagation rate.[75] Formation of PCL/PLA block

copolymers by addition of the LA as a first monomer then followed by the CL has been rarely observed, mostly when transesterification reactions are not present.[76]

In our case, when L-LA was added as the first monomer or both monomers were added at the same time in the polymerization medium, exclusive formation of PLA chains was observed, even after 24 h. Monitoring the reaction by ^{1}H NMR analysis, the complete conversion of 10 equiv of L-LA was achieved after 5 min but no conversion of the same equivalents of ε-CL was obtained, even after 24 h. The ESI-MS analysis further confirmed that only linear oligomers of PLLA were produced, whereas random CL/LA hetero-sequences were never observed. The same results were obtained when the racemic mixture of lactide was used. Analogous behaviors have been previously observed for borohydride diaminobis(phenoxide) lanthanide complexes.[9a] The net reactivities of CL and LA in the copolymerization are reversed relative to their reactivities in the homopolymerizations and, although the reason of the generally higher reactivity of LA than that of CL in the copolymerization is not well elucidated, it is reasonably to hypothesize that the higher coordination ability of the lactide has a predominant role.[77] This effect should be even enhanced in our case, as a consequence of the highly electrophilic character of the yttrium initiator.

2.2.6 Ring-Opening Polymerization of δ-Valerolactone

In the polymerization of δ-valerolactone (Scheme 2.6), complex **1** showed an activity comparable with that showed in the ROP of lactide.

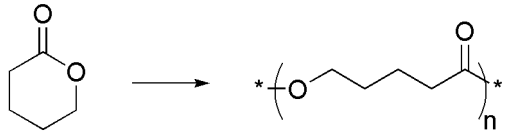

Scheme 2.6: Ring-opening polymerization of δ-valerolactone

The quantitative conversion of 200 equiv of monomer was achieved in 15 min in toluene at room temperature. The molecular weight of the obtained polymer (21.2 KDa, Mw/Mn = 1.39) was in good agreement with the theoretical value calculated considering that a single site of the metal centre is involved in the polymerization reaction.

The reaction kinetic features a pseudofirst-order dependence in δ-valerolactone concentration, as reported in Figure 2.17: the semilogarithmic plot of $\ln([\delta\text{-VL}]_0/[\delta\text{-VL}]_t)$ versus time was linear with a slope of $(2.37 \pm 0.07) \times 10^{-3}$ s^{-1} ($[\delta\text{-VL}]_0 = 0.6$ M). The value of the apparent rate constant is of the same order of magnitude of that observed for the ROP of lactide $(1.1 \pm 0.1) \times 10^{-3}$ s^{-1} for complex **1**. This is coherent with literature data reporting that the reactivity of the cyclic esters towards the ROP depends on the Lewis basicity of the carbonyl groups that is influenced by the ring size.

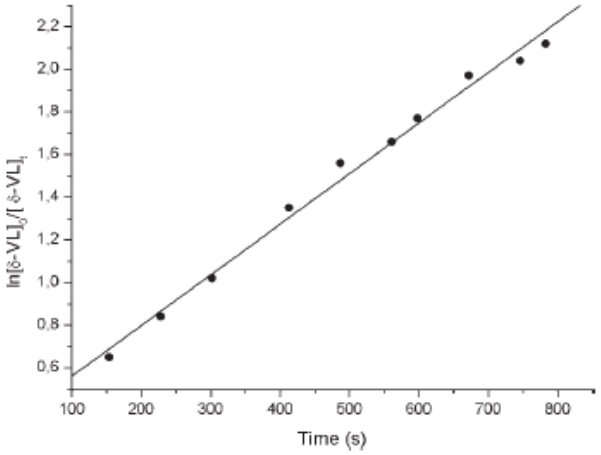

Figure 2.17: Pseudofirst-order kinetic plot for ROP of δ-VL promoted by **1**. Pseudofirst-order rate is (2.37 ± 0.07) $x10^{-3}$ s^{-1}($[\delta\text{-VL}]_0$ = 0.6 M; $[\delta\text{-VL}]_0/[I]_0$ = 100; C_7D_8 as solvent; T = 25 °C).

2.2.7 Polymerization of rac-β-Butyrolactone

Synthetic analogues of natural-origin poly(3-hydroxybutyrate) (PHB) can be prepared by the ring-opening polymerization of β-butyrolactone (BL) using various organometallic catalysts. [78] Few examples of Group 3 metal complexes as efficient initiators for the ROP of β-butyrolactone have been recently reported [79] (Scheme 8).

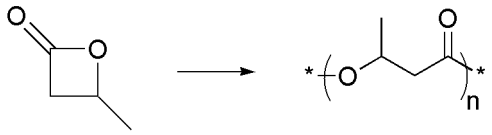

Scheme 2.7: Ring-opening polymerization of rac-β-Butyrolactone

Polymerization results for the ROP of rac-β-butyrolactone promoted by complexes **1** and **4** are shown in Table 2.8.

Table 2.8. Ring-opening Polymerization of *rac*-β-Butyrolactone initiated by complexes **1**

[a]Run	Cat	$[M]/[I]_0$	$[iPrOH]/[I]_0$	Toluene (ml)	Time (h)	[b]Conv (%)	[c]Mn_{GPC} (kDa)	[d]Mn_{calc} (kDa)	[c]PDI
1	**1**	200	//	1	24	27	2.7	4.6	1.31
2	**1**	200	2	1	24	50	2.5	2.9	1.16
3	**1**	613	2	0.1	65	83	1.0	21.9	1.87
4	**1**	1262	//	//	70	76	0.9	82.7	2.00
5	**4**	613	2	0.1	48	62	3.6	10.9	1.91

[a] All reactions were carried out at 90 °C with 10 μmol of initiator. [b] Conversion of rac-BBL as determined by the integration of ^{1}H NMR methine resonances of rac-BBL and PHB. [c]Experimental (uncorrected) Mn and Mw/Mn values determined by GPC in THF using polystyrene standards [d] Mn_{calc} values (in g/mol) were calculated considering one polymer chain per metal center from the equation : Mn_{calc} =86.00 x ([BBL]/[I + iPrOH]) x conversion BBL.

The produced polymers were characterized by GPC, ^{1}H and ^{13}C NMR analysis. Complexes **1** and **4** do not initiate the ROP of rac-β-butyrolactone at room temperature, but they were active in toluene solution at 90 °C.

The PHB produced were atactic, as for all the samples ^{13}C NMR analysis showed carbonyl signals of equal intensity for racemic and meso diads. The ROP process was much slower than those of ε-CL and lactide. For instance, a polymerization experiment performed in the presence of a monomer: Y molar ratio of 200:1 required 24 h to reach 27% of conversion (see run 1, Table 2.8). The produced polymer displayed a molecular weight, evaluated by GPC, lower than the theoretical one, calculated assuming that one polymer chain per metal was produced.

Some experiments were performed by adding two equivalent of 2-propanol and increasing the monomer: Y molar ratio (runs 2 and 3, Table 2.8); the beneficial effect on the control of the polymerization, especially in terms of molecular weight distribution, observed in the lactide ROP was not

evidenced. On the contrary, by increasing the time of reaction as well as the amount of the monomer in the feed, an irregular decrease of the molecular weight and a broadening of the PDI were observed.

These features clearly indicated that secondary reactions occurred at longer polymerization time.

Inspection of the aliphatic regions of the ^{1}H NMR spectra of the produced polymers revealed, in addition to the main polymer chain signals, the presence of minor resonances attributable to end groups. In details, a multiplet at 5.04 ppm and a doublet at 1.2 ppm have been assigned, according to the literature, to isopropyl ester end groups, whereas a multiplet at 4.2 ppm to the α-methynehydroxyl- $CH_2(CH_3)C\mathit{H}OH$ end-groups (Figure 2.18).[80]

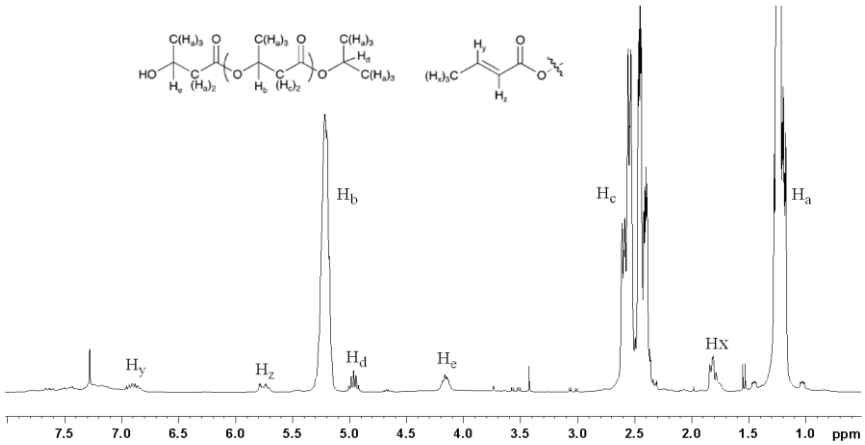

Figure 2.18 . ^{1}H NMR spectrum (400 MHz, $CDCl_3$) of the PBL obtained in run 3

These end groups clearly are the ones expected for the well established coordination-insertion mechanism operating via insertion of the BL

monomer into the Y-alkoxide bond of the initiator, generated *in situ* by the addition of 2-propanol, and followed by the acyl-oxygen cleavage of the lactone. The hydrolysis of the active yttrium alkoxide bond releases the hydroxyl end group. Moreover, in the same ^{1}H NMR spectrum, at lower field unsaturated end groups were also detected. These signals were attributed to *trans*-crotonate groups, probably generated by elimination reaction (see Scheme 2.8) The molar ratio between the end groups was determined by ^{1}H NMR, by integration of the proper signals in the ^{1}H NMR spectrum. By increasing the time of reaction and/or the amount of the monomer in the feed, the percentage of the unsaturated end groups increased, therefore resulting in the observed shortening of the molecular weight and broadening of the PDI of the polymers. Analogous results were obtained with the scandium derivative compound **4**, (cf. runs 3 vs. 5, Table 7), although in the produced PHB a lower amount (≈1/10) of *trans*-crotonate end groups was observed. Formation of *trans*-crotonate end groups was already observed in the case of the anionic polymerization of BL initiated by alkali metal alkoxides [81] and in the presence of aluminum alkoxides.[80,81] The elimination reaction was also observed in the β-butyrolactone ROP promoted by β-diiminate zinc catalysts, leading to degradation of the polymer. [82]

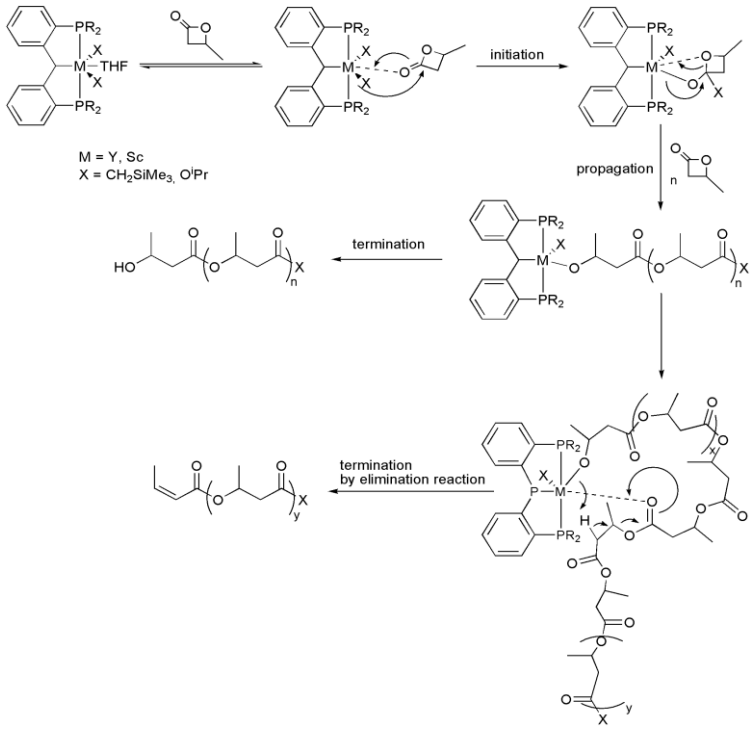

Scheme 2.8.: Polymerization mechanism of *rac*-β-butyrolactone initiated by complexes **1-4**

2.3 CONCLUSIONS

In this chapter, the synthesis and characterization of new yttrium and scandium complexes supported by phosphide phosphine pincer ligands, [(o-$C_6H_4PR_2)_2PH$; **L1**-H: R = Ph; **L2**-H: R = iPr] have been described.

All complexes, [$LM(CH_2SiMe_3)_2(THF)_n$] [M = Y, L = **L1** (**1**), L = **L2** (**3**); M = Sc, L = **L1** (**2**), L = **L2** (**4**)] have been obtained by direct reaction of proligands with metal tris(alkyl) precursors $M(CH_2SiMe_3)_3(THF)_2$ in quantitative yields.

For all complexes NMR analysis were being consistent with structures in which one pincer ligand is coordinated at metal center with a *mer* arrangement.

The behavior of these pincer-based yttrium and scandium complexes was investigated in the ROP of cyclic esters, such as ε-caprolactone, L- and rac-lactide, δ-valerolactone and rac-β-butyrolactone

They resulted very active initiators for the ROP of these monomers.

In the ROP of ε-CL, they showed activities among the highest reported in literature. For yttrium complex **1** a turnover frequency (TOF) is about 4 × 10^4 mol_{CL}/mol_I h) was observed.

Quantitative conversions of high amount of monomer (up to 3000 equivalents) using relatively low amount of the initiator (1 μmol), under mild polymerization conditions, were achieved.

In the ROP of *L*-, *rac*-lactide and δ-valerolactone all compounds allowed quantitative conversion of 200 equivalents of monomer at room temperature, with turnover frequencies up to 650 mol_M/mol_I h.

Complexes **1-4** also promoted the ROP of rac-β-butyrolactone affording atactic low molecular weight poly(hydroxybutyrate) chains bearing unsaturated end groups, probably generated from termination process by elimination reaction.

The studies performed on the catalytic behavior of these systems showed that the catalytic activity is strongly dependent on the nature of the metal center, the structure of the ancillary ligand and the polymerization conditions.

Yttrium initiators showed higher activities than the analogues scandium complexes accordingly with literature data reporting that the complexes of smaller rare earth metals normally show lower activities. For both metals higher catalytic activities were observed for the phenyl substituted complexes. This has been ascribed to the lower electron donating character of the phenyl groups and to the consequent increase of the Lewis acidity of the metal center.

The polymerization medium revealed to play an important role in influencing the catalytic activity. For all complexes, a lower activity was observed when polymerization experiments were performed in THF as a consequence of the presence of a competing coordinating solvent.

The investigations concerning the study of the polymerization mechanism showed that all complexes exhibit a good molar-mass control indicative of a ‘‘single site’’ nature of the catalysts. Linear dependences of Mn versus the percentage conversion, time and the monomer-initiator ratio were observed. The overall results were consistent with a ‘‘controlled- living’’ polymerization model.

These same catalysts, used in combination with several equivalents of alcohol used as chain transfer agent, promoted the “immortal” ROP of *L*-

lactide and ε-CL. These bi-component systems (catalyst and alcohol) allowed to generate a number of growing polymer chains that exceeded the number of catalyst molecules optimizing the productivity and minimizing the contamination of polymer with metal residues.

Yttrium complexes were able to promote the polymerization of L-lactide with a controlled manner also under drastic conditions of reaction, in absence of solvent at 130°C. The resulting polymers have high molecular weights with narrow molecular weight distributions. Under these conditions, both alkyl groups on the metal center are involved in the polymerization process.

Diblock PCL-PLA copolymers were also obtained by sequential addition of the two monomers.

In conclusion, the results of this work highlight the ability of an unusual coordination environment with soft donor atoms to provide stability and reactivity at catalytic systems based on very acid early-transition-metal systems in the ROP of cyclic esters.

The results reported here have been published in references.[83, 84]

3 ZINC COMPLEXES

3.1 INTRODUCTION

In intensive activity to produce polyesters with controlled architecture and tailor-made properties,[85] via ring opening polymerization (ROP) of the related cyclic esters promoted by metal initiators,[86] single-site metal catalysts based on zinc complexes are of great interest. Several important families of single-site zinc catalysts have been developed that exhibit high polymerization activity affording polymers with controlled molecular weights and microstructures.[87]

Neutral catalytic species supported by anionic ancillary ligands of the type LZn-X, where L often is a chelating phenoxy or alkoxides based ligand and X is an alkyl or amide group, have been predominantly employed.[88, 89, 90, 91]

Many recent works have involved the use of zinc complexes bearing a wider variety of anionic and neutral ligand frameworks, such as β-diketiminates,[92, 93] phosphinimine,[94] guanidine–pyridine[95] and tris-pyrazolylborates.[96] All these ligands include nitrogen-based hard donor groups.

Differently, the catalytic behavior of zinc complexes featuring soft donors is scarcely explored. According to the HSAB (Hard and Soft Acids and Bases) theory, zinc ion is a “borderline” soft Lewis acid: this feature may provide some lability for chelating ligands carrying pendant groups with soft donors.

Since phosphine derivatives of Group 12 metals are quite rare, I decided to extend the use of this class of ligands to the coordination chemistry of zinc. Some examples of crystallographically characterized zinc complexes were firstly reported by Darensbourg[97] and more recently by Liang.[98] In all cases phosphine donors are in combination with hard phenoxide or amide additional donors. In this context, the PPP-H =bis(2 diphenylphosphinophenyl)phosphine pincer ligand represents an original coordination environment in which an unusual phosphido anionic donor is flanked by phosphine neutral donors. This architecture proposes uncommon coordination abilities that could introduce lability in the coordination sphere with intriguing and novel reactivity patterns at the metal center.

In this section the synthesis and characterization of new zinc complexes, supported by the bis(2 diphenylphosphinophenyl)phosphine pincer ligand, of type: [(κ^3-PPP)Zn(R)] (R = CH_2CH_3,(**5**); R = $N[Si(CH_3)_3]_2$, (**6**)) have been reported.

Their reactivity as catalysts for the ring-opening polymerization of ε-caprolactone and L and *rac*-lactide. and the ability of zinc amido complex (**6**) to produce random copolymers from L-lactide and ε-caprolactone have been studied.

3.2 RESULTS AND DISCUSSION

3.2.1 Synthesis and Characterization of Complexes

Preparative scale reactions of [(PPP)ZnEt] (**5**) and [(PPP)ZnN(SiMe$_3$)$_2$] (**6**) were carried out in toluene solution by allowing to react the opportune zinc precursor with an equimolar amount of the neutral pro-ligand (Scheme 3.1). Removal of the volatiles under reduced pressure yielded pale yellow solids, that were washed with a minimum amount of cold hexane to obtain the analytically pure complex **5** (yield 83 %) and **6** (yield 91 %).

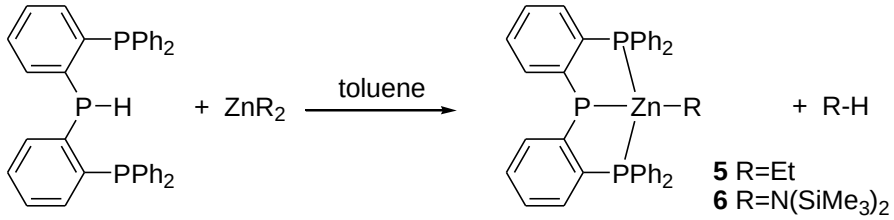

Scheme 3.1: Synthesis of the zinc complexes **5** and **6**.

Both complexes **5** and **6** were characterized by multinuclear and two-dimensional NMR spectroscopy (^{1}H, ^{13}C, ^{31}P NMR and COSY experiments) and elemental analysis.

The ^{1}H NMR spectrum of complex **5** ([C_7D_8], 25°C) showed two signals in the aliphatic region, attributable to the protons of the ethyl group bound to the zinc. In particular, the multiplicity of the methylene signal, ascribable to the coupling with the phosphorous atoms of the ligand, confirmed the

formation of the desired complex.(Fig 3.1) With respect to akin zinc complexes reported in the literature, the signals of the alkyl group bound to the metal resonate at a lower field. This could suggest the location of the alkyl group in the deshielding zone of the adjacent phenyl rings.

The aromatic region of the ^{1}H NMR spectrum features an integration pattern consistent with overall C_s symmetry in which the mirror plane includes the central phosphine donor, the metal, and the alkyl group, and reflects the two peripheral phosphine groups. The two phenyl groups on each peripheral phosphine are diastereotopic, however, their broad signals suggest fluxional behavior on the NMR time scale.

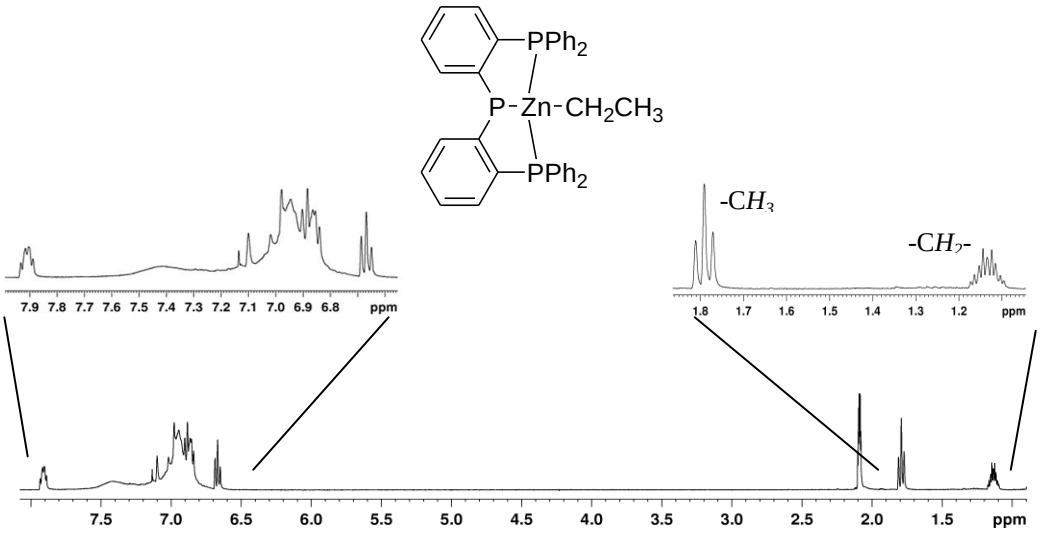

Fig. 3.1: ^{1}H NMR spectrum of complex **5** (400 MHz, toluene-*d8*). In the upper part, an enlargement of the aromatic and alkyl regions are shown.

The ^{31}P NMR spectrum supports this symmetry including only two signals: a doublet for the neutral phosphorous donors, at δ = -5.68 ppm, and a triplet for the anionic phosphido ligand, at δ =-50.32 ppm, that are downfield shifted relative to the corresponding ligand precursor (δ = -10.9 ppm and δ = -53.8 ppm), (Fig.3.2).

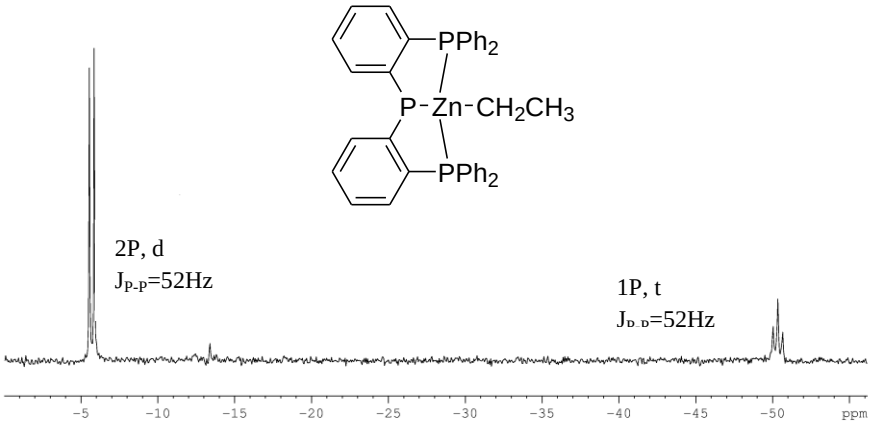

Fig. 3.2:. $^{31}P\{^{1}H\}$ NMR of complex **5** (162.97 MHz, C_6D_6)**.**

Coherently with the supposed symmetry, the ^{13}C NMR spectrum showed ten signals for the *C*H carbons and four signals for the quaternary carbons, the nature of these signals being confirmed by DEPT experiment. The pseudoquartet resonance observed for the α-carbon atom in the ^{13}C NMR spectrum indicates that both phosphine neutral donors are equivalently coordinated to the zinc confirming that the monoanionic phosphido pincer ligand is coordinated to the central metal in a tridentate fashion.

The solution NMR data for the zinc complex **6** indicated a similar situation. The number and the intensity of the NMR signals in the ^{1}H NMR spectrum of complex **6** ([C_6D_6], 25°C) indicated the formation of a symmetrical

complex.(Fig. 3.3) In the aliphatic region one sharp resonance (δ = 0.44 ppm) was observed, attributable to the methyls of the amido group, resulting shifted downfield with respect to that of the $Zn(N(SiMe_3)_2)_2$ precursor (0.21 ppm).

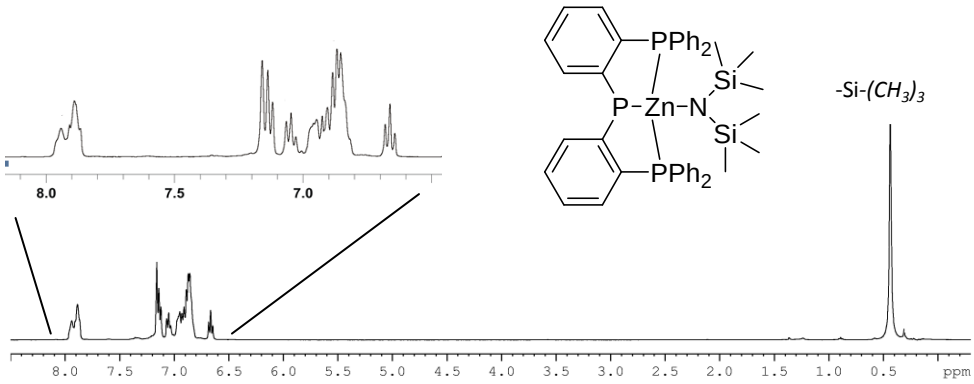

Fig. 3.3: . ^{1}H NMR spectrum of complex **6** (400 MHz, C_6D_6). In the upper part, an enlargement of the aromatic region is shown.

^{31}P NMR spectrum displayed two signals at δ = -12.59 and δ = -53.46 ppm, corresponding to the neutral and anionic phosphorous donors respectively. The ^{13}C NMR spectrum features the same pattern observed for complex **5**.

In summary, the solution NMR data for both complexes indicated that the monoanionic phosphido pincer ligand is coordinated to the central metal in a tridentate fashion with both phosphine neutral donors equivalently coordinating to the zinc. The symmetric situation observed at room temperature could result either from the formation of symmetric complexes or from a fluxional process in action that makes the two sides of the chelate arm equivalent.

Monitoring by ^{1}H and ^{31}P NMR spectroscopy showed that complexes **5-6** were stable at room temperature in benzene and in toluene solution for at last one week. Unexpectedly, the homoleptic complex **7** was isolated as crystalline precipitate from a THF/ hexane solution of complex **6** at room temperature (after 1 month). Reasonably complex **7** was produced by a very slow ligand exchange reaction of complex **6** (Scheme 3.2).[99]

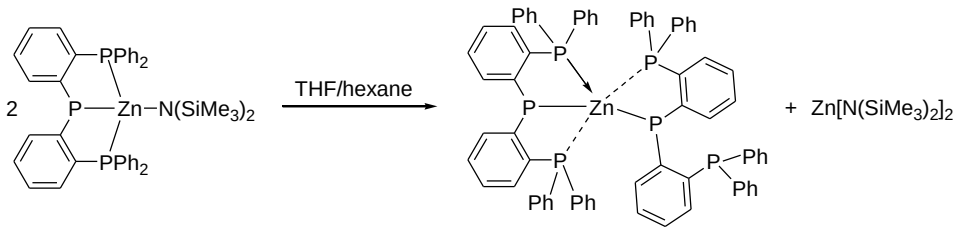

Scheme 3.2: Disproportion reaction of complex **6**

Formation of homoleptic L_2Zn complexes has been reported for undemanding and/or with poor electron-donating ability bidentate ligands,[92b, 100] but it is definitely uncommon for complexes bearing tridentate ligands. Generally, the presence of a bulky chelating ligand around the Zn center inhibits the disproportion reaction. The only examples of homoleptic metal complexes bearing two tridentate pincer ligands have been recently reported.[101]

The crystal structure of **7** is shown in Figure 3.4. Zinc displays a nearly trigonal planar coordination geometry (the sum of the bond angles about the metal is close to 360°) [98b, 103] with three phosphorous atoms (P2, P3 and P1) belonging to two different PPP molecules, acting as bidentate and monodentate ligands, respectively. This coordination geometry is quite

distorted due to the constrain imposed by the bidentate pincer ligand (P2-Zn1-P3 = 85.76(6)°). Bond distances and angles are similar to those reported in the literature for a silyl-phosphido zinc complex.[102]

In this structure P4 and P5 atoms are 2.719(2) Å and 2.801(2) Å far from the metal, respectively and this evidence reveals a weak interaction of the phosphine atoms with Zn center resulting in a pseudo bipyramidal trigonal arrangement (P4-Zn1-P5 = 152.54(5)°). This structure highlights the aptitude of the phosphido pincer ligand in adopting multiple coordination geometries.

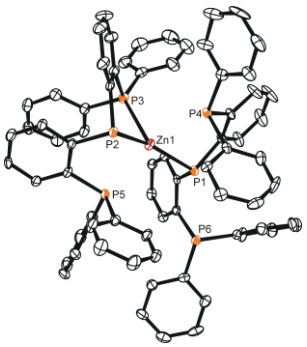

Figure 3.4. ORTEP-3 view of $[PPP]_2Zn$ (**7**). Thermal ellipsoids are shown at 30% probability level. Hydrogen atoms are omitted for clarity. Selected bond distances and angles (Å, °): Zn1-P1 =2.340(2), Zn1-P2 = 2.397(2), Zn1-P3 = 2.463(2), P1-Zn1-P3 = 120.86(6), P1-Zn1-P2 = 152.53(6), P2-Zn1-P3 = 85.76(6).

The homoleptic complex **7** was purposely prepared by reaction of the zinc ethyl precursor with two equivalents of the pincer proligand in toluene solution at 50°C for 12 hours. The ^{31}P NMR spectrum ($[C_7D_8]$, 25°C)

showed a well-resolved multiplet at δ = – 53.0 ppm for the two phosphido donors and a broad resonance, at δ = – 13.8 ppm, for the phosphine phosphorous atoms suggesting an exchange process involving the four neutral phosphine atoms. Raising the temperature up to 80°C, the broad resonance resolved in a sharp multiplet. Probably, due to the high fluxionality of the complex at high temperature, all phosphine arms resulted equivalent on the NMR time scale.

Coordination studies by DFT analysis and variable temperature NMR experiments.

The fluxionality showed by the phosphido pincer complexes **5** and **6** in solution at room temperature and the different denticity assumed by pincer ligands in the homoleptic complex **7** induced to investigate more deeply the coordination behavior of this ligand at the metal center by DFT calculations (Density functional theory) [103] and variable temperature NMR analyses.

To propose a molecular model for the pincer zinc complexes **5** and **6**, DFT calculations were firstly carried out.

In the optimized structures of the expected tetracoordinated species (k^3-PPP), the geometry at Zn atom is best described as distorted tetrahedral with angles ranging from 83.2° to 119.7°. The main distortions are caused by the restricted "bite" angle of each -PPh_2 unit that lowers the corresponding P-Zn-P angles. In these structures the pincer ligand is enforced in a facial binding that is required to create a tetrahedral metal center, this produces a distortion of the pyramidal phosphido phosphorous atom and a near perpendicular orientation of the two bridging aryl rings. Although the frame

of this pincer ligand is more adapted to a meridional configuration, all attempts to optimize a square planar geometry met with failure.

The pincer ligand generally behaves as an anionic tridentate ligand. Alternatively, the PPP ligand may employ only one neutral phosphine donor for the coordination to the metal center resulting in an anionic bidentate ligand. Although the examples of three-coordinate zinc complexes of phosphine are extremely rare,[92b, 100, 104] the bis-chelated zinc species featuring the k^2-PPP ligand were successfully optimized. In these species, the zinc atom is in a trigonal-planar environment (sum of the bond angles are 359.9° and 360.0 for the alkyl and the amide derivative, respectively), coordinated by two phosphorous atoms which form a five-membered chelate ring. The corresponding P-Zn-P bond angles are only slightly larger than in the corresponding tetrahedral Zn species and they are in the range observed for other bis-chelate zinc complexes with a N-Zn-N environment (80.7-84.4°).[105] Also in these species, the phosphido phosphorous donor is in a pyramidal arrangement suggesting that the lone pair is not involved in a multiple bonding with Zn. Calculations show that the free energy difference (at 298 K) between the tetrahedral and the trigonal species is low, it is only -4.1 kcal/mol for the alkyl derivative and -3.9 kcal/mol for the amide derivative. The negative values favour the tetrahedral isomers.

The behavior of complexes **5** and **6** in solution was also studied by variable temperature ^{1}H and ^{31}P NMR experiments performed in the range -60 ÷ 80°C in [C_7D_8] toluene.

In the ^{1}H NMR spectrum of complex **5** at – 60°C, all the signals appeared as well resolved peaks (Figure 3.5). As the temperature increases, the signals attributed to the protons of the two diastereotopic phenyl rings become broader and merge at a coalescence temperature (T_C) of 40 °C, indicating

the formation of a C_{2v} symmetric species. In particular, while some of these signals overlapped with the solvent, a well resolved signal at δ 7.21 ppm, accounting for eight nuclei, was observed for the protons named H_G. Due to the complexity of the aromatic region line shape analysis was not possible in this case.

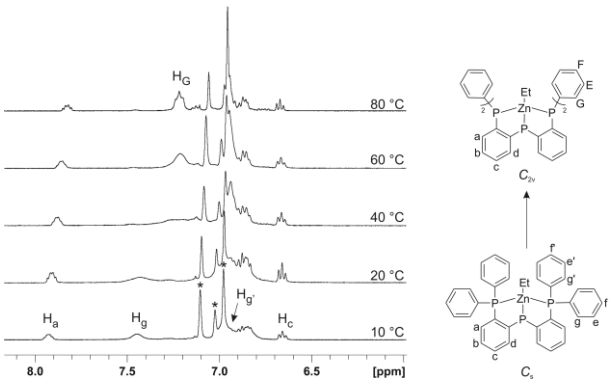

Figure 3.5 Selected region of variable-temperature ^{1}H NMR spectra of complex **5**

Acquisition of the ^{31}P NMR spectra at variable temperature was inconclusive; the signals of each phosphorous atom remain unchanged in the range -60 ÷ 80°C.

Upon cooling complex **6** from 20 to -60 °C the aromatic area of the ^{1}H NMR spectra exhibited broadening of some of the signals even if no coalescence was observed, i.e. if a fluxional process is active, it has a low energy barrier which is still overcome at -60 °C.(Fig. 3.6) On the other hand, variable temperature ^{31}P NMR spectra, accumulated in the same range of temperature, showed that the signal of neutral phosphorous donors progressively loses its multiplicity and appears as a broad peak at – 60°C, while the peak of the phosphido ligand preserves its multiplicity.

Thus, the low-temperature NMR experiments lean towards the hypothesis that a fluxional process is active affording a C_s symmetric species on the NMR time scale.

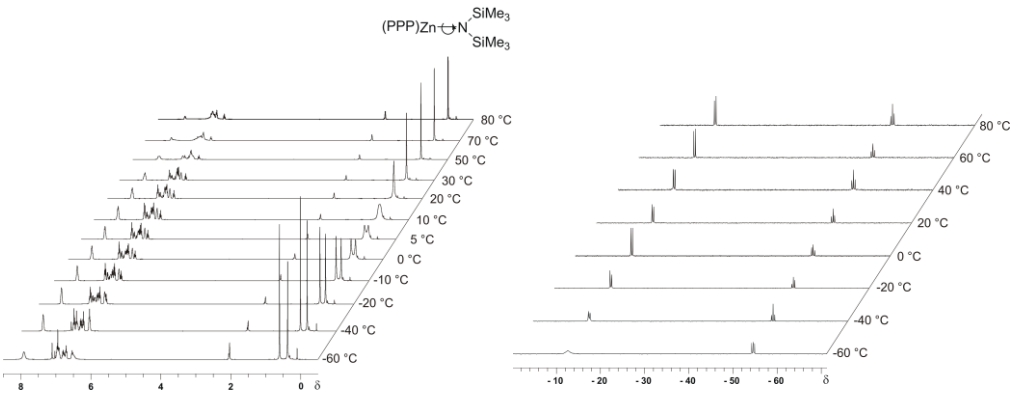

Figure 3.6: Variable-temperature ^{1}H NMR spectra (on the left) and ^{31}P NMR spectra (on the right) of complex **6** in toluene-*d*8. The temperature for each spectrum is shown at the right

Looking to the aliphatic area of the ^{1}H NMR spectra it can be observed that, as the temperature decreases, the sharp room temperature $SiMe_3$ resonance splits into two singlets at a coalescence temperature (T_C) of 10 °C at δ 0.33 ppm, as would be expected for freezing the amido group rotation. The free energy of activation for the fluxional process was calculated from the line shape analysis of the $SiMe_3$ methyl protons to be $\Delta G^{\ddagger} = 13.93 \pm 0.03$ kcal mol^{-1} at 298 K. Activation parameters resulted to be $\Delta H^{\ddagger} = 14.8 \pm 0.3$ kcal mol^{-1} and $\Delta S^{\ddagger} = 2.9 \pm 1.1$ cal mol^{-1} K^{-1}

Upon raising the temperature from 20 to 80 °C a broadening of the signals was observed (Figure 3.6). Although the complexity of the spectrum did not allow a precise assignment of each signal, the simplified pattern observed at

80 °C is compatible with the presence of a C_{2v} symmetric species as supposed for complex **5**.

A picture accounting for the observed behavior can be depicted as follows.

At low temperature a C_s-symmetric structure in which the monoanionic phosphido pincer ligand is coordinated to the central metal in a tridentate fashion, is present in solution. The broadening observed when approaching room temperature for complex **5** and 40 °C for complex **6**, indicates the existence of a fluxional process which, at those temperatures, proceeds at a rate comparable to the NMR time scale.

Increasing the temperature, the observed patterns indicate the formation of an averaged-C_{2v} symmetric species, in which the two phenyl rings on each phosphorous result equivalent. Two plausible explanations can account these results.

A fast equilibrium between the two possible diastereomers derived from the inversion of the pyramidal anionic phosphido atom would lead to a C_{2v} symmetry on the NMR time scale.

A similar fluxional process was hypothesized for a germanium complex bearing a [NP^-] ligand.[106]

Alternatively, the reversible dechelation of one arm of the pincer ligand, through the formation of a tricoordinate species for which a free rotation about the P-C (phenyl) bound is possible, could account for these observations. The fluxionality of k^2 species has been studied in depth for complexes of hemilabile ligands with redundant donor atoms.[107] Additionally, the k^2 coordination of the related PNP ligand has been recently observed for uranium halide complexes [108] and in the case of phosphido pincer zinc complexes is supported by DFT calculations.

3.2.2 Ring-Opening of ε-caprolactone

The phosphido pincer complexes **5-6** were tested as initiators for the ROP of ε-caprolactone (see Scheme 3) under a variety of polymerization conditions. Representative results were summarized in Table 1. The obtained polymers were characterized by ^{1}H NMR and GPC analyses.

Both complexes **5** and **6** resulted efficient initiators for the ROP of ε-CL to give high molecular weight polymers.

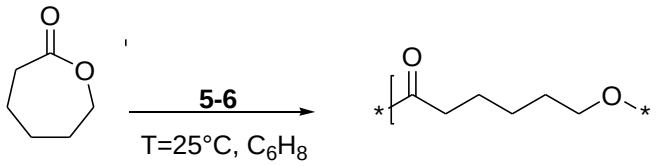

Scheme 3.3: Ring-opening polymerization of ε-caprolactone initiated by complexes **5-6**

At room temperature, complex **5** showed moderate catalytic activity in the ROP of ε-CL, about 100 equivalents of monomer were converted after eight hours (run 1, Table 3.1).

Not unexpectedly, an increase in the temperature up to 50 °C led to a higher conversion of the monomer, showing a productivity of 9.6 10^{3} g PCL (mol Zn)$^{-1}$ h^{-1}, without any increase in the polydispersity index (run 2, Table 3.1).

To probe the importance of the nature of the initiating group we tested in the ROP of ε-caprolactone the amide-zinc derivative complex **6**. As expected, this showed a much higher activity than that of complex **5** under the same reaction conditions (cfr runs 1 and 4).

Table 3.1. Ring Opening Polymerization of ε-CL by **5** and **6**

Run[a]	**Cat**	**[iPrOH]$_0$/[I]$_0$**	**T (°C)**	**Time**[b] **(min)**	**Con (%)**	**Mn**[c]$_{GPC}$ **(kDa)**	**Mn**[d]$_{th}$ **(kDa)**	**PDI**[c]
1	**5**	-	25	480	46	19.7	10.5	1.20
2	**5**	-	50	100	70	47.1	15.9	1.20
3	**5**	2	25	480	100	9.1	11.4	1.11
4	**6**	-	25	360	89	130.7	20.3	1.72
5	**6**	-	50	100	80	136.0	18.3	1.74
6	**6**	-	70	50	62	55.8	14.2	1.83
7	**6**	2	50	100	100	13.8	11.4	1.19
8	**6**	4	50	100	100	5.5	5.7	1.14
9	**6**	10	50	100	100	2.7	2.3	1.12
10[e]	**6**	10	50	100	100	22.4	22.8	1.21
11[f]	**6**	10	50	120	100	56.1	57.1	1.85

[a]All reactions were carried out with [**I**]$_0$ = 5 mM and [ε-CL] = 1 M in toluene (2 mL). [b] Reaction time was not necessarily optimized. [c]Experimental M_n (corrected using the Mark–Houwink factor of 0.56) and PDI values were determined by GPC analysis in THF using polystyrene standards. [d]Calculated Mn of PCL (in gmol^{-1}) =114,13 x ([ε-CL]/[iPrOH]) x conversion ε-CL. [e] [ε-CL]/[**6**] = 2000; [f] [ε-CL]/[**6**] = 5000

Kinetic studies for the polymerization of ε-CL with both compounds **5** and **6** were also performed to establish the reaction orders with respect to monomer.

Conversion of the monomer with time was monitored by ^{1}H NMR in C_7D_8 at different temperatures (25 and 50 °C) until monomer consumption was almost completed (conversion>80 %).

Plots of ln($[\varepsilon\text{-CL}]_0/[\varepsilon\text{-CL}]$) vs time were linear, indicating the first order dependence on monomer concentration for both catalysts. The pseudofirst-order kinetic plot for catalyst **6** is shown in Fig. 3.7.

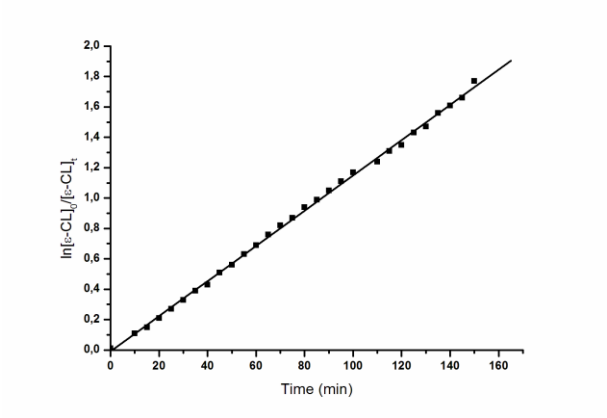

Figure 3.7. Pseudofirst-order kinetic plot for ROP of ε-CL promoted by **(6)**. Pseudofirst-order rate costant is $(1{,}6 \pm 0{,}1) \times 10^{-3}$ min^{-1} R= 0.99896 ($[\mathbf{6}]_0$ = 3 mM, $[\varepsilon\text{-CL}]_0$ = 0.6M; $[\varepsilon\text{-CL}]_0/[\mathbf{6}]_0$ = 100; toluene-d_8 as solvent; T = 50°C).

The kinetic constant for catalyst **6** $(1{,}6 \pm 0{,}1) \times 10^{-3}$ min^{-1} was double than that observed for catalyst **5** $(8{,}8 \pm 0{,}2) \times 10^{-4}$ min^{-1} under the same reaction conditions.

To provide further evidences about the polymerization mechanism, the nature of the initiating groups of the active species was evaluated by NMR

analysis of the chain end groups of a properly prepared low molecular weight polymer.

The ^{1}H NMR spectrum of poly(ε-caprolactone) oligomer, derived from the reaction of **6** with 20 equiv of ε-CL, exhibited characteristic resonances consistent with the presence of amido -$N(SiMe_3)_2$ and CH_2OH hydroxyl chain end groups.

These observations supported the hypothesis that the reaction followed the classical nucleophilic route and was initiated by the transfer of the labile ligand (amide or alkyl) to the monomer with the subsequent oxygen-acyl bond cleavage of the cyclic ester.

The molecular weight distributions of the produced polymers are monomodal, although the measured Mn values are several times larger than the calculated Mn_{th} values assuming the growth of one polymer chain per zinc-initiator. This suggested that, possibly, only a fraction of zinc complex was involved in catalysis, most likely as a result of an inefficient initiation by the poor nucleophilic ethyl and amide groups.[93b]

Upon addition of isopropanol the productivity of both complexes is considerably improved (cfr runs 1 vs 3 and 4 vs 7). The addition of iPrOH expected to generate *in situ* the more efficient alkoxide-Zn initiating species and indeed higher conversions of the monomer were achieved at room temperature. Consequently, a more efficient control on the molecular weights was also obtained as demonstrated by the good agreement between the theoretical and experimental values.

The catalytic ability of compound **6** to promote ROP of ε–CL in the presence of several equivalents of alcohol as chain transfer agent, was also assessed.[109] Upon addition of an excess of iPrOH, complex **6** provided an

efficient binary catalytic system for the controlled ROP of ε-CL (runs 7-9, Table 3.1).

The ^{1}H NMR analysis of chain end-groups of the obtained polymers showed the presence of a single family of polymer chains with $–CH_2OH$ (3.65 ppm) and iPrOC(O)- (1.22 ppm and 5.01 ppm) chain end groups.

A strict dependence of molar masses of PCLs on the monomer/alcohol ratio was observed, indicating that the number of polymer molecules becomes larger, proportionally to the number of added alcohol equivalents.

The narrow polydispersity index and the good agreement between experimental and theoretical molecular weights confirmed that the rate constant for the transfer between growing chains and resting alcohols or the dormant hydroxy-end-capped polymer chains (k_{tr}) was far greater than that for the chain propagation (k_p) (Scheme 3.4).

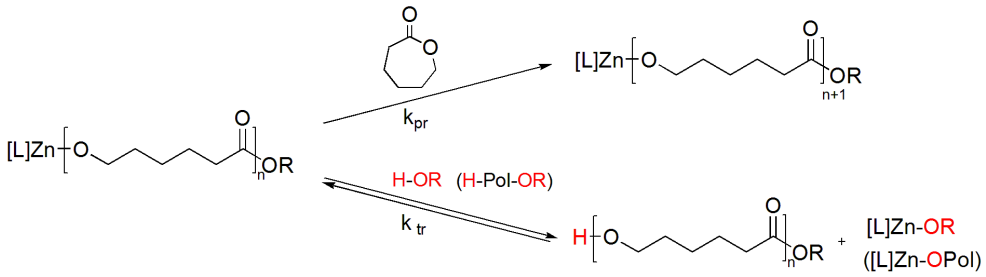

Scheme 3.4: ROP of ε-CL catalyzed promoted by the binary catalytic system **5-6**/ iPrOH

Most interestingly, 10 μmol of complex **6** allowed to convert up to 5000 equiv. of ε-CL in the presence of 10 equiv. of *i*PrOH as a transfer agent (runs 10 and 12). Under these experimental conditions, only trace amounts of the metal contaminant is present in the final product.

Also in this case, a strict agreement between the theoretical and experimental molecular weight was observed. The molecular weight distributions (*M*w/*M*n) were slightly broader (1.21-1.85) and this may be due to bulk transfer properties, resulting in an increase of chain termination reactions as the concentration of monomer is increased.[110]

3.2.3 Polymerization of L-and rac-Lactide.

The polymerization of L-lactide and *rac*-lactide (Scheme 3.5) using the zinc amide complex **6** has been studied; representative results are summarized in Table 3.2.

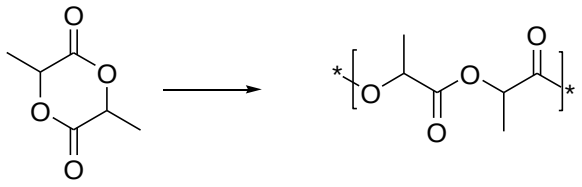

Scheme 3.5. Ring-opening polymerization of L- and *rac*-lactide initiated by complex **6**

Complex **6** resulted highly active in the ROP of lactide. High conversion, about 150 equivalents of the monomer within 1 hour, under mild polymerization conditions was observed (at room temperature in toluene solution, see run 12, Table 3.2).

Table 3.2. Ring Opening Polymerization of **L-** and ***rac*-LA** by **(6).**

Run[a]	**Monomer**	**Solvent**	**Time (min)**	**Yield (%)**	Mn_{GPC}[b] **(kDa)**	Mn_{th}[c] **(kDa)**	**PDI**[b]	P_r[d] **(%)**
12	L-LA	toluene	60	70	389.2	20.2	1.73	-
13	L-LA	THF	60	-	-	-	-	-
14	L-LA	CH_2Cl_2	60	79	177.7	22.8	1.31	-
15[e]	L-LA	toluene	20	91	8.8	8.7	1.05	-
16	*rac*-LA	toluene	60	75	228.2	21.6	1.78	71
17	*rac*-LA	CH_2Cl_2	60	80	133.4	23.1	1.61	77
18[f]	*rac*-LA	CH_2Cl_2	300	43	18.5	12.4	1.57	80

[a]All reactions were carried out at 25°C with $[\mathbf{6}]_0$ = 5 mM and [L-LA] = 1 M in 2 mL of solvent. [b]Experimental M_n (corrected using the Mark–Houwink factor of 0.58) and PDI values were determined by GPC analysis in THF using polystyrene standards. [c]Calculated *Mn* of PLA (in $gmol^{-1}$) =144,14 x ([L-LA]/[iPrOH]) x conversion L-LA. [d]P_r is the probability of racemic linkages. [e] $[iPrOH]_0/[\mathbf{6}]_0$ =2. [f]Temperature = 0°C.

The reactivity of complex **6** toward lactide was higher than that toward ε-CL under the same polymerization conditions (cf run 4 in Table 3.1 vs run 12 in Table 3.2). This behavior is not very common since polymerization of ε-CL is frequently faster than that of lactide, although some examples of zinc complexes with opposite reactivity towards these two monomers have been recently reported.[92b 111]

The influence of solvent on the polymerization of L-lactide was also investigated. The productivity (79%) was slightly improved when the polymerization was performed in a more polar solvent such as methylene dichloride (run 14). Differently, a complete loss of activity was observed in the presence of tetrahydrofuran most probably as a result of competitive

coordination of the solvent onto the metal center (run 13) that inhibits substrate coordination and polymerization.

As already observed for polymerization of ε-caprolactone, the experimental *Mn* values of the PLAs produced by **6** were several times larger than the calculated Mn_{th} values. However, a very good control on the molecular weights and a very narrow polydisperity index can be reached by adding isopropanol.

Kinetics studies showed that polymerization of LA by **6** followed a first order dependency on the concentration of monomer as revealed by Figure 3.8. At ambient temperature, the rate constant (k_{app}) was 1,7 ± 0,02 $\times 10^{-2}$ min^{-1}, about one order of magnitude higher than that of complex **6** in the polymerization of CL (k_{app}=1,0$\times 10^{-3}$ min^{-1}) under the same polymerization conditions.

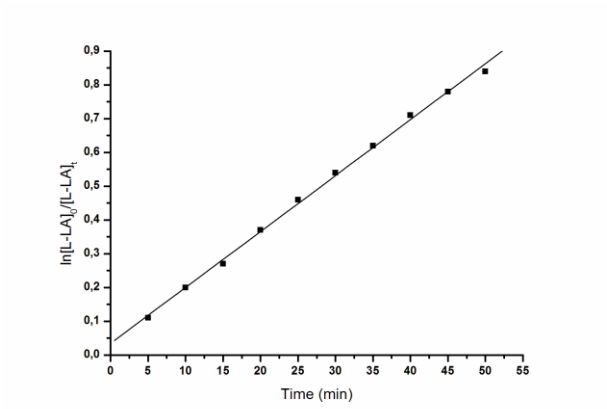

Figure 3.8. Pseudofirst-order kinetic plot for ROP of L-LA promoted by **6**. Pseudofirst-order rate costant is
(1,7 ± 0,02) $\times 10^{-2}$ min^{-1} (R= 0.99898, $[\mathbf{6}]_0$ = 3 mM, $[L\text{-}LA]_0$ = 0.6M; $[L\text{-}LA]_0/[\mathbf{6}]_0$ = 100; toluene-d_8 as solvent; T = 25°C)

Compound **6** was also tested for the ROP of *racemic* lactide (runs 16–18, Table 3.2) displaying equally good activity. The resulting polymers were prevailingly heterotactic with P_r values (probability of racemic linkages between monomer units) in the range 0.71–0.80.

It is worthwhile to note that the tacticity of the polymer is significantly influenced by the solvent and temperature used. For instance, changing the solvent from toluene to methylene dichloride at 25 °C resulted in an increase in P_r from 71 % to 77%. Lowering the temperature from 25 to 0 °C, P_r increased from 77% to 80%.

DFT computational analysis

In order to gain further insight into the role played by the coordinated pincer ligand in the ROP of ε-caprolactone and lactide, DFT computational analysis was carried out. [103]

The coordination of the monomer is a prerequisite for the insertion reaction, all attempts carried out on the metal complex with the k^3-coordinated pincer ligand finally led to the departing of the monomer from the metal centre. Whereas, it has succeeded in locate the coordination adducts between the metal complex and monomer only when the metal complex featuring the k^2-coordinated PPP ligand has been considered.

The intermediates and transition states we found are similar to those reported in literature.[112]

For demonstration, the reaction path for ring opening polymerization of caprolactone is given in Figure 3.9.

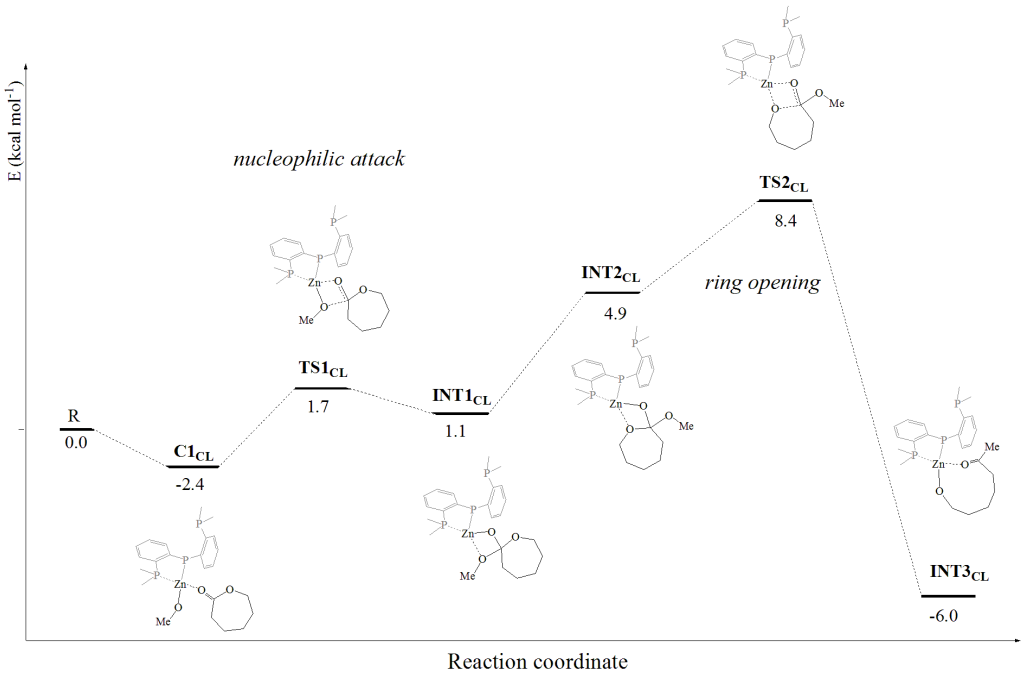

Figure 3.9. Calculated energy values (kcal mol^{-1}) for ring opening polymerization of ε-caprolactone.

The ring-opening starts with the nucleophilic attack of the initiating group at the carbonyl carbon of the coordinated monomer. This step corresponds to the C=O insertion into the Zn-OMe bond. The formed intermediate (**INT1$_{CL}$**) does not efficiently prepare the ring opening of the monomer, as no interaction between the endocyclic oxygen O_i of the monomer with the zinc is found. Rotation around the O_e–C vector next affords new intermediate (**INT2$_{CL}$**) which allows the O_i atom of the monomer units to approach the zinc in readiness for ring opening. Cleavage of the heterocycle then occurs on passing through the **second transition state**. The

dissociation of the carbonyl group allows the reorientation of the opened monomer molecule chain forming a species similar to the starting complex. The DFT calculations suggest that the k^2 coordination is an indispensable prerequisite for coordination of the monomer at the metal centre and for opening a straightforward reaction pathways at the metal centre. Thus the hemilabile character of the ligand is a crucial factor for the reactivity of the metal catalytic system.

3.2.4 Random Copolymerization of L-Lactide and ε-Caprolactone

To gain further insight into the ROP of cyclic esters by phosphido zinc complexes, the behavior of complex **6** in the random ε-CL/L-LA copolymerization was investigated. (Scheme 3.6)

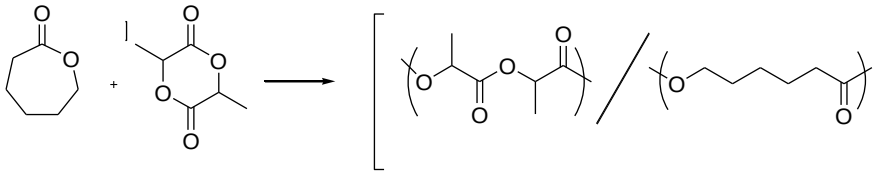

Scheme 3.6: Random copolymerization of L-Lactide and ε-Caprolactone initiated by complex **6**

The polymerizations were carried out in the melt at 110 ° C at various molar ratio of L-lactide and ε-caprolactone. The products were characterized by ^{13}C and ^{1}H NMR, GPC, and DSC. The results of these random copolymerizations are summarized in Tables 3.3

Table 3.3. Copolymerization of L-Lactide and ε-Caprolactone by **(6)**

Run	[LA]/[CL]	Con (%)[a]	%LA[a] in polymer	% LA-CL[a] heterodiadi	Mn^{b}_{GPC} (kDa)	Mn^{c}_{th} (kDa)	PDI[b]
19	0/100	0/100	0	0	338,3	22,8	3,18
20	10/90	100/87	6	9	229,3	20,8	2,46
21	30/70	100/73	25	40	176,2	20,3	2,50
22	50/50	100/82	40	57	93,5	23,8	3,31
23	70/30	100/77	62	78	185,7	25,5	2,20
24	90/10	98/63	91	35	95,2	26,8	4,25
25	100/0	100/0	100	0	187,2	28,8	2,88
26[e]	50/50	92/35	61	68	216.1	17.3	1.80
27[d]	50 /50	100/77	42	69	67,4	46,2	1,70
28	50/50	100/76	44	63	204,9	46,1	2,12

All reactions were carried out in the melt at 110°C, for 1 hour, using 10 μmol of (6) and [M]/[I] = 200. [a]Obtained from ^{1}H NMR spectroscopy. [b]Experimental M_n and PDI values determined by GPC in THF using polystyrene standards [c]Theorical Mn = [(M/I) × (% conversion of L-lactide) × (mol wt of L-lactide)] + [(% conversion of ε-caprolactone) × (mol wt of ε-caprolactone)]. [d] [M]/[I] = 400 and reaction time = 15 hours.[e] Reaction time = 10 minutes.

The chemical compositions of the copolymers were determined by ^{1}H NMR spectroscopy through the ratio between the intensity of methylene signal (observed around 4.00 ppm) of the CL segment and the values of the methine signal of polylactide (around 5.20 ppm).(Fig.3.10)

The percents of lactide and ε-caprolactone units in the polymer chains corresponded well with the monomer feed ratios, (run 20-24, table 3.3), and

less with monomer-initiator ratio (run 22 vs run 28, table 3.3) and with the time of reaction, (run 22 vs run 27, table 3.3)

In all the cases, the percent conversion of lactide was 92-100%, while the percent conversion of ε-caprolactone ranged from 63 to 87% (Table 3.3).

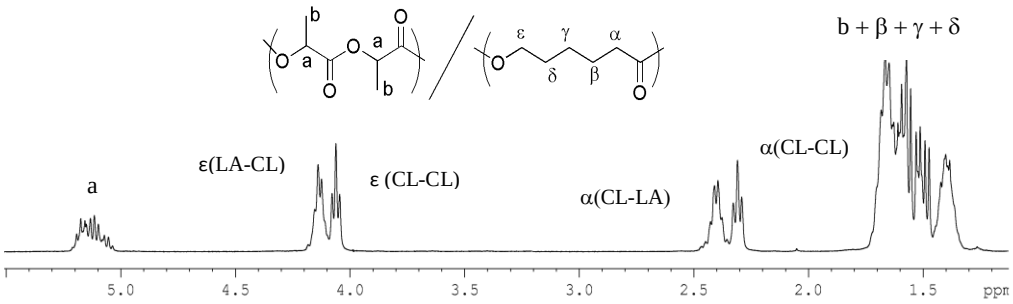

Fig. 3.10: ^{1}H NMR spectrum ($CDCl_3$, 25°C) of a copolymer L-LA/ε-CL, run 22, table 3.3.

This result is consistent with the reactivity of complex **6** toward the two monomers in the related homopolymerizations.

The percentage of CL-LA heterodiads in the copolymers was calculated by comparing the intensity of the signals of the methylene protons close to the carbonyl (-CH_2-C=O and -$COOCH_2$-) of the CL-LA heterosequences with the same methylene protons for the CL-CL homosequences, which appear at higher field (Fig 3.10)

The increase of the percentage of L-lactide in the feed from 0 to 100% resulted in the increasing of ε-caprolactone and lactide linkages as showed by the resonances assigned to ε(CL-LA) and α(CL-LA) that is indicative of a higher propensity for random copolymerization behavior.(Fig. 3.11)

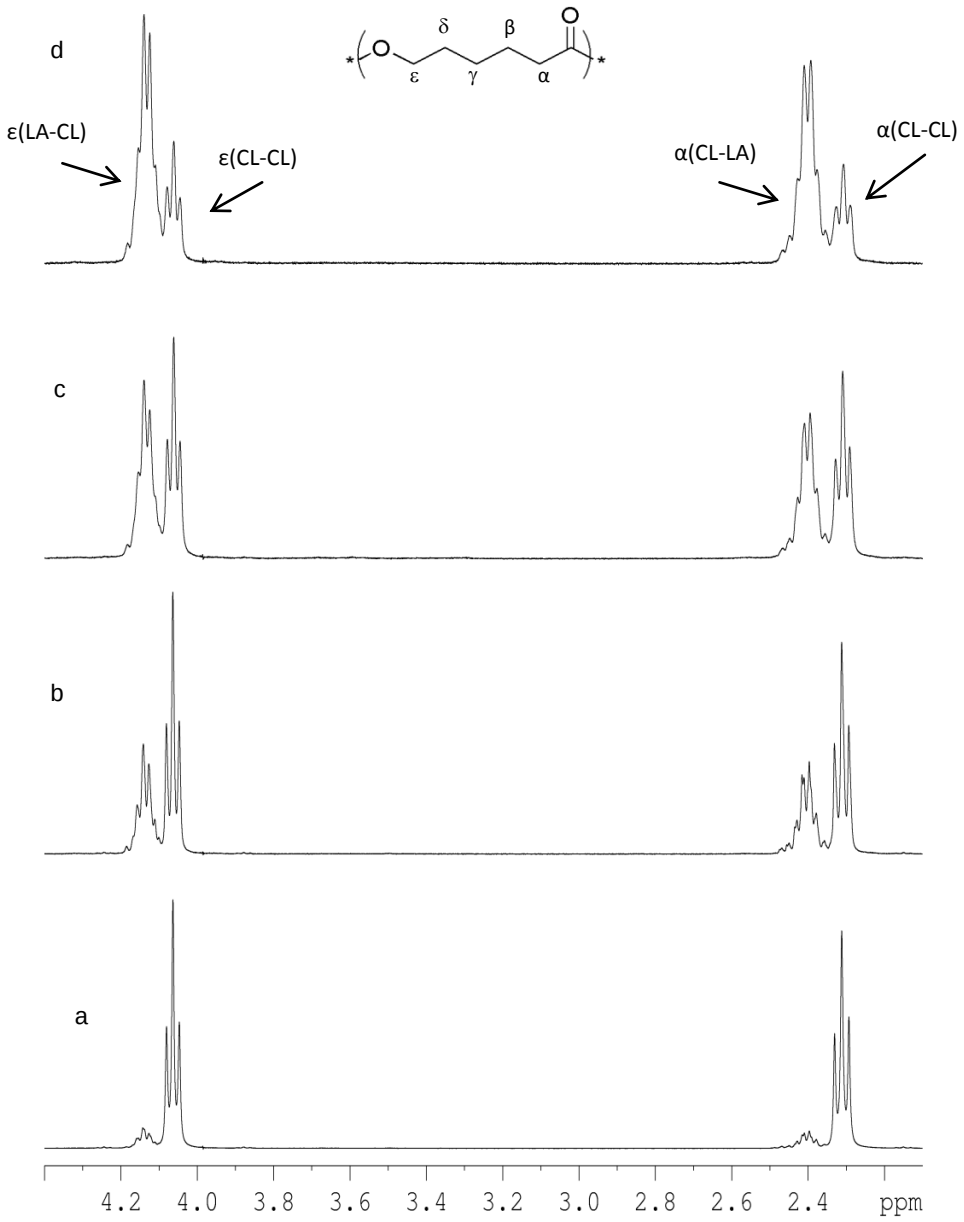

Fig 3.11: ^{1}H NMR ($CDCl_3$, 25°C) spectra of the copolymers showing the e- and a-methylene ranges in the copolymers of run 20 (a), run 21 (b), run 22 (c) and run 23 (d) in table 3.3.

In addition, the chain microstructures of the copolymers were assessed by analysis of the carbonyl region of the ^{13}C NMR spectra (between 174 and 172 ppm). The ^{13}C NMR spectra of the copolymers obtained by runs 21 and 22 are shown in Figure 3.12. The resonances were assigned according to the reported literature.[113] In particular, the resonances of the carbonyl region (between 175 and 165 ppm) are very sensitive to the chemical environments and the triads sequences signals have been used to calculate the average length of the blocks.[114]

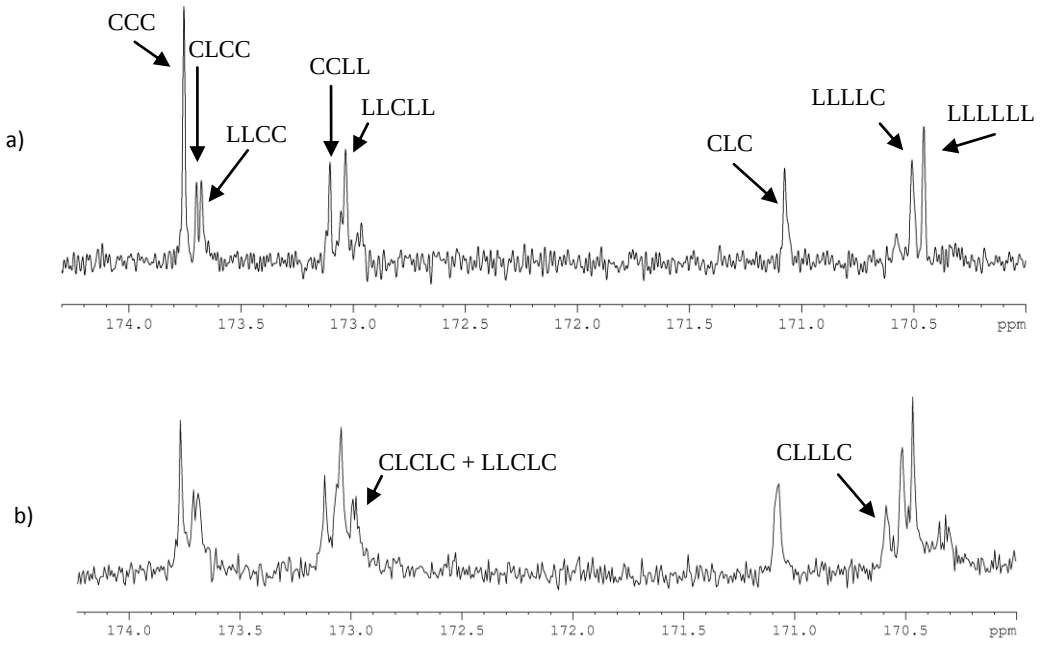

Figure 3.12. Carbonyl range of ^{13}C NMR spectrum ($CDCl_3$, 25 °C) of copolymers obtained in run 21 (a) and 22 (b) of Table 3.3.

Also the ^{13}C NMR analysis confirm a random copolymerization behavior and an average length of the blocks of both monomers close to two [114, 115] was found.

A weak resonance at 171.1 ppm, relative to the carbonyl group of a sequence of type CL-LA-CL in which a single "lactic" ester unit was flanked by two unit of caprolactone, was detected. This is evidence that transesterification reactions can occur during the polymerization process and they contribute to the randomization of the copolymers' structures.[110]

This is also confirmed by the quite large polydispersity indexes observed for these copolymers, (2.20 – 4.25).

The thermal properties of the copolymers were analyzed by differential scanning calorimetry. (DSC). The thermal parameters such as melting temperature and glass transition temperature are listed in Table 3.4 for polycaprolactone, polylactide, and their copolymers.

Table 3.4. Thermal Properties of Copolymers of L-Lactide and ε-Caprolactone by (**6**)

Run	% LA[a]	Tg[b] (°C)	Tg[c] (°C)	Tc[b] (°C)	Tm[b] (°C)
29	0	-59	-59	30	58
30	6	-53	-53	8	40
31	25	-31	-34	n.d.	n.d.
32	40	-19	-18	n.d.	n.d.
33	62	9	6	n.d.	n.d.
35	91	42	43	98	152
35	100	55	55	108	163

[a]Obtained from ^{1}H NMR spectroscopy. [b]The glass transition temperature (Tg), the crystallization temperature (Tc), and the melting temperature (Tm) of copolymers were determined from the second heating at heating rate of 5 °C/min. [c]Theorical values calculated by Fox equation according to the literature report.[25]

Three copolymers obtained are amorphous (runs: 21, 22, 23, table 3.3 and 3.4), while two copolymers show melting and crystallization points, (runs: 20 and 24, table 3.3 and 3.4).

The thermal properties for the copolymers are very dependent on the composition of the monomers incorporated in the polymer chains. For example, the Tg of the copolymers increased, in a linear way, from -59°C (pure polycaprolactone) to 55 °C (pure polylactide) as the percent of lactide units in the copolymer increased (Figure 3.13) with a strict agreement between the experimental values and the values calculated from Fox law.

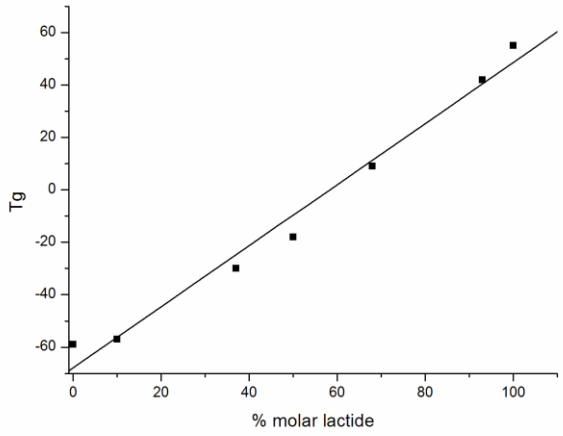

Figure 3.13: Plot of the dependence of Tg of the copolymers on the molar % lactide.

3.3 CONCLUSIONS

In this chapter, the preparation and characterization of new Zn(II) complexes of the type [(*o*-$C_6H_4PPh_2)_2P$ ZnR], (R= Et (**5**) or $N(SiMe_3)_2$ (**6**)), have been reported.

The ethyl zinc (**5**) and amido zinc (**6**) complexes were obtained by reaction of the opportune Zn precursor with one equivalent of proligand.

Both complexes have been obtained in a monoligaded form in which the pincer ligand is in a tridentate coordination mode.

Variable temperature ^{1}H and ^{31}P NMR studies highlighted a marked flexibility of the phosphido pincer ligand in the coordination at the metal center.

This is also evident in the crystal structure of the homoleptic [(*o*-$C_6H_4PPh_2)_2P]_2$-Zn complex **7**, obtained by reaction of the zinc precursor with two equivalents of proligand. This complex displays a nearly trigonal planar coordination geometry in which two different pincer ligands are present acting as bidentate and monodentate ligands respectively. This structure describes one of the rare examples of three-coordinate zinc complexes of phosphine and demonstrates the facility of the phosphido pincer ligand to adopt variable coordination geometries.

Catalytic studies demonstrated that both zinc complexes **5** and **6** are efficient initiators for the ring-opening polymerization of ε-caprolactone, under mild polymerization conditions.

Quantitative conversions of 200 equivalents were obtained in 100 minutes at 50°C, showing a productivity of about 10×10^3g PCL $(mol\ Zn)^{-1}h$, with relative narrow polydispersity indexes.

The molecular weight distributions of the polymers are monomodal, although the measured Mn values are several times larger than the calculated Mn values assuming the growth of one polymer chain per zinc-initiator.

Upon addition of alcohol, to generate *in situ* the alkoxide-Zn initiating specie, the activity and control on the polymerization were considerably improved.

Moreover, the use of several equivalents of alcohol as chain transfer agent allowed to obtained a number of polymer molecules proportional to the number of added alcohol equivalents. In this way, many equivalents of monomer have been converted using small amount of metal catalyst, increasing productivity.

Zinc amido complex (**6)** was also active in the polymerization of L- and rac-lactide, affording 70% conversion of 200 equivalents of the monomer within 1 hour at room temperature.

It showed good stereoselectivity for ROP of *rac*-lactide: heterotactic poly(lactic acid) with Pr up to 80% has been obtained.

Preliminary results showed that the amide zinc complex **6** is an active catalyst for the random copolymerization of L-lactide and ε-caprolactone. The NMR spettroscopic analysis of these complexes showed that the percents of lactide and caprolactone units in the polymer chains corresponded well with the monomer feed ratios. The thermal properties for the copolymers are very dependent on the composition of the monomers incorporated in the polymer chains. The Tg of the copolymers increased, in a linear way, from -59°C (pure polycaprolactone) to 55 °C (pure polylactide) as the percent of lactide units in the copolymer increased with a

strict agreement between the experimental values and the values calculated from Fox law.

In conclusion, the results of this work show that the incorporation of phosphide diphosphine ligand framework , for zinc-based complex, furnish an interesting coordinative flexibility of the ancillary ligand. A DFT study about the ring opening polymerization mechanism promoted by these zinc complexes highlighs the importance of the hemilabile behavior of ancillary ligand during the polymerization reaction for allowing a straightforward coordination of the monomer to the metal center.

This results have been reported in a work accepted by *Chemistry-A European Journal.*

4 ALUMINUM COMPLEXES

4.1 INTRODUCTION

Aluminum compounds have traditionally played an important role in the field of Ring Opening Polymerization of cyclic esters.

In particular, aluminum alkoxide [116] and aryloxides [117] based initiator systems are suited candidates for this kind of catalysis due to their high Lewis acidity and low toxicity [118]. Chelating ligands combining N- and O-donors, SALEN [119]- and SALAN [120]- type, have been involved in the design of well-defined aluminum complexes. This kind of aluminum initiators was found to be active for polymerization of lactones and lactides with excellent steroselectivity in polymerization of *rac*- and *meso*- lactide, (Fig.4.1).

Coates and Ovitt [119e] reported the only example of an efficient catalyst (**1a**) for the preparation of highly syndiotactic polylactide from *meso*-lactide.

Spassky's catalyst [119a] (**1b**) and Feijen's catalyst [119b] (**2**) are the first chiral complexes described as highly selective for synthesis of isotactic PLA from polymerization of *rac*-lactide.

In comparison with the possibility to obtain isotactic stereoblock PLA with racemic mixture of chiral compound **2,** Nomura *et al.* [119c] reported the a achiral Al-based system (**3**) which is able to generate a highly stereoblock PLA from *rac*-lactide.

Gibson's catalyst [120] is the first SALAN ligand-based aluminium complex reported to able of producing isotactic PLA from *rac*-lactide.

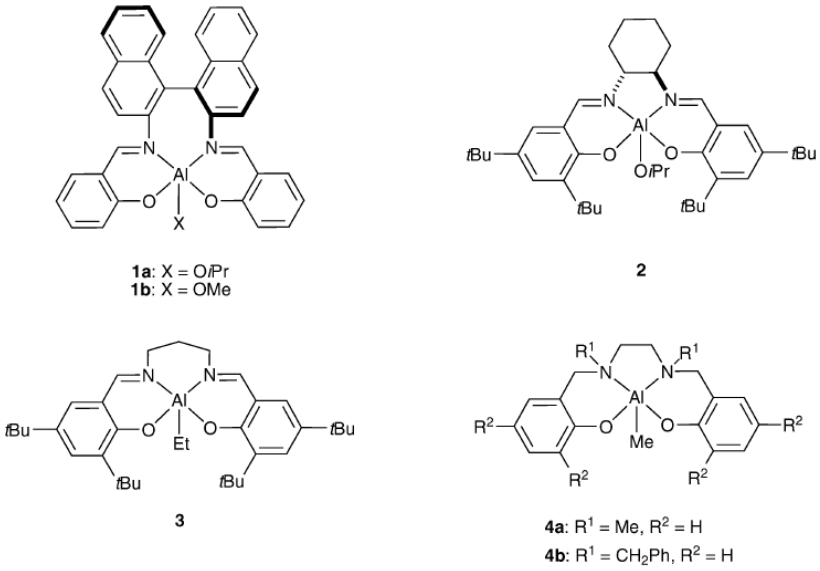

Fig.4.1:SALEN and SALAN aluminum complexes active in the ROP of lactones

Aluminium bearing polydentate ligands containing soft donors are definitively less investigated.

Recently Liang *et al.* explored the coordination chemistry of new amido phosphine aluminum complexes, in which the metal is stabilized by hybrid chelating ligands incorporating both hard and soft donors, such as bidentate [NP]- and tridentate [PNN]- ligands [121], (Fig.4.2).

However these aluminum complexes were investigated as initiators for catalytic α-olefin polymerization, whereas the examples of aluminum complexes with phosphorous-containing polydentate ligands are extremely rare in the ROP of cyclic esters.

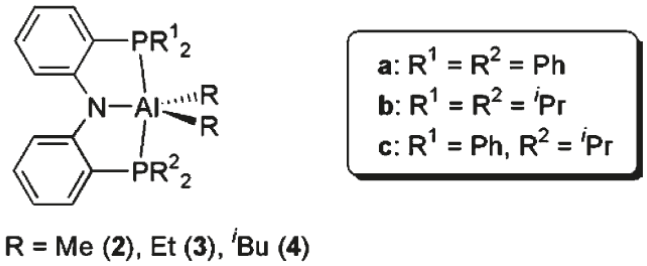

Fig:4.2: Amido diphosphine aluminum complexes

As an extension of the previous work, the use of phosphide pincer ligand to the coordination chemistry of aluminum has been extended.

New aluminum complexes of the type [(κ^3-(R)PPP)Al(R')] (PPP-H: = bis (2 diphenylphosphinophenyl)-phosphine and bis(2 diisopropylphosphinophenyl)-phosphine) have been synthesized and characterized.

Then their ability as catalysts for ROP of cyclic monomers, *L*- and *rac*-lactide, and ε-caprolactone has been studied.

4.2 RESULTS AND DISCUSSION

4.2.1 Synthesis and Characterization of Complexes

The synthesis of the aluminum complexes **8-10** is described in scheme 4.1. Alkane elimination reactions of the proligands and an equivalent of AlR_3 in dry toluene at 90 °C produced the corresponding dialkyl complexes [R'-PNP]- AlR_2 : R=Me, R' = Ph (**8**); R=Me, R' = iPr (**9**), R=iBu, R' = Ph (**10**).

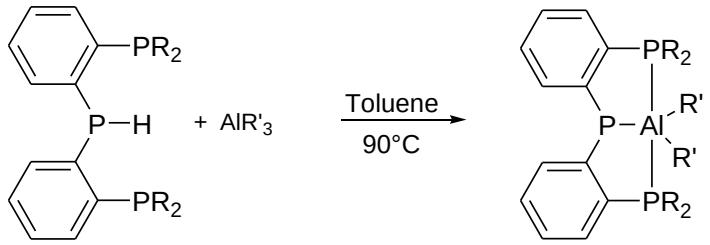

Complex	R	R'
8	Ph	CH_3
9	iPr	CH_3
10	Ph	iBu

Scheme 4.1: Synthesis of the aluminum complexes **8-10**.

The volatiles were removed under reduced pressure and all organoaluminum complexes were isolated, after crystallization in THF, as colorless or pale-yellow solids in high yields.

All complexes **8-10** were characterized by NMR spectroscopy (^{1}H, ^{13}C, ^{31}P NMR) and elemental analysis.

All aluminum complexes are soluble in hydrocarbon solvents, they are extremely sensitive to air and moisture but stable under an inert atmosphere for a prolonged period of time, even at elevated temperatures.

NMR and elemental analysis were being coherent with structures consisting of one *PPP* pincer ligand and two alkyl groups at the metal centre. The solution NMR data are all consistent with a high symmetric five-coordinate structure, in which the phosphido diphosphine ligand is coordinated in a tridentate fashion and the two alkyl groups are equivalents.

The ^{1}H NMR spectrum of complex **8** (C_6D_6, RT), (Fig. 4.3) showed a single signal in the aliphatic region, attributable to the protons of the methyl groups bound to the metal center. The multeplicity of the methyl signal (a triplet of doublets), is ascribable to the coupling with the phosphorous atoms of the ligand.

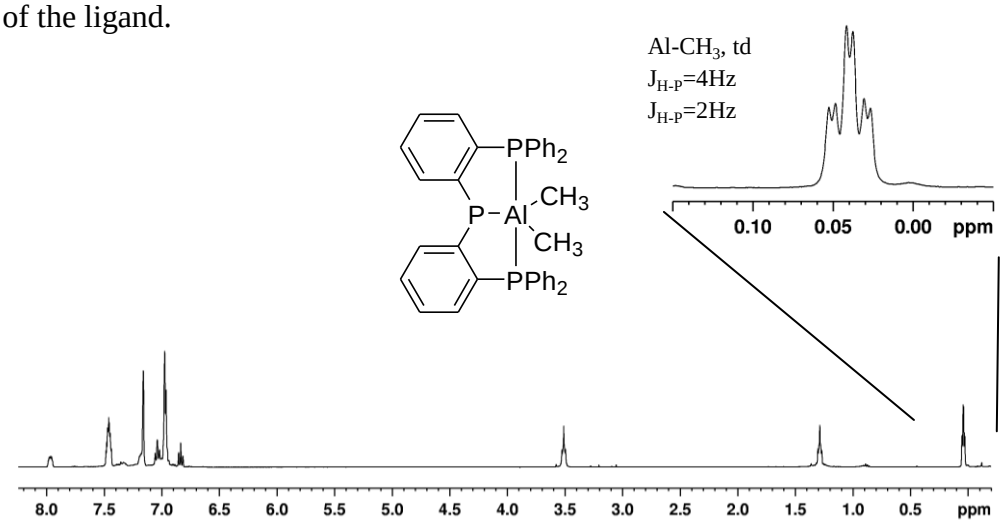

Fig.4.3: ^{1}H NMR spectrum of complex **8** in C_6D_6 at room temperature with an enlargement of the aliphatic region.

The ^{31}P MR spectrum supported the hypothesis of a κ^3 pincer ligand showing only two signals: a doublet for the neutral phosphorous donors, at δ = -16.38 ppm, and a triplet for the anionic phosphido ligand, at δ = - 61.93 ppm, (Fig. 4.4). These signals are upfield shifted relative to the corresponding ligand precursor (δ = -10.9 ppm and δ = -53.8 ppm).

Analogous shifts were observed for diarylamido diphosphine aluminium complexes reported by Liang.[121]

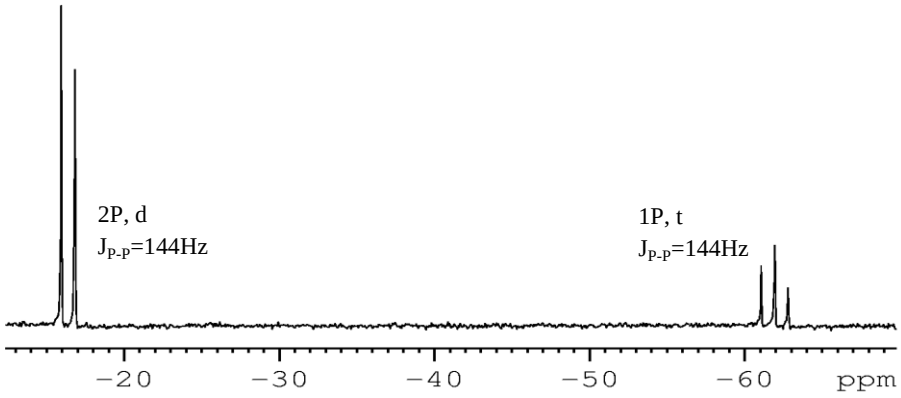

Fig. 4.4: 31P{^{1}H} NMR spectrum of complex 8 (161.97 MHz, C_6D_6).

Coherently, in the $^{13}C\{^1H\}$NMR spectrum a triplet of doublets was observed at δ = -7.02 ppm for the equivalents α-carbons of the methyl groups thus further confirming the κ^3-coordination of the phosphido ligand at the metal centre.

The NMR analysis of complexes **9** and **10** showed that they exhibited, in benzene-d_6 solution, the same symmetry discussed for complex **8**. In the $^{31}P\{^1H\}$NMR spectra single resonances (doublets) for the neutral phosphorous donors (δ= -6.29 ppm and -11.18) and a triplet for the anionic

phosphido donor at -65.20 ppm -57.75 were observed for **9** and **10** respectively.

The α-carbons of complex **9** showed a ^{13}C chemical shift, at δ = -6.30 ppm, relatively downfield as compared to that observed for the [Ph-PPP] methyl aluminium derivative. This difference is attributable to bulkier and more electron-releasing properties of the isopropyl substituents. [122]

4.2.2 Ring-Opening Polymerization of ε-caprolactone (ε-CL)

The phosphido pincer aluminium complexes **8-10** were tested as initiators for the ROP of ε-caprolactone (see Scheme 4.2) under a variety of polymerization conditions.

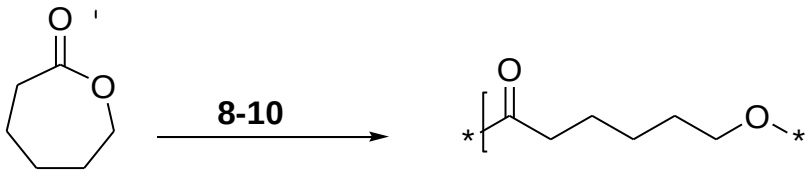

Scheme 4.2: Ring-opening polymerization of ε-caprolactone initiated by complexes **8-10**

Representative results were summarized in Table 3.1. The obtained polymers were characterized by ^{1}H NMR and GPC analyses.

Aluminum complexes bearing Al-alkyl bounds are generally not active in the polymerization of cyclic esters. Infact, alkoxide initiators have to be generated in situ by alcoholysis of amido and alkyl complexes with alcohols.

Worth of noting, compounds **8-10** exhibit reasonable activity toward the ROP of ε-CL in the absence of alcohols (runs 1-4, Table 4.1). At room temperature complex **8** converted 150 equivalents of monomer in six hours, (run 1, table 3.1). A considerable increase in the reactivity was observed by reasing the reaction temperature thus almost quantitative conversions of 200 equivalents of ε-caprolactone were achieved in 75 min.

Table 4.1: Ring Opening Polymerization of ε-caprolactone by complex (**8**), [iPr-PPP]-$AlMe_2$ (**9**) and [Ph-PPP]-$Al(iBu)_2$ (**10**).

Run[a]	Cat	[iPrOH]/[I]	Solvent	Time (min)	Conv (%)	Mn[b] (kDa)	Mn_{th}[c] (kDa)	PDI
1[d]	**8**	0	toluene	360	74	17.6	16.9	1,51
2	**8**	0	toluene	75	88	77.7	20.1	1,89
3	**9**	0	toluene	75	53	17.1	12.1	1.30
4	**10**	0	toluene	180	100	26.9	22.8	1,67
5	**8**	2	toluene	5	84	13.6	9.6	1,10
6	**9**	2	toluene	5	81	10.8	9.2	1.20
7	**10**	2	toluene	75	100	11,6	22,8	1.30
8	**8**	4	toluene	5	100	5.3	5.7	1.15
9	**8**	10	toluene	5	70	2.7	1.6	1.12
10[d]	**8**	2	THF	120	43	3.3	3.7	1.20
11[d]	**8**	2	CH_2Cl_2	120	8	nd	nd	nd

[a]All reactions were carried out with $[I]_0$ = 5 mM and [ε-CL] = 1 M at 70°C. [b]Experimental M_n and M_w/M_n values (corrected using the Mark–Houwink factor of 0.58) were determined by GPC analysis in THF using polystyrene standards. [c]Calculated Mn of PCL (in $gmol^{-1}$) =114,13 x ([ε-CL]/[I_0 + iPrOH]) x conversion ε-CL. [d] Reactions performed at room temperature.

The labile alkyl groups directly bonding with aluminum significantly affected the catalytic activity. Complex **10,** bearing isobutyl labile substituents, showed significantly lower activity than methyl derivatives **8** and **9**, (run 2 vs run 4, table 4.1) This is in agreement with the lower nucleophilicity of bulkier alkyl groups and the consequent difference in the initiation efficiency.

The number averaged molecular weight (Mn) values of the resulting polymers from the complexes **8-10** initiated reactions were in agreement with the calculated molecular weight (Mth) values assuming the growth of one polymer chain per aluminium-initiator. The molecular weight distributions were monomodal, although quite large polydispersity indexes were observed (PDIs =1.67-1.89).

Upon activation with isopropyl alcohol (iPrOH), the productivity of complexes was drastically improved (cfs 2-3 with 5-6 runs, Table 4.1). The addition of iPrOH is expected to generate *in situ* the more efficient alkoxide-Al initiating specie, thus higher conversions of the monomer were achieved. Additionally, a more efficient control on the molecular weights was also obtained as demonstrated by narrower distribution of molecular weights (PDI ranging from 1.10 to 1.20) and the good agreement between the theoretical and experimental values (runs 5-6, table 4.1).

The effect of the alcohol /monomer molar ratio was also examined. Increasing the alcohol/initiator ratio (10:1) polymer chains with reduced molecular weights and narrower polydispersities (PDI= 1.12) were achieved (run 9, Table 4. 1). This confirms that the excess of alcohol acts as an efficient chain transfer agent and that the growing chain/2-propanol exchange is very fast with respect to the chain propagation.

The influence of solvent on the polymerization of ε-CL was also investigated. The productivity was significantly depressed when the polymerization runs were performed in a more polar solvent (methylene dichloride) or in a coordinating solvent as THF (runs 10,11, table 4.1). This is often observed as a result of competitive coordination of the solvent onto the metal center that inhibits substrate coordination and polymerization.

To examine the effect of the monomer/initiator molar ratio on the ring-opening polymerization of ε-caprolactone a number of experiments with different monomer /initiator (M/I) molar ratios were carried out. The molecular weight Mn of the resulting polymers increase linearly with the increase in the M/I molar ratio (Fig. 4.5). This further proved the controlled character of the polymerization reaction.

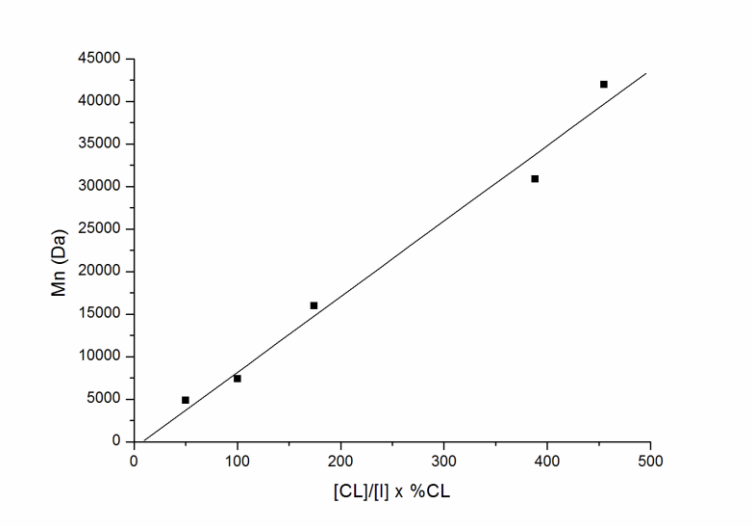

Fig.4.5: Linear relationship observed between Mn and monomer/ initiator ratio of polycaprolactone catalyzed by complex 8 at 70°C in toluene.

To establish the termination and initiation steps of the polymerization reaction, end-group analysis of low molecular weight PCL was performed by NMR spectroscopy. The ^{1}H NMR spectrum of the sample clearly showed a douplet at 1.22 ppm and a septet at 5.01 ppm, diagnostic of the isopropoxide chain-end group.(Fig.4.6)

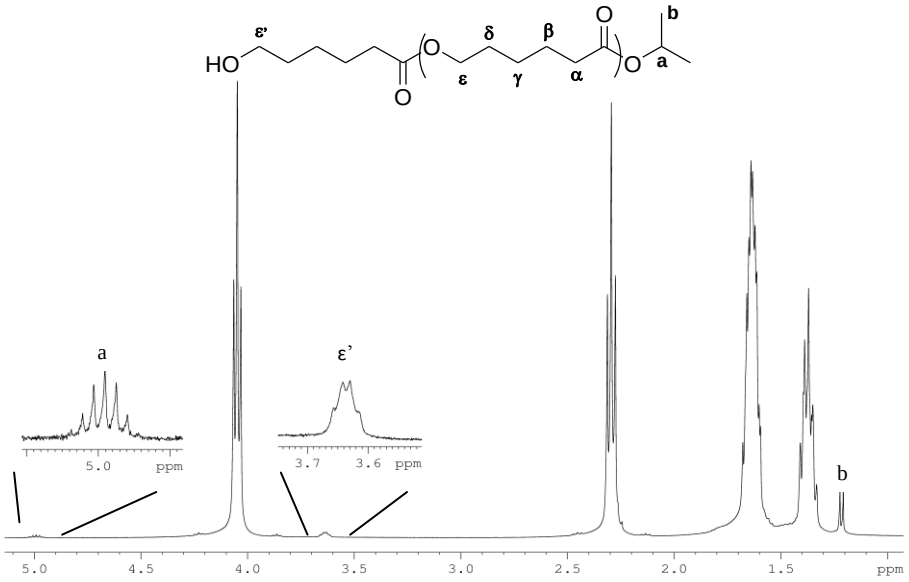

Fig.4.6: ^{1}H NMR spectrum (RT, $CDCl_3$) of a sample of the PCL with isoproxide chain-end group

Kinetic studies for the polymerization of ε-CL with complexes **8-10** were also performed to establish the reaction orders with respect to monomer. Conversion of the monomer with time was monitored by ^{1}H NMR in C_7D_8 until monomer consumption was almost completed (conversion>80 %).

Plots of ln($[\varepsilon\text{-CL}]_0/[\varepsilon\text{-CL}]$) versus time were linear, indicating that the polymerization processes are first-order in monomer concentration for all catalysts investigated.

For complex **8** the rate constants (k_{app}) for polymerizations of CL performed under the same polymerization conditions, in absence (Fig. 4.7) and in presence of two equivalents of alcohol (Fig. 4.8) were $2.15 \pm 0.05 \times 10^{-4}$ s^{-1} and $4.35 \pm 0.15 \times 10^{-3}$ s^{-1} respectively. The rate constant resulted about one

order of magnitudine higher when the polymerization was performed in presence of alcohol as activator.

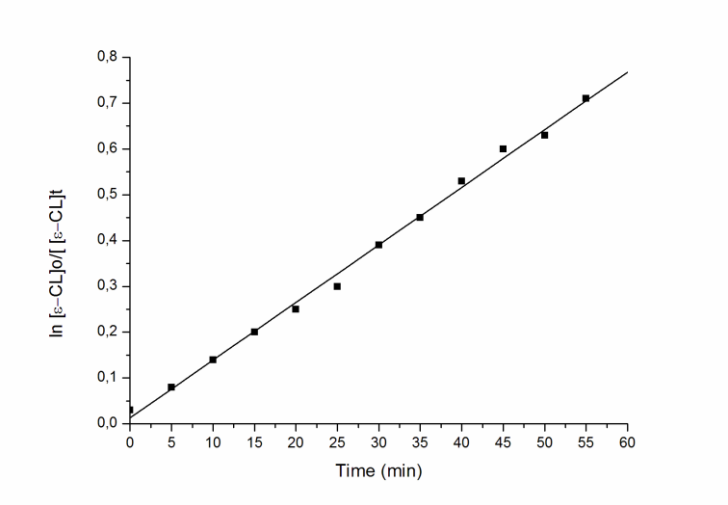

Figure 4.7. Pseudofirst-order kinetic plot for ROP of ε-CL promoted by **8** Pseudofirst-order rate costant is $k = (2.15 \pm 0.05) \times 10^{-4}$ s^{-1} $k = (1.29 \pm 0.03) \times 10^{-2}$ min^{-1} R = 0.996 ($[\mathbf{8}]_0$ = 6 mM, $[\varepsilon\text{-CL}]_0/[\mathbf{8}]_0$ = 100; toluene-d_8 as solvent; T = 50°C).

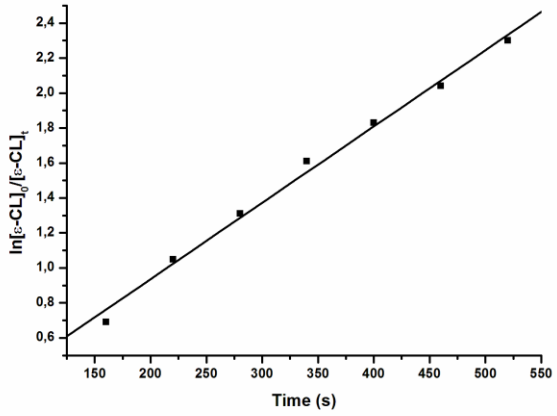

Figure 4.8: Pseudofirst-order kinetic plot for ROP of ε-CL promoted by **8** with [iPrOH]/[I] = 2 Pseudofirst-order rate costant is $k = (4.35 \pm 0.15) \times 10^{-3}$ s^{-1} R = 0.997 ($[\mathbf{8}]_0$ = 6 mM, $[\varepsilon\text{-CL}]_0/[\mathbf{8}]_0$ = 100; toluene-d_8 as solvent; T = 50°C).

The same effect on the reactivity was observed for complex **9** and **10**. The reaction kinetics, in presence of alcohol, feature a pseudofirst-order dependence in CL concentration: the semilogarithmic plots of $\ln([\varepsilon\text{-CL}]_0/[\varepsilon\text{-CL}]_t)$ versus time were linear with a slope of $(4.77\pm 0.22) \times 10^{-3}\ s^{-1}$ and $(1.01\pm 0.49) \times 10^{-3}\ s^{-1}$ for **9** and **10** respectively.

4.2.3 Ring-Opening Polymerization of of L-and rac-Lactide.

The polymerization of *L*-lactide and *rac*-lactide (Scheme 4.3) using the aluminum complexes **8** and **9** has been studied.

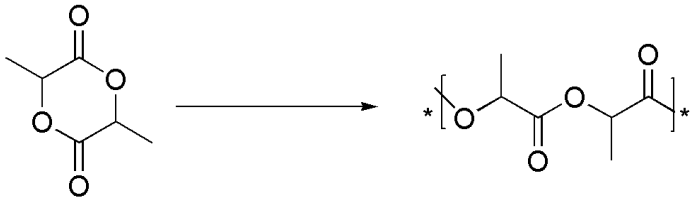

Scheme 4.3. Ring-opening polymerization of *L*- and *rac*-lactide initiated by complexes **8-9**

The reactions were carried out in toluene at 70 °C, and the representative polymerization results are summarized in Table 4.3. Low conversion of L-lactide was achieved from reaction initiated by complexes **8** after 16 h (run 18, table 4.2).

Table 4.2. ROP of L- and rac-lactide by complexes **8** and **9**.

Run[a]	**Cat**	**[iPrOH]/[I]**	**M**	**Time (h)**	**Conv (%)**	**Mn^{b}_{GPC} (kDa)**	**Mn^{c}_{th} (kDa)**	**PDI**[b]
12	8	0	L-LA	16	11	10,3	3,2	1,43
13	8	2	L-LA	16	76	4,3	7,3	1,12
14	9	2	L-LA	21	91	18.3	13.1	1.12
15	8	2	*rac*-LA	21	36	5.6	5.2	1.12
16	9	2	*rac*-LA	21	71	8.5	10.2	1.10

[a]All reactions were carried out with $[I]_0$ = 5 mM and [M] = 1 M in 2 mL of toluene at 70 °C. [b]Experimental M_n and M_w/M_n values (corrected using the Mark–Houwink factor of 0.58) were determined by GPC analysis in THF using polystyrene standards. [c]Calculated Mn of PLA (in $gmol^{-1}$) =144,13 x ([M]/[I_0 + iPrOH]) x conversion M.

The measured Mn value of the polymers produced is several times larger than the calculated Mc value with broad PDI, as already showed in the ROP of ε-caprolactone, because of the poor efficiency of the alkyl groups as initiators.

Upon activation with isopropyl alcohol complex **8** showed good activity in the ROP of lactide affording about 80% conversion of 200 equivalents of the monomer within 16 hours 70 °C in toluene solution. Moreover the experimental Mn value is in good agreement with the theorical one, Mn_{th}, assuming growth of one polymer chai per Al-initiator and with PDI of 1.12 (run 13, table 4.2) Similar activity was observed for complex **9** under the same reaction conditions, (run 14, table 4.2).

Polymerization of *rac*-lactide was explored to evaluate the stereospecificty of polymerization. The aluminum complexes **8** and **9** showed catalytic activity in polymerization of *rac*-lactide similar to that obtained for *L*-lactide. They show a good control of the molecular weights of the polymers

and PDI of 1.1. The homonuclear decoupled ^{1}H NMR spectra of the methine region of the PLA samples revealed a slightly heterotactic microstructure with a Pr [123] values of about 60%

4.3 CONCLUSIONS

In this chapter new alkyl aluminum complexes supported by phosphide phosphine pincer ligands, [(*o*-$C_6H_4PR_2)_2PH$; **L1**-H: R = Ph; **L2**-H: R = iPr], has been prepared.

All complexes, [LAlR], [L = **L1** and R = Me (**8**); L = **L2** and R = Me (**9**); L = **L1** and R = iBu (**10**)].were synthesized by alkane elimination reactions of the proligands with an equivalent of tris(alkyl) aluminum compound.

The solution NMR data are all consistent with a high symmetric five-coordinate structure of metal complexes, in which the phosphido diphosphine ligand is coordinated to metal in a tridentate fashion.

Aluminum complexes (**8**-**10**) have been tested in the ROP of L-, rac-lactide and ε-caprolactone.

All compounds resulted active initiators for the ROP of ε-CL at room temperature in toluene, converting 150 equivalents of monomer in six hours. A considerable increase in the reactivity was observed by raising the reaction temperature at 70°C, thus almost quantitative conversions of 200 equivalents of ε-CL were achieved in 75 minutes.

The experimental number averaged molecular weight (Mn_{exp}) values of the resulting polymers were in good agreement with those calculated (Mn_{th}) values assuming the growth of one polymer chain per Al-initiator.

These compounds represent a rare example of aluminum alkyl complexes active as catalyst in ROP of ε-caprolactone even without alcohol activation.

However the addition of alcohol in medium of reaction allowed to improve the activity and control on polymerization reaction. Almost quantitative conversions of 200 equivalents of monomer were achieved in just 5

minutes, obtained polymers with controlled molecular weights and very narrow polydispersity indexes (PDI = 1.1).

Aluminum complexes (**8**-**10**) showed also good activity in the polymerization of *L*- and *rac*-lactide, affording about 80% conversion of 200 equivalents of the monomer within 16 hours, at 70°C. The results proved a good molar-mass control of polymerization, indicative of a ‘‘single site’’ nature of the catalysts and of a ‘‘controlled- living’’ polymerization model.

They showed no stereocontrol on polymerization of *rac*-lactide: the obtained polymers exhibit a slightly heterotactic microstructures.

In conclusion, in this chapter the first examples of aluminum complexes bearing ancillary ligand pincer, with purely phosphorous atoms, have been reported.

Worth of noting all these pincer-based alkyl aluminum complexes have been shown active in the Ring Opening Polymerization of caprolactone and lactide, without alcohol activation.

These innovative polymerization studies highlight the possibility to develop new and original coordination environments for this kind of metal.

5 CONCLUDING REMARKS

The main objective of the whole research project work described in this PhD thesis is the exploration of a new class of ligands of pincer type as original coordinative environment for the design of new metal catalysts for the ring opening polymerization (ROP) of cyclic esters.

In this family of ligands, the anionic central donor is an unusual phosphido phosphorous atom flanked by two phosphine neutral donors. The choice to include in the ligand skeleton all donor atoms with "soft" character determined interesting consequences on the stability and reactivity of the different metal complexes investigated in this work.

For hard Lewis acid metals, such as the Group 3 metals, yttrium and scandium, the coordination of a chelating ligand with soft donors represented an innovative combination. The outcome of this has been an increased acidity of the metal centre with a considerable improvement of the activity of the catalytic species. The described yttrium complexes resulted, at the best of our knowledge, among the most active catalysts for the ring opening polymerization of ε-caprolactone.

For a "borderline" soft Lewis acid metal such as zinc, the coordinative flexibility of the phosphido donor, that can serve as an efficient σ and possibly π donor moiety, revealed to be crucial for the catalytic activity. In fact, NMR analysis and DFT calculations demonstrated that the coordination of the monomer at the reactive metal centre was possible thanks to the hemilability of the ligand in the coordination at the zinc. The pincer zinc complexes investigated in this work revealed to be efficient

initiators for the homopolymerization and for the random copolymerization of L-lactide and ε-caprolactone

They showed also good stereoselectivity for ROP of *rac*-lactide producing polymers with highly heterotactic microstructures.

The use of phosphorous based ancillary ligands in the coordination chemistry of aluminum is a scarcely explored field thus the phosphido pincer aluminum complexes described in this work represent one of the first examples.

All the synthesized alkyl aluminum complexes resulted to be active in the ROP of caprolactone and lactide and worth of noting, they showed significant catalytic activities also without alcohol activation. This behavior is quite uncommon for aluminum based catalysts. In fact, for the amido and alkyl aluminium derivatives the activation of the metal complex with an alcohol is an indispensable step to generate *in situ* the more efficient alkoxide-Al initiating specie.

The catalytic activity observed for the pincer-based alkyl aluminum complexes is probably due to the ability of the phosphido ligand to effectively transfer electronic charge at the metal center improving the nucleophilic character of the initiator group, thus favoring the initiation step by the alkyl group.

For all metal systems investigated, the phosphido pincer ligands provided high stability to the oxophilic metal centre allowing the use of these catalysts even in the presence of several equivalents of alcohol as chain agent without catalyst deactivation.

Operating under such “immortal” polymerization conditions (*i*ROP) offers clear advantages of optimizing the productivity and minimizing the contamination of polymer with metal residues.

All discussed results showed that this class ligands, based on purely “soft” donors can be a promising alternative to more traditional ligands with hard donors, such as N- and O-, abundantly reported in literature .

6 EXPERIMENTAL PROCEDURES

6.1 MATERIALS AND METHODS

All manipulations of air- and/or water-sensitive compounds were carried out under a dry nitrogen atmosphere using a Braun Labmaster drybox or standard Schlenk line techniques.

Glassware and vials used in the polymerization were dried in an oven at 120 °C overnight and exposed to vacuum-nitrogen cycle thrice. Hexane and THF (Carlo Erba) were purified by distillation from sodium benzophenone ketyl. Toluene (Carlo Erba) was purified by distillation from sodium. Dichloromethane and dichloromethane-d_2 were distilled over calcium hydride under a nitrogen atmosphere before use. Anhydrous yttrium trichloride and scandium trichloride (Aldrich) were used as received. Anhydrous yttrium trichloride and scandium trichloride (Aldrich) were used as received. Zinc-bis(trimethylsilyl)amide, Diethylzinc, $AlMe_3$, $Al(iBu)_3$ were purchased from Aldrich and used as received and all were stored in the glovebox.

The phosphido-diphosphine ligands [(o- $C_6H_4PR_2)_2P$-H; R = iPr; R = Ph] were prepared according to previously published procedures.

Lactide (Aldrich) was purified by crystallization from dry toluene and stored over P_2O_5. iPrOH was purified by distillation over sodium. Racemic β-butyrolactone, ε-CL, δ-valerolactone, and γ-valerolactone (Aldrich reagents) were dried with CaH_2 for 24 h at room temperature and then

distilled under reduced pressure. All other chemicals were commercially available and used as received unless otherwise stated.

6.2 INSTRUMENTS AND MEASUREMENTS

The NMR spectra were recorded on Bruker Avance 400 spectrometer (^{1}H, 400. MHz; ^{13}C, 100.62 MHz; ^{31}P 161.97 MHz) at 25 °C, unless otherwise stated.

Deuterated solvents were purchased from Cambridge Isotope Laboratories, Inc. and degassed and dried over activated 3 Å molecular sieves prior to use. Chemical shifts (δ) are listed as parts per million and coupling constants (*J*) in hertz. ^{1}H NMR spectra are referenced using the residual solvent peak at δ = 7.16 for C_6D_6 and δ = 7.27 for $CDCl_3$, δ= 5.32 for CD_2Cl_2. ^{13}C NMR spectra are referenced using the residual solvent peak at δ =128.39 for C_6D_6 and δ = 77.23 for $CDCl_3$.

^{31}P NMR spectra are referenced externally using 85% H_3PO_4 at δ = 0.00.

Elemental analyses were performed in the microanalytical laboratory of the institute.

The molecular weights (M_n and M_w) and the molecular mass distribution (M_w/M_n) of polymer samples were measured by GPC at 30 °C, using THF as solvent, flow rate of eluant 1 mL/min, and narrow polystyrene standards as reference. The measurements were performed on a Waters 1525 binary system equipped with a Waters 2414 RI detector using four Styragel columns (range 1000-1 000 000 Å). Every value was the average of two

independent measurements. It was corrected using the Mark–Houwink factor of 0.58 for polylactide and 0.56 for polycaprolactone according to the literature.

Electrospray ionization-mass spectrum (ESI-MS) were acquired using a Micromass Quattro micro API triple quadrupole mass spectrometer equipped with an electrospray ion source (Waters, Milford, MA). Acetonitrile was added to the samples, and the solutions were continuously infused into the electrospray ionization (ESI) ion source at a rate of 10 L/min using the instrument syringe pump. The LCQ ion source was operating at 4 kV, and the capillary heater was set to 100 °C. Nitrogen was used as nebulizing gas, damping gas and collision gas in the mass analyzer. Positive ion mode was used for all analyses. No cationizing agents were used for ESI measurements because Naþ, Kþ, and Hþ adduct ions were detectable at a high intensity. The origin of these alkali metals was apparently the ambient contaminants.

Glass transition temperatures (Tg), the crystallization temperature (Tc) and melting temperature (Tm) of the copolymers were measured by differential scanning calorimetry (DSC) using a DSC 2920 TA Instruments in nitrogen flow. Samples were first heated to 200°C at a rate of 10°C/min and cooled to 20°C for two cycles. The samples were then cooled to -100°C, by liquid nitrogen, followed by heating to 200°C at a heating rate of 5°C/min to determine their thermal properties (Tg, Tc, and Tm).

Density functional theory (DFT) calculations were performed with the program suite Gaussian 03.[71] All geometries were optimization without constraints at the BP86 level, i.e., employing the exchange and correlation functionals of Becke[72] and Perdew,[73, 74]respectively. The 6-31G(d) basis set was used all atoms. The structures of transition state between were

located by applying Schlegel's synchronous-transit-guided quasi-Newton (QST2) method as implemented in Gaussian 03. Single-point energies were computed at the BP86/6-311G(d,p) level using the previously DFT optimized structures to obtain more reliable energy values. Frequency calculations were performed on all structures to confirm that the reactants and products had no imaginary frequencies and that transition states possessed only one imaginary frequency. The relative energies, at 0 K, were thus corrected for vibrational zero-point energies (ZPE, not scaled). Cartesian coordinates of all DFT optimized structures are available on request.

Single crystals of **7**, suitable for X-Ray analysis were obtained at 253 K from an hexane/THF solution. Data collection was performed in flowing N_2 at 173 K on a Bruker-Nonius kappaCCD diffractometer (MoKα radiation, CCD rotation images, thick slices, φ scans + ω scans to fill the asymmetric unit). Cell parameters were determined from 326 reflections in the range $3.54° \leq \theta \leq 19.89$. Semiempirical absorbtion corrections (multi-scan SADABS) were applied. The structure was solved by direct methods (SIR 97 package) and refined by the full matrix least-squares method (SHELXL program of SHELX97 package) on F^2 against all independent measured reflections, using anisotropic thermal parameters for all non-hydrogen atoms. H atoms were placed in calculated positions with Ueq equal to those of the carrier atom and refined by the riding method. 712 refined parameters, $R_1 = 0.0864$; $wR_2 = 0.1744$ (on reflections with $I>2\sigma(I)$) and $R_1 = 0.2062$, $wR_2 = 0.2247$ on all reflections. Max. and min. residual electron density ($e \cdot Å^{-3}$): +0.713 and –0.541.

Crystallographic data for the structural analysis have been deposited with the Cambridge Crystallographic Data Center, CCDC N° 835164. Copies of

this information may be obtained free of charge from the Director, CCDC, 12, Union Road, Cambridge CB2 1EZ [Fax +44(1223)336-033] or e-mail deposit@ccdc.cam.ac.uk or http://www.ccdc.cam.ac.uk.

6.3 POLYMERIZATION EXPERIMENTS

Kinetic Experiments

In a Braun Labmaster glovebox, initiator solution from a stock solution in THF was injected to a 6-mL vial loaded with monomer and suitable amounts of dry solvent. After specified time intervals, a small amount of the polymerization mixture was transferred in a different via containing wet $CDCl_3$. The first fraction was subjected to monomer conversion determination which was monitored by integration of monomer versus polymer methine or methyl resonances in ^1H NMR ($CDCl_3$).

Oligomers for MALDI-TOF Measurements

To the stirred THF solution (1,5ml) of monomer (0.1M) the fresh prepared solution of metal complex (0.02M) in THF (0.5 mL) was injected at 20 °C ($[M]_0/ [I]_0 = 20$). The polymerization mixture was stirred for 15 min. and then quenched with hexane the precipitated oligomers were collected and dried in air and used for MALDI-TOF measurement.

6.3.1 Polymerization of ε-Caprolactone

A typical experiment, in a Braun Labmaster glovebox, a flask was charged sequentially with a solution of metal-complex in dry solvent, to which iso-propanol was eventually added, and monomer. The mixture was immediately stirred with a magnetic stir bar at required temperature for the

predicted time. After specified time an aliquot of the reaction mixture was sampled with a pipette for determining the monomer conversion by ^{1}H NMR spectroscopy ($CDCl_3$, 400 MHz). The reaction mixture was quenched by adding wet n-hexane. The polymer was then precipitated with excess n-hexane, filtered and further dried in a vacuum oven at 40 °C for 16 h.

6.3.2 Polymerization of L- and rac-Lactide

A typical experiment, in a Braun Labmaster glovebox, a 12-mL vial was charged with a solution of monomer in dry solvent and a solution of the metal initiator in dry solvent, to which *iso*-propanol was eventually added. The mixture was immediately stirred with a magnetic stir bar at required temperature for the predicted time. After specified time an aliquot of the reaction mixture was sampled with a pipette for determining the monomer conversion by ^{1}H NMR spectroscopy ($CDCl_3$, 400 MHz). The reaction mixture was quenched by adding wet *n*-hexane. The polymer was then precipitated with an excess of *n*-hexane, filtered and dried in a vacuum oven at 40 °C for 16 h.

6.3.3 Polymerization of δ-Valerolactone

In a typical experiment in a Braun Labmaster glovebox, a Schlenk flask was charged with a solution of metal initiator in toluene and a solution of the monomer in 2 ml of toluene. The mixture was stirred with a magnetic stir

bar at the required temperature. An aliquot of the crude material was sampled by pipette for determining monomer conversion by 1H NMR spectroscopy (CDCl3, 400 MHz), the reaction was quenched with wet n-hexane. The polymer was precipitated with excess n-hexane, then filtered, and dried in a vacuum oven at 60 _C for 16 h.

6.3.4 Polymerization of rac-β-Butyrolactone

In a typical experiment, in a Braun Labmaster glovebox, a Schlenk flask was charged with a solution of metal initiator in toluene, to which 2-propanol was possibly added, and β-butyrolactone. The mixture was stirred with a magnetic stir bar at 90 °C. An aliquot of the crude material was sampled by pipette for determining monomer conversion by ^{1}H NMR spectroscopy ($CDCl_3$, 400 MHz), the reaction was quenched with wet n-hexane. The polymer was precipitated with excess n-hexane, then filtered, and dried in a vacuum oven at 60 °C for 16 h.

6.3.5 Synthesis of Diblock PCL-PLA Copolymers

In a typical experiment, in a Braun Labmaster glovebox, a 6- mL vial was charged with a solution of metal initiator in 2 mL of toluene and ε-caprolattone. The solution was stirred for 5 min at room temperature. A solution of L-lactide in 2 mL of toluene was added to the mixture, which

was stirred for 15 min at room temperature. The resultant viscous mixture was quenched with wet n-hexane. The copolymer was precipitated with excess n-hexane, filtered, washed with methanol, and dried in a vacuum oven at 60 °C for 16 h.

6.3.6 Random Copolymerization of L-Lactide and ε-Caprolactone

In a typical experiment, in a Braun Labmaster glovebox, a flask equipped with a magnetic stirring bar was charged with metal-complex, L-Lactide and ε-caprolactone. The reaction mixture was stirred for 60 min at 110°C. After the reaction mixture was allowed to cool to room temperarure, 1 mL of $CDCl_3$ was added and the reaction mixture, the resulting solution was analyzed by ^1H NMR spectroscopy. The product was dissolved in CH_2Cl_2 and precipitated in n-hexane, then filtered and dried under vacuum oven at 40 °C for 16 h.

6.4.SYNTHESIS AND CHARACTERIZATION OF COMPLEXES

6.4.1 Synthesis and Characterization of [(o-$C_6H_4PPh_2)_2$P-$Y(CH_2SiMe_3)_2(THF)$]

Synthesis of $Y(CH_2SiMe_3)_3(THF)_2$

Anhydrous yttrium trichloride (586 mg, 3.00 mmol) was slurried in THF (30 mL) and stirred at 55 °C for 30 min. The solvent was removed in vacuo, and the solid residue was suspended in hexane (40 mL). The suspension was cooled to -78 °C, and a solution of $LiCH_2SiMe_3$ (856 mg, 9.10 mmol) in hexane (20 mL) was added. The suspension was stirred at 0 °C for 3 h. The reaction mixture was filtered, and the white solid was extracted with an additional 2 × 10 mL hexane. LiCl was filtered off, and the solvent was removed from the filtrate in vacuo to yield 1.22 g (82%) of colorless microcrystals. ^{1}H NMR (400 MHz, RT, C_6D_6): δ -0.71 (d, J_{Y-H} = 2.3 Hz, 6 H, Y*C*H_2), 0.27 (s, 27 H, Si*C*H_3), 1.30 (m, 8 H, THF), 3.93 (m, 8 H, THF). ^{13}C{^{1}H} NMR (100.62 MHz, RT, C_6D_6): δ 4.6 (Si*C*H_3), 25.0 (THF), 33.7 (d, J_{Y-C} = 35.7 Hz, Y*C*H_2), 70.8 (THF).

Synthesis and Characterization of [(o-$C_6H_4PPh_2)_2$P-$Y(CH_2SiMe_3)_2(THF)$]

A THF solution (3 mL) of (o-$C_6H_4PPh)_2$P-H ligand (0.170 g, 0.31 mmol) was added slowly into a THF solution (2 mL) of [$Y(CH_2SiMe_3)_3(THF)_2$] (0.152 g, 0.31 mmol), to give a red solution. After being stirred for 60 min, all volatiles were removed in vacuum, and the residue red solid was washed

with cold hexane and then dried up at reduced pressure for 3 h. Yield 0.266 g (98%). The crude solid was recrystallized from hexane at -20 °C (Yield after crystallization 63.4%).

^{1}H NMR (400 MHz, RT, C_6D_6): δ 7.63 (m, 2H, Ar), 7.50 (m, 8H, Ar), 7.01–6.88 (14H, Ar), 6.83 (t, J_{H-H} = 7 Hz, 2H, Ar), 6.64 (t, J_{H-H} = 7, 2H, Ar), 3.62 (b, 4H, α-THF), 1.26 (b, 4H, β-THF), 0.23(s, 18H, $CH_2Si\mathit{Me_3}$), 0.11 (d, J_{Y-H} = 3 Hz, 4H,

$\mathit{CH_2}SiMe_3$).

$^{13}C\{^{1}H\}$ NMR (100.62 MHz, C_6D_6): δ 156.60 (s, Ar), 135,35 (s, Ar), 134.76 (s, Ar), 133.97 (s, Ar), 129.77 (s, Ar), 129.56 (s, Ar), 129.32 (s, Ar) 133.80 (s, Ar), 125.35 (s, Ar), 70.10 (s, 4C, α-THF), 41.54 (d, 2C, J = 40 Hz, $\mathit{CH_2}SiMe_3$), 25.71 (s, 4C, β-THF), 4.96 [s, 6C, $CH_2Si(\mathit{CH_3})_3$].

^{31}P NMR (161.97 MHz, RT, C_6D_6): δ 7.42 (q, 1P, $J_{Y-P} = J_{P-P}$ = 50 Hz), -1.04 (dd, 2P, J_{Y-P} = 29 Hz, J_{P-P} = 50 Hz).

ELEM. ANAL. (%) calcd for $C_{48}H_{58}OP_3Si_2Y$: C, 64.85; H, 6.58; found: C 64.93, H 6.41.

6.4.2 Synthesis and Characterization of $[(o\text{-}C_6H_4PPh_2)_2P\text{-}Sc(CH_2SiMe_3)_2(THF)]$

Synthesis of $Sc(CH_2SiMe_3)_3(THF)_2$

Anhydrous scandium trichloride (404 mg, 2.62 mmol) was slurried in THF (30 mL) and stirred at reflux for the night. The solvent was removed in vacuo, and the resulting solid residue was suspended in hexane (40 mL). The suspension was cooled to -78 °C, and a solution of $LiCH_2SiMe_3$ (741

mg, 7.87 mmol) in hexane (20 mL) was slowly added. The suspension was stirred at 0 °C for 3 h and at room temperature for an additional hour. The reaction mixture was filtered and the residual white solid was extracted with an additional 2 × 10 mL hexane. All organic solutions were collected and the solvent was removed in vacuo to yield 500 mg (71%) of colorless powder.

^{1}H NMR (400 MHz, RT, C_6D_6): δ -0.20 (s, 6 H, Sc*C*H_2SiMe$_3$), 0.28 (s, 27 H, Si*C*H_3), 1.34 (m, 8 H, THF), 3.98 (m, 8 H, THF).

Synthesis and Characterization of [(o-$C_6H_4PPh_2)_2$*P-Sc(*$CH_2SiMe_3)_2$*(THF)]*

A THF solution (3 mL) of (o-$C_6H_4PPh_2)_2$P-H ligand (0.120 g, 0.22 mmol) was slowly added into a THF solution (2 mL) of [Sc($CH_2SiMe_3)_3$($THF)_2$] (0.097 g, 0.22 mmol) to give a red solution. After being stirred for 60 min, all volatiles were removed in vacuum, and the residue red solid was washed with cold hexane and then dried up at reduced pressure for 3 h. Yield 0.180 g (91%) of complex was obtained. The crude product was recrystallized from hexane at -20 °C. Yield after crystallization 66%.

^{1}H NMR (400 MHz, RT, C_6D_6): δ 7.63 (m, 2H, Ar), 7.50 (m, 8H, Ar), 7.34 (m, 2H, Ar), 7.05–6.95 (m, 12H, Ar), 6.84 (t, J = 7.5 Hz, 2H, Ar), 6.64 (t, J = 7.5, 2H, Ar), 3.80 (b, 8H, α-THF), 1.33 0.72 (s 4H, *C*H_2SiMe$_3$). (b, 8H, β-THF), 0.19 (s, 18H, CH_2Si*Me*$_3$).

^{13}C{^{1}H} NMR (100.62 MHz, C_6D_6): δ 138.22 (d, J = 12 Hz, Ar), 135.52 (m, Ar), 134.77 (s, Ar), 134.62 (s, Ar), 134.45 (s, Ar), 134,25 (Ar), 133.42 (s, Ar), 129.48 (s, Ar), 129.29(Ar), 129.01 (Ar), 128.94 (Ar), 128.71 (Ar), 128.56 (Ar), 125.54 (Ar), 70.21 (s, 4C, α-THF), 47.92 (m, 2C, *C*H_2SiMe$_3$), 25.59 (s, 4C, β-THF), 4.33 (s,6C,CH_2Si(*C*$H_3)_3$).

^{31}P NMR (161.97 MHz, RT, C_6D_6): δ 11.81 (t, 1P, J_{P-P} = 44 Hz), -0.75 (d, 2P, J_{P-P} = 44 Hz).

ELEM. ANAL. (%) calcd for $C_{52}H_{66}O_2P_3$ Sc Si_2: C, 68.10; H, 7.25; found 68.25, 7.12.

6.4.3 Synthesis and Characterization of [(o-$C_6H_4P^iPr_2)_2$P-Y($CH_2SiMe_3)_2$(THF)]

A THF solution (3 mL) of (o-$C_6H_4PiPr_2)_2$P-H ligand (0.100 g, 0.24 mmol) was slowly added into a THF solution (2 mL) of [Y($CH_2SiMe_3)_3(THF)_2$] (0.118 g, 0.24 mmol), to give a red solution. After being stirred for 60 min, all volatiles were removed in vacuum, and the red solid residue was washed with cold hexane, and then dried up at reduced pressure for 3 h. Yield 0.174 g (97%) of complex was obtained. Compound was obtained as crystalline powder from n-hexane solution at -20 °C.

^{1}H NMR (400 MHz, RT, C_6D_6): δ 7.88 (m, J_{H-H} = 6Hz, J_{H-P} = 3Hz, 2H, Ar), 7.01 (m, 2H, Ar), 6.82 (m, 2H, Ar), 3.66 (b, 4H, α-THF), 2.23 (m, 4H, *CH*($CH_3)_2$), 1.40 (b, 4H, β-THF), 1.18 (dd, 12H, J_{H-H} = 15Hz, J_{H-P} = 6Hz, CH(*CH_3*)$_3$), 1.01 (dd, 12H, J_{H-H} = 15Hz, J_{H-P} = 6Hz, CH(*CH_3*)$_3$) 0.37 (s, 18H, CH_2Si*Me_3*), 0.03 (d, J_{Y-H} = 3 Hz, 4H, CH_2SiMe_3).

^{13}C{^{1}H} NMR (62.90 MHz, RT, C_6D_6): δ 157.63 (m, 2C ipso, Ar), 134.63 (m, 2C, o-PAr), 133.29 (m, 2C ipso, Ar), 132.58 (d, 2C, J = 2.5Hz, o-$PiPr_2$, Ar), 129.59 (d, 2C, J = 2.8Hz, Ar), 123.80 (s, 2C, Ar), 69.44 (s, 4C, α-THF), 44.24 (d,2C, J = 37Hz, *CH_2*Si($CH_3)_3$), 25.89 (s, 4C, β-THF), 24.0 [s, 4C, *CH*($CH_3)_2$], 19.99 [s, 8C, CH(*CH_3*)$_2$], 5.10 [s, 6C, CH_2Si(*CH_3*)$_3$].

^{31}P NMR (161.97 MHz, RT, C_6D_6) d 19.25 (q, 1P, $J_{Y\text{-}P} = J_{P\text{-}P} = 50$ Hz), 17.50 (t, 2P, $J_{Y\text{-}P=}$ 56 Hz, $J_{P\text{-}P} = 50$ Hz).

ELEM. ANAL. (%) calcd for $C_{36}H_{66}OP_3Si_2Y$: C, 57.43; H, 8.84; found C, 57.58; H, 8.78.

6.4.4 Synthesis and Characterization of [(o-$C_6H_4P^iPr_2)_2$P-Sc($CH_2SiMe_3)_2$(THF)]

A THF solution (3 mL) of (o-$C_6H_4PiPr_2)_2$P-H ligand (0.250 g, 0.60 mmol) was slowly added into a THF solution (2 mL) of [Sc($CH_2SiMe_3)_3$(THF)$_2$] (0.270 g, 0.60 mmol) to give a red solution. After being stirred for 60 min, all volatiles were removed in vacuum, and the residual red solid was washed with cold hexane and then dried up at reduced pressure for 3 h. A sticky orange solid of complex was obtained. Yield 0.410g (96%).

^{1}H NMR (400 MHz, RT, C_6D_6): δ 7.85 (q, $J_{H\text{-}H} = 8$Hz, $J_{H\text{-}P}$ 0 3Hz, 2H, Ar), 7.03 (m, 2H, Ar), 6.90 (m, 2H, Ar), 6.84 (m, 2H, Ar), 3.82 (b,4H, α-THF), 2.25 (m, $J_{H\text{-}H} = 7$ Hz 4H, *CH*($CH_3)_2$), 1.39 (b, 4H, β-THF), 1.19 (m, 12H, $J_{H\text{-}H} = 7$ Hz, CH(*CH_3*)$_2$), 1.05 (dd, 12H, $J_{H\text{-}H} = 7$ Hz, CH(*CH_3*)$_2$) 0.31 (s, 18H, CH_2Si*Me_3*), 0.16 (s, 4H, *CH_2*SiMe_3).

^{13}C{^{1}H} NMR (75.47 MHz, C_6D_6): δ 142.20 (s, Ar), 132.06 (s, Ar), 131.90 (s, Ar), 130.09 (s, Ar), 130.06 (s, Ar), 128.58 (s, Ar), 128.01 (s, Ar), 127.70 (s, 2C, Ar), 123.33 (s, Ar), 123.30 (s, Ar), 68.27 (s, 2C, α-THF), 23.44 [s, 2C, *CH_2*Si($CH_3)_3$], 25.71 (s, 2, β-THF), 19.57 [s, 4C, *CH*($CH_3)_2$], 19.09 [s, 8C, CH(*CH_3*)$_2$], 1.46 [s, 6C, CH_2Si(*CH_3*)$_3$].

$^{31}P\{^{1}H\}$ NMR (161.97 MHz, RT, C_6D_6) δ 30.21 (t, 1P, J_{P-P} = 50 Hz), 14.67 (d, 2P, J_{P-P} = 50 Hz).

ELEM. ANAL. (%) calcd for $C_{36}H_{66}OP_3$ Sc Si_2: C, 60.99; H, 9.38; found: C, 60.75; H, 9.19.

6.4.5 Synthesis and Characterization of [(o-$C_6H_4PPh_2$)$_2$P-Zn(CH_2CH_3)]

A toluene solution (5 ml) of PPP-H =bis(2-diphenylphosphinophenyl)phosphine) ligand (200 mg, 0,4 mmol) was added slowly into a toluene solution (2 ml) of $ZnEt_2$ (99 mg, 0,8 mmol) at -20°C. The mixture was stirred at room temperature overnight. Volatiles were removed under vacuum and the residue was washed with cold hexane and then dried up at reduced pressure to afford a light yellow powder (0.215g, 83% yield).

^{1}H NMR (400 MHz, [C_7D_8] toluene, 25°C): δ 7.90 (m, 2H, Ar), 7.41 (br, 2H, Ar), 7.02-6.88 (m, 22H, Ar), 6.67 (t, 2H, J_{H-P} = 8 Hz, Ar), 1.78 (t, 3H, J_{H-H} = 8 Hz, ZnCH_2*CH_3*), 1.12 (m, 2H, Zn*CH_2*CH_3).

$^{13}C\{^{1}H\}$ NMR (100.62 MHz, [C_6D_6] benzene, 25°C): δ 157.56 (td, 2C, J_{C-P} = 42 Hz, Ar), 138.17 (dt, 2CH, J_{C-P} = 22 Hz, J_{C-P} = 4 Hz Ar), 136.95 (d, 2C, J_{C-P} = 42 Hz, Ar), 134.12 (d, 4CH, J_{C-P} = 16 Hz, Ar), 133.81 (s, 2CH, Ar), 129.94 (br, 4CH, Ar), 129.45 (d, 2CH, J_{C-P} = 6 Hz, Ar), 129.03 (br, 4CH, Ar), 126.53 (s, 2CH, Ar), 16.02 (s, C, -CH_2*CH_3*), 2.44 (q, C, J_{C-P} = 19 Hz, -*CH_2*CH_3). Some of the signals overlapped with the solvent.

^{31}P NMR (161.97 MHz, [C_6D_6] benzene, 25°C): δ -5.68 (d, 2P, J_{P-P} = 52 Hz), -50.32 (t, P, J_{P-P} = 52 Hz).

ELEMENTAL ANALYSIS calcd (%) for $C_{38}H_{33}P_3Zn$: C 70.44, H 5.13 found: C 70.89, H 5.23.

6.4.6 Synthesis and Characterization of $[(o\text{-}C_6H_4PPh_2)_2P\text{-}Zn(N(SiMe_3)_2)]$

A toluene solution (5 ml) of PPP-H =bis(2-diphenylphosphinophenyl)phosphine) ligand (150 mg, 0,3 mmol) was added slowly into a toluene solution (5 ml) of $Zn[N(SiMe_3)_2]_2$ (105 mg, 0,3 mmol). The mixture was stirred at 90°C for three hours. Volatiles were removed under vacuum and the residue was washed with cold hexane and then dried up at reduced pressure to afford a yellow powder (0.213g, 91% yield).

^{1}H NMR (400 MHz, [D_6] benzene, 25°C): δ 7.94 (br, 2H, H_a), 7.89 (br, 4H, H_g), 7.14 (t, 4H, $J_{H\text{-}H}$ = 7.6 Hz, H_f), 7.05 (t, 2H, $J_{H\text{-}H}$ = 7.2 Hz, H_e), 6.96 (br, 2H, H_d), 6.94 – 6.82 (m, 12H, H_b, $H_{e'}$, $H_{f'}$, $H_{g'}$), 6.66 (t, 2H, $J_{H\text{-}H}$ = 7.6 Hz, H_c), 0.44 (s, 18H, NSi(CH_3)$_3$).

^{13}C{^{1}H} NMR (100.62 MHz, [D_6] benzene, 25°C): δ 156.47 (td, 2C, $J_{C\text{-}P}$ = 40 Hz, $J_{C\text{-}P}$ = 20 Hz, Ar), 138.22 (dt, 2CH, $J_{C\text{-}P}$ = 23 Hz, $J_{C\text{-}P}$ = 4 Hz, Ar), 136.15 (2C, $J_{C\text{-}P}$ = 48 Hz, $J_{C\text{-}P}$ = 20 Hz, Ar) 135.42 (t, 4CH, $J_{C\text{-}P}$ = 7 Hz, Ph), 133.98 (d, 2CH, $J_{C\text{-}P}$ = 6 Hz, Ar), 133.57 (t, 4CH, $J_{C\text{-}P}$ = 6 Hz, Ph), 133.03 (m, 2C, Ar), 132.71 (m, 2C, Ar), 131.15 (s, 2CH, Ar), 129.74 (d, 2CH, $J_{C\text{-}P}$ = 7 Hz, Ar), 129.47 (d, 4CH, $J_{C\text{-}P}$ = 6 Hz, Ph), 128.77 (t, 4CH, $J_{C\text{-}P}$ = 4 Hz, Ph), 126.92 (s, 2CH, Ar), 6.81 (s, 3CH_3, NSi*(CH_3)$_3$*), 6.78 (s, 3CH_3, NSi*(CH_3)$_3$*).

^{31}P NMR (161.97 MHz, [C_6D_6] benzene, 25°C): δ -12.59 (d, 2P, J_{P-P} = 62 Hz), -53.46 (t, P, J_{P-P} = 62 Hz).

ELEMENTAL ANALYSIS calcd (%) for $C_{42}H_{46}P_3Zn$: C 64.73, H 5.95
found: C 64.92, H 5.33

6.4.7 Synthesis and Characterization of [(o-$C_6H_4PPh_2$)$_2$P]$_2$-Zn

A toluene solution (1 ml) of PPP-H =bis(2-diphenylphosphinophenyl)phosphine ligand (50 mg, 0,1 mmol) was added slowly into a toluene solution (1 ml) of $ZnEt_2$ (6 mg, 0,05 mmol) at room temperature. The mixture was stirred at 50 °C overnight. Volatiles were removed under vacuum and the residue was washed with cold hexane and then dried up at reduced pressure to afford a light yellow powder (0.091 g, 78% yield). Crystals suitable for RX analysis were obtained by recrystallization from a THF / hexane solution at -20 °C..

^{1}H NMR (400 MHz, [C_7D_8] toluene, 25°C): δ 7.93 (m, 4H, Ar), 6.95-6.70 (m, 48H, Ar), 6.56 (m, 4H, Ar),

^{31}P NMR (161.97 MHz, [C_7D_8] toluene, 25°C): δ – 13.87 (b, 4P), δ -54.90 (m, 2P)

^{31}P NMR (161.97 MHz, [C_7D_8] toluene, 80°C): δ – 12.96 (m, J_{P-P} = 52 Hz, 4P),

δ -52.96 (2 dd overlapped, J_{P-P} = 52 Hz, 2P)

ELEMENTAL ANALYSIS calcd (%) for $C_{72}H_{56}P_6Zn$: C 73.76, H 4.81
found: C 74.29, H 5.44

6.4.8 Synthesis and Characterization of $[(o\text{-}C_6H_4PPh_2)_2P\text{-}Al(Me)_2]$

To a toluene solution of Ph-PPP-H (0,4 mmol in 5ml of solvent), at room temperature, was added a solution of $AlMe_3$ (0,5mmol in 5ml of toluene).
The reaction solution was heated at 90°C with stirring overnight.
The resulting yellow solution was dried in vacuo to yield a pale yellow powder. The solid was dissolved in THF and allowed to stir at room temperature for 5 minutes. The volatiles were removed in vacuo and the resulting powder was washed with hexane and dried. (85% yield).
^{1}H NMR (400 MHz, C_6D_6): δ 7.97 (m, 2H, Ar), 7.46 (br, 8H, Ar), 7.04 (t, 2H, Ar, $J_{H\text{-}P}$= 7 Hz), 7.02 – 6.85 (br, 14H, Ar), 6.83 (t, 2H, Ar, $J_{H\text{-}P}$= 7 Hz), 0.04 (td, 6H, Al-*CH*$_3$, $^3J_{H\text{-}P}$= 4 Hz, $^3J_{H\text{-}P}$= 2 Hz).
$^{13}C\{^1H\}$ NMR (100.62 MHz, C_6D_6): δ 152.44 (dt, 2C_{ipso}, $J_{C\text{-}P}$ = 34.36 Hz, $J_{C\text{-}P}$ = 21.20 Hz, Ar), 133.97 (d, 8C, $J_{C\text{-}P}$ = 7.04 Hz, Ar), 133.86 (s, 2C, Ar), 133.22 (dt, 2Cipso, $J_{C\text{-}P}$ = 7.04 Hz, $J_{C\text{-}P}$ = 4.02 Hz, Ar), 133.30 (m, 4C_{ipso}, Ar), 129.62 (s, 4C, Ar), 129.55 (d, 2C, $J_{C\text{-}P}$ = 3.02 Hz, Ar), 128.92 (t, 8C, $J_{C\text{-}P}$ = 4.02 Hz, Ar), 128.54 (s, 2C, Ar), 125.88 (s, 2C, Ar), -7.02 (td, 2C, $J_{C\text{-}P}$ = 20.0 Hz, $J_{C\text{-}P}$ = 7.02 Hz, Al-*C*H$_3$).
^{31}P NMR (162.97 MHz, C_6D_6): δ -16.38 (d, 2P, $J_{P\text{-}P}$ = 144 Hz), -61.93 (t, 1P, $J_{P\text{-}P}$ = 144 Hz)
ELEMENTAL ANALYSIS calcd (%) for $C_{38}H_{34}AlP_3$: C 74.75, H 5.61 found: C 74.22, H 4.96.

6.4.9 Synthesis and Characterization of [(o-$C_6H_4P^iPr_2)_2$P-Al$(Me)_2$]

To a toluene solution of iPr-PPP-H (0,4 mmol in 5ml of solvent), at room temperature, was added a solution of $AlMe_3$ (0,5mmol in 5ml of toluene).
The reaction solution was heated at 90°C with stirring overnight.
The resulting yellow solution was dried in vacuo to yield a pale yellow powder. The solid was dissolved in THF and allowed to stir at room temperature for 5 minutes. The volatiles were removed in vacuo and the resulting powder was washed with hexane and dried. (80% yield).
^{1}H NMR (400 MHz, C_6D_6): δ 7.91 (m, 2H, Ar), 7.05 (m, 4H, Ar), 6.94 (m, 2H, Ar), 3.32, 2.18 (m, 4H, J_{H-H} = 11 Hz, C*H*$(CH_3)_2$), 1.08 (dd, 12H, J_{H-H} = 11 Hz, J_{H-P} = 24 Hz, CH(C*H*$_3)_2$), 1.02 (dd, 12H, J_{H-H} = 11 Hz, J_{H-P} = 24 Hz, CH(C*H*$_3)_2$), 0.14 (td, 6H, , J_{H-P} = 2 Hz, J_{H-P} = 6 Hz, Al-C*H*$_3$).
^{13}C{^{1}H} NMR (100.62 MHz, C_6D_6): δ 153.40 (m, 2C_{ipso}, Ar), 133.65 (m, 2C, Ar), 132.65 (m, 2C_{ipso}, Ar), 131.08 (d, 2C, J_{C-P} = 2 Hz), 128.26 (d, 2C, J_{C-P} = 4 Hz), 123.72 (m, 2C, Ar), 23.33 (d, 4C, J_{C-P} = 8 Hz, *C*H$(CH_3)_2$), 19.34 (m, 8C, CH(*C*H$_3)_2$), -6.30 (t, 2C, , J_{C-P} = 20 Hz, Al-*C*H$_3$).
^{31}P NMR (162.97 MHz, C_6D_6): δ -6.29 (d, 2P, J_{P-P} = 132 Hz), -65.20 (t, 1P, J_{P-P} = 132 Hz).
ELEMENTAL ANALYSIS calcd (%) for $C_{26}H_{42}AlP_3$: C 65.81, H 8.92 found: C 44.89, H 9.96.

6.4.10 Synthesis and Characterization of [(o-$C_6H_4PPh_2)_2P$-Al($^iBu)_2$]

To a toluene solution of Ph-PPP-H (0,4 mmol in 5ml of solvent), at room temperature, was added a solution of $Al[CH_2CH(CH_3)]_3$ (0,4mmol in 5ml of toluene).

The reaction solution was heated at 90°C with stirring overnight.

The yellow solution was dried in vacuo. The resulting powder was washed with cold hexane and dried to yield a pale yellow powder. (91% yield).

^{1}H NMR (400 MHz, C_6D_6): δ 7.68 (m, 2H, Ar), 7.53 (t, 8H, J_{H-P}= 7 Hz, Ar), 7.02 (m, 14H, Ar), 6.95 (t, 2H, J_{H-P}= 7 Hz, Ar), 6.80 (t, 2H, J_{H-P}= 7 Hz, Ar), 2.05 (m, 2H, , J_{H-H}= 6.4 Hz, Al-CH_2CH(C$H_3)_2$), 1.09 (d, 12H, J_{H-H}= 6.4 Hz, Al-$CH_2CH(CH_3)_2$), 0.69 (m, 4H, Al-$CH_2CH(CH_3)_2$).

$^{13}C\{^1H\}$ NMR (100.62 MHz, C_6D_6): δ 152.77 (m, $2C_{ipso}$, Ar), 142.98 (m, $2C_{ipso}$, Ar), 136.48 (m, $4C_{ipso}$, Ar), 134.82 – 134.24 (m, 8C, Ar), 130.04 (br, 2C, Ar), 129.95 (s, 4C, Ar), 129.25 (t, 4C, J_{C-P} = 6 Hz, Ar), 129.21 – 129.03 (m, 8C, Ar), 126.35 (s, 2C, Ar), 28.99 (s, 4C, Al-CH_2CH($CH_3)_2$), 27.73 (s, 2C, Al-$CH_2CH(CH_3)_2$), 23.10 (m, 2C, Al-$CH_2CH(CH_3)_2$).

^{31}P NMR (162.97 MHz, C_6D_6): δ -11.18 (d, 2P, J_{P-P} = 122 Hz), -57.75 (t, 1P, J_{P-P} = 122 Hz).

ELEMENTAL ANALYSIS calcd (%) for $C_{44}H_{46}AlP_3$: C 70.07, H 6.67 found: C 76.38, H 6.81.

REFERENCES

[1] a) *Biopolymers - Polyesters I Biological Systems and Biotechnological Production* (Eds.: Y. Doi, A. Steinbüchel), Wiley-VCH,Weinheim, **2002.**
b) *Biopolymers - Polyesters II Properties and Chemical Synthesis* (Eds.: Y. Doi, A. Steinbüchel), Wiley-VCH,Weinheim**, 2002;**
c) *Biopolymers - Polyesters III Application and Commercial Products* (Eds.: Y. Doi, A. Steinbüchel), Wiley-VCH,Weinheim**, 2002**
[2] S. Jacobsen, P. Degée, H. Fritz, P. Dubois, R. Jérôme, *Polym. Eng. Sci.* **1999**, 39, 1311-1319.
[3] M. Vert, *Biomacromolecules*, **2005**, 6, 538-546.
[4] O. Dechy-Cabaret, B. Martin-Vaca, D. Bourissou, *Chem. Rev.*, **2004**, 104, 6147-6176.
[5] O.Wolf, M. Crank, M. Patel, F. Marscheider-Weidemann, J. Schleich, B.Hüsing, G.Angerer, *Techno-economic Feasibility of Large-scale Production of Bio-based Polymers in Europe, tech. rep. EUR 22103 EN, European Commission*, **2005**
[6] *Bioplastic Magazine*, (Ed.: M. Thielen), **2006**, 26-27.
[7] B. Nagel, H. Dellweg, L. M. Gierasch, *Pure Appl. Chem*. **1992**, 64, 143–168.
[8] DIN V54900 *"PrKfung der Kompostierbarkeit von Kunststoffen"(*German standard test method "Probing the compostability of plastics").
[9] Ragauskas, A. J.; Williams, C. K.; Davison, B. H.; Britovsek, G.; Cairney, J.; Eckert, C. A.; Fredrick, W. J., Jr.; Hallett, J. P.; Leak, D. J.; Liotta, C. L.; Mielenz, J. R.; Murphy, R.; Templer, R.; Tschaplinski, T. "*The path forward for biofuels and biomaterials", Science* **2006**, 311, 484–489
[10] P. T. Anastas, J. C. Warner, *Green Chemistry: Theory and Practice*, Oxford University press, New York, USA, **1998**
[11] S. Mecking, *Angew. Chem. Int. Ed.*, **2004**, 43, 1078-1085.
[12] A. C. Albertsson, I. K. Varma, *Biomacromolecules*, **2003,** 4, 1466-1486.
[13] R. Auras, B. Harte, S. Selke, *Macromol. Biosci*., **2004**, 4, 835–864
[14] http://www.natureworksllc.com /. http://www.mitsui.com
[15] H. Kricheldorf, *Chemosphere*, **2001**, 43, 49–54
[16] J. O. Iroh, in *Polymer Data Handbook*, Ed. J. E. Mark, Oxford University Press, New York, **1999**, pp. 361–362.
[17] M. C. Rocca, G. Carr, A. B. Lambert, D. J. Mac Quarrie and J. H. Clark, S. A. Solvay, US patent 2003/6531615 B2, **2003**
[18] M. Minami and S. Kozaki, US patent 2003/0023026 A1, **2003.**
[19] V. R. Sinha, K. Bansal, R. Kaushik, R. Kumria and A. Trehan, *Int. J. Pharm*., **2004**, 278, 1–23
[20] R. A. Gross and B. Kalra, *Science*, **2002**, 297, 803–807
[21] P. Joshi and G. Madras, *Polym. Degrad. Stab*., **2008**, 93, 1901–1908.
[22] C. X. F. Lam, S. H. Teoh and D. W. Hutmacher, *Polym. Int*., **2007**, 56, 718–728

[23] D. W. Hutmacher, T. Schantz, I. Zein, K. W. Ng, S. Hin, T. Kim and C. Tan, J. *Biomed. Mater. Res*., **2001**, 55, 203–216.
[24] Y. Ikada and H. Tsuji, Macromol. *Rapid Commun*., **2000**, 21, 117–132.
[25] O. Coulembier, P. Deg ee, J. L. Hedrick and P. Dubois, *Prog. Polym. Sci.,* **2006**, 31, 723
[26] a)Chiellini, E.; Solaro, R. *Adv. Mater*. **1996**, 8, 305–313;
b) Qian, H.; Bei, J.; Wang, S. *Polym. Degrad. Stab*. **2000**, 68, 423–429;
c) Ghosh, S. J. *Chem. Res*. **2004**, 241–246
[27] a) Sinclair, R. G. USP 4045418; **1977**;
b) Sinclair, R. G. USP 40457537; **1977**.
[28] Wehrenberg, R.H. *Mater. Eng*.**1981**, 94, 63.
[29] a) Grijpma, D. W.; Hofslot, R. D. A.; Super, H.; Nijenhuis, A. J.; Pennings, A. *J. Polym. Eng. Sci*. **1994**, 34, 1674–1684.
b) Corbin, P. S.;Webb, M. P.; McAlvin, J. E.; Fraser, C. L. *Biomacromolecules* **2001**, 2, 223–232.
c) PCT Patent application PCT/NL93/00235, **1993.**
[30]) Schindler, A.; Jeffcoat, R.; Kimmel, G. L.; Pitt, C. G.; Wall, M. E.; Zweidinger, R. *In Contemporary Topics in Polymer Science*; Pearce, E. M., Schaefgen, J. R., Eds.; Plenum Press: New York, **1977**; Vol. 2, p 251;
b) Song, C. X.; Sun, H. F.; Feng, X. D. *Polym. J* **1987**, 19 (5), 485–494
[31] a) Song, C. X.; Feng, X. D. *Macromolecules* **1984**, 17, 2764–2767.
b) Qian, H. T.; Bei, J. Z.;Wang, S. G. *Polym. Degrad. Stab*. **2000**, 68, 423–429.
c) Huang, M. H.; Li, S. M.; Coudane, J.;Vert, M. *Macromol. Chem. Phys*. **2003**, 204, 1994–2001.
d) Jeon, O.; Lee, S.-H.; Kim, S. H.; Lee, Y. M.; Kim, Y. H. *Macromolecules* **2003**, 36, 5585–5592.
e) Lahcini, M.; Castro, P. M.; Kalmi, M.; Leskala, M.; Repo, T. *Organometallics* **2004**, 4547–4549.
f) Wang, J. L.; Dong, C. M. Macromol. *Chem. Phys*. **2006**, 207, 554.
g) Zhao, Z. X.; Yang, L.; Hu, Y. F.; He, Y.; Wei, J.; Li, S. M. *Polym. Degrad. Stab*. **2007**, 92, 1769–1777.
h)Wie, Z.; Liu, L.;Yu, F.;Wang, P.; Qu, C.; Qi, M. *Polym. Bull*. **2008**, 61, 407–413.
[32] a) Vanhoorne, P.; Dubois, Ph.; Jerome, R.; Teyssie, Ph. *Macromolecules* **1992**, 25, 37–44.
b) Shen, Y.; Zhun, K. J.; She, Z.; Yao, K.-M. *J. Polym. Sci., Part A: Polym. Chem*. **1996**, 34, 1799–1805.
c) Bero, M.; Kasperczyk, J. *Macromol. Chem. Phys*. **1996**, 197, 3251–3258.
d) Hiljanen-Vainio, M. P.; Orava, P. A.; Seppala, J. V. J. Biomater. *Mater. Res.* **1997**, 34, 39–46.
e) Kister, G.; Cassanas, G.; Bergounhon, M.; Hoarau, D.; Vert, M. *Polymer* **2000**, 41, 925–932.
f) Baimark,Y.; Molloy, R. *ScienceAsia* **2004**, 30, 327–334.
g) Fay, F.; Renard, E.; Langlois, V.; Linossier, I.; Vallee-Rhel, K. *Eur. Polym. J*. **2007**, 43, 4800–4813.
h) Calandrelli, L.; Calarco, A.; Laurienzo, P.; Malinconico, M.; Petillo, O.; Peluso, G. *Biomacromolecules* **2008**, 9, 1527–1534.

[33] W. H. Carruthers, G. L. Dorough, F. J. van Natta, *J. Am. Chem. Soc*., **1932**, 54, 761-772.
[34] C. Braud, R. Devarieux, A. Atlan, C. Ducos and V. Michel, *J. Chromatogr., B: Biomed. Sci. Appl.*, **1998**, 706, 73–82
[35] N. Kawashima, S. Ogawa, S. Obuchi, M. Matsuo, T. Yagi in *Biopolymers, Vol. 4* (Eds.: A. SteinbKchel, Y. Doi), Wiley-VCH, Weinheim, **2002**, pp. 251 – 274
[36] A. Mahapatro, A. Kumar and R. A. Gross, *Biomacromolecules*, **2004**, 5, 62–68.
[37] J. Wu, T. L. Yu, C. T. Chen, C. C. Lin, *Coord. Chem. Rev*., **2006**, 250, 602-626.
[38] N. E. Kamber, W. Jeong, R. M. Waymouth, *Chem. Rev*., **2007**, 107, 5813-5840.
[39] Duda, A.; Penczek, S. *Thermodynamics, kinetics and mechanisms of cyclic esters polymerisation. In Polymers from Renewable Resources: Biopolyesters and Biocatalysis;* Scholz, C.; Gross, R. A., Eds.; ACS Symposium Series; Oxford University Press: Washington, DC, **1996,**; Vol. 5, pp 317-343.
[40] a) Z. Tang , X. Chen , Q. Liang , X. Bian, L. Yang , L. Piao, et al. *J Polym Sci Part A Polym Chem* **2003**; 41,1934–41;
b) K. M. Stridsberg, M. R. and A. C. Albertsson, *Adv. Polym. Sci*., **2002**, 157, 41-65.
[41]H. R. Kricheldorf, I. K. Saunders. *Polylactones, 19. Anionic polymerization of L-lactide in solution. Die Makromo.l Chem.*, **1990**;191(5):1057–66.
[42] Platel, R. H.; Hodgson, L. M.; Williams, C. K. *Polym Rev* **2008**, 48, 11–63.
[43] Abdessamad, A.; Redshaw, C. *Polym Chem* **2010**, 1, 801–826-
[44] B. O'Keefe, M. Hillmyer,W. Tolman, *J. Chem. Soc. Dalton. Trans.* **2001**, 2215–2224.
[45] M. Labet, W. Thielmans, *Chem. Soc. Rev*., **2009**, 38, 3484-3504.
[46] P. Degée, P. Dubois, R. Jerôme, S. Jacobsen, H. G. Fritz, *Macromol. Symp*., **1999**, 144-289.
[47] a) Degee, P.; Dubois, P.; Jerome, R.; Jacobsen, S.; Fritz, H.-G. *Macromol. Symp*. **1999**, 144, 289;
b) Al(OiPr)3 is known to exist as a mixture of at least two aggregates, namely, a trimer and a tetramers, see: Kowalski,
A.; Duda, A.; Penczek, S. *Macromolecules* **1998**, 31, 2114.
[48] (a) Chabot, F.; Vert, M.; Chapelle, S.; Granger, P. *Polymer* **1983**, *24*, 53.
(b) Schwach, G.; Coudane, J.; Engel, R.; Vert, M. *Polym. Int.* **1998**, *46*, 177.
[49] McClain, S. J.; Ford, T. M.; Drysdale, N. E., *Polym. Prep*. **1992**, 33, 463–464.
[50] A.P. Gupta, V. Kumar, *Eur. Polym. J*.,**2007**, 43, 4053-4074.
[51] Amgoune, A.; Thomas, C. M.; Roisnel, T.; Carpentier, J.-F. *Chem.;Eur. J*. **2006**, 12, 169–179.
[52] a) Amgoune, A.; Thomas, C. M.; Carpentier, J.-F. *Pure Appl. Chem.*, **2007**, 79, 2013–2030;
b)Bambirra, S.; Bouwkamp, M. W.; Meetsma, A.; Hessen, B., *J. Am. Chem. Soc*., **2004**, 126, 9182–9183;
c) Arnold, P. L.; Buffet, J.-C.; Blaudeck, R. P.; Sujecki, S.; Blake, A. J.; Wilson, C. *Angew Chem Int Ed Engl* **2008**, 47, 6033–6036;
d) Cheng, J.; Cui, D.; Chen, W.; Hu, N.; Tang, T.; Huang, B. *J Organomet Chem* **2004**, 689, 2646–2653.
[53] a) Yao, Y.; Luo, Y.; Chen, J.; Zhang, Z.; Zhang, Y.; Shen, Q. *J Organomet Chem* **2003**, 679, 229–237;
b) Luo, Y.; Yao, Y.; Shen, Q.; Yu, K.; Weng, L. *Eur J Inorg Chem* **2003**, 318–323;
c) Luo, Y.; Yao, Y.; Shen, Q.; Sun, J.; Weng, L. *J Organomet. Chem*., **2002**, 662, 144–149;

d) Yao, Y.; Ma, M.; Xu, X.; Zhang, Y.; Shen, Q.; Wong, W.-T. *Organometallics* **2005**, 24, 4014–4020;
e) Yao, Y.; Xu, X.; Liu, B.; Zhang, Y.; Shen, Q.; Wong, W.-T. *Inorg Chem* **2005**, 44, 5133–5140.
[54] a) Sanchez-Barba, L. F.; Hughes, D. L.; Humphrey, S. M.; Bochmann, M. *Organometallics* **2005**, 24, 3792–3799;
b) Sanchez-Barba, L. F.; Hughes, D. L.; Humphrey, S. M.; Bochmann, M. *Organometallics* **2006**, 25, 1012–1020.
[55] a) S. McLain, N. Drysdale. U.S. patent 5 028 667 (**1991**).
[56] a)Stevels, W. M.; Ankone, M. J. K.; Dijkstra, P. J.; Feijen, J. , *Macromolecules* **1996**, 29, 3332–3333.
b). Stevels, W. M.; Ankone, M. J. K.; Dijkstra, P. J.; Feijen, J. ,*Macromolecules***1996**, 29, 6132–6138.
c). Simic, V.; Girardon, V.; Spassky, N.; Hubert-Pfalzfraf, L. G.; Duda, A., *Polym. Degr.Stab*. **1998**, 59, 227–229.
[57] a)S. Arndt, J. Okuda. *Chem. Rev.* **2002,** 102, 1953
b) S. Zhou, S. Wang, G. Yang, Q. Li, L. Zhang, Z. Yao, Z. Zhou and H.-B. Song, *Organometallics*, **2007**, 26, 3755.
[58] a) Ajellal, N.; Lyubov, D. M.; Sinenkov, M. A.; Fukin, G. K.; Cherkasov, A. V.; Thomas, C. M.; Carpentier, J. F.; Trifonov, A. A. *Chem—Eur J* **2008**, 14, 5440–5448;
b) Cai, C.-X.; Amgoune, A.; Lehmann, C. W.; Carpentier, J.-F. *Chem Commun* **2004**, 330–331;
c) Mahrova, T. V.; Fukin, G. K.; Cherkasov, A. V.; Trifonov, A. A.; Ajellal, N.; Carpentier, J.-F. *Inorg Chem* **2009**, 48, 4258– 4266;
d) Grunova, E.; Kirillov, E.; Roisnel, T.; Carpentier, J.-F. *Organometallics* **2008**, 27, 5691–5698;
e) Amgoune, A.; Thomas, C. M.; Carpentier, J. F. *Macromol Rapid Commun* **2007**, 28, 693–697.
[59] a) Bonnet, F.; Cowley, A. R.; Mountford, P. *Inorg Chem* **2005**, 44, 9046–9055;
b) Save, M.; Schappacher, M.; Soum, A. *Macromol Chem Phys* **2002**, 203, 889–899.
[60] Ma, H. Spaniol T.; Okuda, *J. Angew Chem Int Ed Engl* **2006,** 45, 7818–7821
[61] Platel, R. H.; Hodgson, L. M.; White, A. J. P.; Williams, C. K. *Organometallics* **2007**, 26, 4955–4963.
[62] a)Mankad, N. P.; Rivard, E. Harkins, S. B.; Peters, J. C. *J AmChem Soc* **2005**, 127, 16032–16033; b) Whited, M. T.; Rivard, E.; Peters, J. C. *Chem Commun* **2006**, 1613–1615.
[63] (a) Grunova, E.; Kirillov, E.; Roisnel, T.; Carpentier, J.-F. *Organometallics* **2008**, 27, 5691–5698.
[64] (a) Yao, Y.; Zhang, Z.; Peng, H.; Zhang, Y.; Shen, Q.; Lin, *J. Inorg Chem* **2006**, 45, 2175–2183. (b) Xue, M. Y. Y.; Shen, Q.; Zhang, J. *J Organomet Chem* **2005**, 690, 4685–4691
[65] Penczek, S. S. R.; Duda, A.; Baran, *J. Macromol Symp* **2003**, 201, 261–270
[66] Shang, X.; Liu, X.; Cui, D. J Polym Sci Part A*: Polym Chem* **2007**, 45, 5662–5672
[67] Liu, X.; Shang, X.; Tang, T.; Hu, N.; Pei, F.; Cui, D.; Chen, X.; Jing, X. *Organometallics* **2007**, 26, 2747–2757
[68] The k_{app} value for the bis(thiophosphinicamido)yttrium complex, [(bis(P,P'-diisopropylthiophosphinic)-2,2-dimethylpropylene

diamido)(bis(trimethylsilyl)amido)yttrium], reported as one of the highest active yttrium initiators, is 19×10^{-3} s^{-1} at 10 mM catalyst concentration. See Hodgson, L. M.; White, A. J. P.; Williams, C. K. J Polym Sci Part A: Polym Chem 2006, 44, 6646–6651
[69] Ma, H.; Okuda, J. *Macromolecules* **2005**, 38, 2665–2673.
[70] Ma, H.; Spaniol, T. P.; Okuda, *J. Inorg Chem* **2008**, 47, 3328–3339.
[71] N. Ajellal, J-F. Carpentier, C. Guillaume, S. M. Guillaume,M H. Valentin Poirier, Y. Sarazin*a* and A. Trifonov,*Dalton Trans.* **2010**, 39, 8363-8376.
[72] S.Inoue, *J. Polym. Sci*., **2000**, 38, 2861-2871.
[73] Martin, E.; Dubois, P.; Jerome, R. *Macromolecules* **2003**, 36, 5934–5941
[74] (a) Jacobs, C.; Dubois, P.; Teyssie, P.; Jerome, R. *Macromolecules* **1991**, 24, 3027-3034. (b) Shen, Y.; Shen, Z.; Zhang, Y.; Yao, K. *Macromolecules* **1996**, 29, 8289–8295. (c) Simic, V.; Pensec, S.; Spassky, N. *Macromol Symp* **2000**, 153, 109–121. d) Song, C. X.; Feng, X. D. *Macromolecules* **1984**, 17, 2764– 2767; e) B.M. Chamberlain, B.A. Jazdzewski, M. Pink, W.B. Tolman, *Macromolecules*, **2000**, 33, 3970-3977.
[75] (a) Shen, Y.; Zhu, K. J.; Shen, Z.; Yao, K.-M. *J Polym Sci Part A: Polym Chem* **1996**, 34, 1799–1805. (b) Duda, A.; Biela, T.; Libiszowlski, J.; Penczek, S.; Dubois, P.; Mecerreyes, D.; Jerome, R. *Polym Degrad Stab* **1998**, 59, 215
[76] (a) Florczak, M. L. J.; Monsnacek, J.; Duda, A.; Penczek, S. *Macromol Rapid Commun* **2007**, 28, 1385–1391. (b) Pappalardo, D.; Annunziata, L.; Pellecchia, C. *Macromolecules* **2009**, 42, 6056. (c) Amgoune, A.; Thomas Christophe, M.; Roisnel, T.; Carpentier, J.-F. *Chem—Eur J* **2006**, 12, 169–179.
[77] (a) Nomura, N.; Akita, A.; Ishii, R.; Mizuno, M. *J Am Chem Soc* **2010**, 132, 1750. (b) Florczak, M.; Duda, A. *Angew Chem Int Ed Engl* **2008**, 9088–9091.
[78] (a) Tanahashi, N.; Doi, Y. *Macromolecules* **1991**, 24, 5732– 5737. (b) Kemnitzer, J. E.; McCarthy, S. P.; Gross, R. A. *Macromolecules* **1993**, 26, 1221–1229, and references cited therein
[79] (a) Amgoune, A.; Thomas Christophe, M.; Ilinca, S.; Roisnel, T.; Carpentier, J.-F. *Angew Chem Int Ed Engl* **2006**, 45, 2782–
2784. (b) Ajellal, N.; Bouyahyi, M.; Amgoune, A.; Thomas, C. M.; Bondon, A.; Pillin, I.; Grohens, Y.; Carpentier, J.-F. *Macromolecules*
2009, 42, 987–993. (c) Kramer, J. W.; Treitler, D. S.; Dunn, E. W.; Castro, P. M.; Roisnel, T.; Thomas, C. M.; Coates, G. W. *J Am Chem Soc* **2009**, 131, 16042–16044
[80] Kurcok, P.; Duboist, P. J. R. *Polym Int* **1996**, 41, 479–485.
[81] Kurcok, P.; Kowalczuk, M.; Hennek, K.; Jedliiiski, Z. *Macromolecules* **1992**, 25, 2017.
[82] Rieth, L. R.; Moore, D. R.; Lobkovsky, E. B.; Coates, G. W. *J Am Chem Soc* **2002**, 124, 15239–15248.
[83] M. Mazzeo, M. Lamberti, I. D'Auria, S.Milione, J. C. Peters, C. Pellecchia, *J. of Polym. Sci. Part A: Polym. Chem.*, **2010,** 48, 1374-1382.
[84] I. D'Auria, M. Mazzeo, D. Pappalardo, M. Lamberti, C. Pellecchia, *J. of Polym. Sci. Part A: Polym. Chem.*, **2010,** 49, 403-413.
[85] a) T. Biela, A. Kowalski, J. Libiszowski, A. Duda, S. Penczek, *Macromol. Symp.* **2006**, *240*, 47-55;
b)M. J. Stanford, A. P. Dove, *Chem. Soc. Rev.* **2010**, *39*, 486–494.
[86] a) B. J. O'Keefe, M. A. Hillmyer, W. B. Tolman, *J. Chem. Soc., Dalton Trans.* **2001**, 2215-2224;
b) O. Dechy-Cabaret, B. Martin-Vaca, D. Bourissou, *Chem. Rev.* **2004**, *104*, 6147-6176.

c) J. Y. Wu, T.-L.; Chen, C.-T., C.-C. Lin, *Coord. Chem. Rev.* **2006**, *250*, 602-626.
d)A. Arbaoui, C. Redshaw, *Polym. Chem.* **2010**, *1*, 801–826.
[87] a) P. J. Dijkstra, H. Du, J. Feijen, *Polym. Chem.* **2011**, *2*, 520–527.
b) C. M. Thomas, *Chem. Soc. Rev.*, **2010**, *39*, 165-173.
[88] a) L. E. Breyfogle, C. K. Williams, V. G. Young, Jr., M. A. Hillmyer, W. B. Tolman, *Dalton Trans.* **2006**, 928-936;
b) C. K. Williams, L. E. Breyfogle, S. K. Choi, W. Nam, V. G. Young, Jr., M. A. Hillmyer, W. B. Tolman, *J. Am. Chem. Soc.* **2003**, *125*, 11350-11359;
c) C. K. Williams, N. R. Brooks, M. A. Hillmyer, W. B. Tolman, *Chem. Commun.* **2002**, 2132-2133
[89] a) H.-Y. Chen, H.-Y. Tang, C.-C. Lin, *Macromolecules* **2006**, *39*, 3745-3752.
b) H.-Y. Chen, M.-Y. Liu, K. Sutar Alekha, C.-C. Lin, *Inorg. Chem.* **2010**, *49*, 665-674
[90] a) J. Ejfler, S. Szafert, K. Mierzwicki, L. B. Jerzykiewicz, P. Sobota, *Dalton Trans.* **2008**, 6556-6562;
b) M. H. Chisholm, J. C. Gallucci, H. Zhen, J. C. Huffman, *Inorg. Chem.* **2001**, *40*, 5051-5054.
[91] a) V. Poirier, T. Roisnel, J.-F. Carpentier, Y. Sarazin, *Dalton Trans.* **2009**, 9820-9827.
b) V. Poirier, T. Roisnel, J.-F. Carpentier, Y. Sarazin, *Dalton Trans.* **2011**, *40*, 523-534.
[92] a) M. Cheng, A. B. Attygalle, E. B. Lobkovsky, G. W. Coates, *J. Am. Chem. Soc.* **1999**, *121*, 11583-11584.
b) H.-Y. Chen, B.-H. Huang, C.-C. Lin, *Macromolecules* **2005**, *38*, 5400-5405
[93] a) M. H. Chisholm, J. C. Gallucci, K. Phomphrai, *Inorg. Chem.* **2005**, *44*, 8004-8010.
b) A. P. Dove, V. C. Gibson, E. L. Marshall, A. J. P. White, D. J. Williams, *Dalton Trans.* **2004**, 570-578;
c) F. Drouin, P. O. Oguadinma, T. J. J. Whitehorne, R. E. Prud'homme, F. Schaper, *Organometallics* **2010**, *29*, 2139-2147;
d) B. M. Chamberlain, M. Cheng, D. R. Moore, T. M. Ovitt, E. B. Lobkovsky, G. W. Coates, *J. Am. Chem. Soc.* **2001**, *123*, 3229-3238.
[94] C. A. Wheaton, P. G. Hayes, *Chem. Commun.* **2010**, *46*, 8404-8406.
[95] J. Boerner, U. Floerke, K. Huber, A. Doering, D. Kuckling, S. Herres-Pawlis, *Chem.--Eur. J.* **2009**, *15*, 2362-2376.
[96] M. H. Chisholm, N. W. Eilerts, J. C. Huffman, S. S. Iyer, M. Pacold, K. Phomphrai, *J. Am. Chem. Soc.* **2000**, *122*, 11845-11854
[97] D. Darensbourg, J., M. S. Zimmer, P. Raney, D. L. Larkins, *Inorg. Chem.* **1998**, *37*, 2852-2853.
[98] a) L.-C. Liang, W.-Y. Lee, C.-H. Hung, *Inorg. Chem.* **2003**, *42*, 5471-5473.
b) L.-C. Liang, W.-Y. Lee, T.-L. Tsai, Y.-L. Hsua, T.-Y. Leeb, *Dalton Trans.* **2010**, *39*, 8748–8758
[99] L. M. Broomfield, J. A. Wright, M. Bochmann, *Dalton Trans.* **2009**, 8269-8279.
[100] a) M. Cheng, D. R. Moore, J. J. Reczek, B. M. Chamberlain, E. B. Lobkovsky, G. W. Coates, *J. Am. Chem. Soc*, **2001**, *123*, 8738-8749.
b) E. Grunova, T. Roisnel, J.-F. Carpentier, *Dalton Trans.* **2009**, 9010-9019.
[101] a) T. Cantat, B. L. Scott, D. E. Morris, J. L. Kiplinger, *Inorg. Chem.* **2009**, *48*, 2114-2127.
b) Z. Liu, W. Gao, J. Zhang, D. Cui, Q. Wu, Y. Mu, *Organometallics* **2010**, *29*, 5783-5790
[102] S. C. Goel, M. Y. Chiang, W. E. Buhro, *J. Am. Chem. Soc.* **1990**, *112*, 5636-5637.

[103] DFT calculations were carried out by Doc. S. Milione in the Chemistry Department.
[104] a) M. Bochmann, G. C. Bwembya, R. Grinter, A. K. Powell, K. J. Webb, M. B. Hursthouse, K. M. A. Malik, M. A. Mazid, *Inorg. Chem.* **1994**, *33*, 2290–2296.
b) P. L. o. a. E. Hey-Hawkins, F. Majoumo-Mbe, *Organometallics* **2005**, *24*, 5287–5293.
[105] P. C. Andrews, C. L. Raston, B. W. Skelton, A. H. White, *Organometallics* **1998**, *17*, 779.
[106] K. Izod, W. McFarlane, B. Allen, W. Clegg, R. W. Harrington, *Organometallics* **2005**, *24*, 2157-2167
[107] P. J. Heard, *Chem. Soc. Rev.* **2007**, *36*, 551–569.
[108] a) T. Cantat, B. L. Scott, D. E. Morris, J. L. Kiplinger, *Inorg. Chem.* **2009**, *48*, 2114-2127
b) T. Cantat, C. R. Graves, B. L. Scott, K. J. L., *Angew. Chem., Int. Ed.* **2009**, *48*, 3681 – 3684.
[109] N. Ajellal, J.-F. Carpentier, C. Guillaume, S. M. Guillaume, M. Helou, V. Poirier, Y. Sarazin, A. Trifonov, *Dalton Trans.* **2010**, *39*, 8363-8376.
[110] S. Penczek, R. S., A. Duda, J. Baran, *Macromol. Symp.* **2003**, *201*, 261
[111] D. Darensbourg, J., O. Karroonnirun, *Inorg. Chem.* **2010**, *49*, 2360-2371
[112] a)J. L. Eguiburu, M. J. Fernandez-Berridi, F. P. Cossío, J. San Román., *Macromolecules* **1999**, *32*, 8252-8258.
b) H. von Schenck, M. Ryner, A. Albertsson, M. Svensson, *Macromolecules* **2002**, *35*, 1556-1562.
c) E. L. Marshall, V. C. Gibson, H. S. Rzepa, *J. Am. Chem. Soc.* **2005**, 6048-6051.
d) N. Barros, P. Mountford, S. M. Guillaume, L. Maron, *Chem. Eur. J.* **2008**, *14*, 5507-5518.
e) J. Liu, J. Ling, X. Li, Z. Shen, *J. Mol. Catal. A: Chem.* **2009**, *300*, 59–64.
f) H. E. Dyer, S. Huijser, N. Susperregui, F. Bonnet, A. D. Schwarz, R. Duchateau, L. Maron, P. Mountford, *Organometallics* **2010**, 3602-3621.
g) N. Susperregui, M. U. Kramer, J. Okuda, L. Maron, *Organometallics* **2011**, *30*, 1326-1333.
h) J. Börner, I. dos Santos Vieira, A. Pawlis, A. Döring, D. Kuckling, S. Herres-Pawlis, *Chem. Eur. J.* **2011**, *17*, 4507 – 4512.
[113] a) Kasperczyk, J.,Bero, M., *Makromol. Chem*., **1991**, 192, 1777-1787.
b) Kasperczyk, J.,Bero, M., *Makromol. Chem*., **1993**, 194, 913-925
[114] Vanhoorne, P., Dubois, Ph., Jerome, R., Teyssié, Ph., *Macromolecules*, **1992**, 25, 37-44.
[115] a)J. Kasperczyk, M. Bero, *Makromol. Chem.* **1991**, *192*, 1777-1787.
b) J. Kasperczyk, M. Bero, *Makromol. Chem.* **1993**, *194*, 913-925.
[116] Dubois, P.; Jacobs, C.; Jerome, R.; Teyssie´, P. *Macromolecules* **1991**, 24, 2266–2270
[117] Liu, Y.-C.; Ko, B.-T.; Lin, C.-C. *Macromolecules* **2001**, 34, 6196.
[118] (a) Webster, O. W. *Science* **1991**, 251, 887.
(b) Aida, T.; Inoue, S. *Acc. Chem. Res*. **1996**, 29, 39.
(c) Aida, T. *Prog. Polym. Sci*. **1994**, 19, 469.
[119] a) N. Spassky, M. Wisniewski, C. Pluta and A. Le Borgne, *Macromol. Chem. Phys*., **1996**, 197, 2627;
b) Z. Zhong, P. J. Dijkstra and J. Feijen, *Angew. Chem., Int. Ed*., **2002**, 41, 4510;
c) N. Nomura, R. Ishii, M. Akakura and K. Aoi, *J. Am. Chem. Soc*., **2002**, 124, 5938;
d) T. M. Ovitt andG.W.Coates, *J. Am. Chem. Soc*., **2002**, 124, 1316.

e) T. M. Ovitt and G. W. Coates, *J. Am. Chem. Soc*., **1999**, 121, 4072
[120] P. Hormnirun, E. L. Marshall, V. C. Gibson, A. J. P. White and D. J. Williams, *J. Am. Chem. Soc*., **2004**, 126, 2688
[121] P.-Y. Lee and L.-C. Liang, *Inorg. Chem*. **2009**, 48, 5480–5487
[122] (29) Barron, A. R. J. Chem. Soc., Dalton Trans. 1988, 3047–3050. (32) Healy, M. D.; Ziller, J. W.; Barron, A. R. Organometallics 1991, 10,
597–608. (33) Power, M. B.; Bott, S. G.; Atwood, J. L.; Barron, A. R. J. Am. Chem. Soc. 1990, 112, 3446–3451. (34) Power, M. B.; Bott, S. G.; Clark, D. L.; Atwood, J. L.; Barron, A. R. Organometallics 1990, 9, 3086–3097.
[123] Pr is the probability of racemic linkages between monomer units and is determinated from the methine region of the homonuclear decoupled ^{1}H NMR spectrum.